EFFECTS OF STRONTIUM ON THE OXIDATION OF MOLTEN ALUMINUM ALLOYS CONTAINING SILICON AND MAGNESIUM

By

PUI KEI YUEN

Department of Mining and Metallurgy

McGill University, Montreal

June 2001

A Thesis submitted to the Faculty of Graduate Studies and Research in partial fulfillment of the requirements of the degree of Master of Engineering

© Pui Kei Yuen, 2001



National Library of Canada

Acquisitions and Bibliographic Services

395 Wellington Street Ottawa ON K1A 0N4 Canada Bibliothèque nationale du Canada

Acquisitions et services bibliographiques

395, rue Wellington Ottawa ON K1A 0N4 Canada

Your Me Votre reference

Our the Notre reference

The author has granted a nonexclusive licence allowing the National Library of Canada to reproduce, loan, distribute or sell copies of this thesis in microform, paper or electronic formats.

The author retains ownership of the copyright in this thesis. Neither the thesis nor substantial extracts from it may be printed or otherwise reproduced without the author's permission.

L'auteur a accordé une licence non exclusive permettant à la Bibliothèque nationale du Canada de reproduire, prêter, distribuer ou vendre des copies de cette thèse sous la forme de microfiche/film, de reproduction sur papier ou sur format électronique.

L'auteur conserve la propriété du droit d'auteur qui protège cette thèse. Ni la thèse ni des extraits substantiels de celle-ci ne doivent être imprimés ou autrement reproduits sans son autorisation.

0-612-79107-6

Canadä

ABSTRACT

In the presence of air and oxygen, oxidation of a molten aluminum alloy will easily take place. The oxidation not only harms the operation by contributing to melt losses, but the processing of the oxides present in the melt and refractory is also costly in time and money. Refractory accretions formed due to the interactions between the oxide-layer and base refractory material, especially alumina-lined ones, are a significant problem for the industry. Aluminum alloys containing magnesium are known to oxidize much more easily and rapidly. In the foundry, oxidation of molten aluminum-magnesium alloy is more prominent than that of pure aluminum. Magnesium has a higher affinity for oxygen, causing it to oxidize more easily than aluminum. In previous studies of oxidation of aluminum alloys, it has been found that strontium additions to the alloy reduce the amount of oxidized layer in an undisturbed melt.

The effects of strontium additions on the oxidation behavior of commercial A356, A357 and 5182 aluminum alloys were investigated by monitoring sample weight gains with time with a thermo-gravimetric balance at 700, 750, and 800°C. Sample surfaces were examined using electron microscope and x-ray diffraction techniques. It was found that in the absence of Sr, the A356 and A357 samples gained substantial amounts of weight through the preferential oxidation of magnesium. Samples containing strontium had significantly lower weight gains. For the high magnesium-containing 5182 alloy, an increase of incubation period before the onset of significant oxidation is associated with the presence of strontium. This change in oxidation behavior was linked to the presence of strontium containing oxide species in the oxidizing surface.

RÉSUMÉ

En présence d'air et d'oxygène, les alliages d'aluminium s'oxydent très facilement. L'oxydation ne cause pas seulement du tort aux opérations contribuant par perte de matériel, mais le traitement des oxydes présents dans le bain fondu et des réfractaires est aussi coûteux en temps et en argent. L'accroissement d'oxyde réfractaires formés dû à l'interaction entre la couche d'oxyde et les briques réfractaires, spécialement ceux d'alumines, sont des problèmes important dans l'industrie. Les alliages d'aluminium contenant du magnésium sont connus pour s'oxyder beaucoup plus facilement et rapidement. Dans les fonderies, les problèmes reliés à l'oxydation des alliages d'aluminium-magnésium liquide est beaucoup plus prononcé que pour ceux de l'aluminium pur. Le magnésium possède une affinité plus grande pour l'oxygène, ce qui cause une oxydation plus rapide que celle de l'aluminium. Lors d'études précédentes sur l'oxydation des alliages d'aluminium, il a été trouvé que des additions de strontium réduisent la quantité d'oxyde produit en surface dans un bain en fusion non troublé.

Les effets d'additions de strontium sur l'oxydation d'alliages commerciaux A356, A357 et 5182 a été investigué en faisant l'acquisition du gain de poids dans une balance thermo-gravimetrique à 700, 750 et 800°C. La surface des échantillons a été examinée utilisant le MEB et la diffraction des rayons X. Il a été trouvé qu'en absence de strontium, les alliages A356 et A357 gagnent substantiellement du poids dû à l'oxydation préférentielle du magnésium. Les échantillons contenant du strontium ont eu des gains de poids significativement inférieur. Pour l'alliage contenant une haute teneur en magnésium (5182), une augmentation de la période d'incubation avant l'oxydation rapide a été associée à la présence de strontium. Ce changement de comportement d'oxydation a été relié avec la présence d'oxyde contenant du strontium dans la surface oxydée.

ACKNOWLEDGEMENTS

I would like to express my sincere gratitude to Professor R.A.L. Drew and Professor John Gruzleski for their excellent supervision and guidance during the entire project. Their enthusiasm and their support throughout the project have been extremely encouraging, and remained as a great source of inspiration.

I would like to thank all the specialists and lab technicians for providing me with all the required tools and suggestions in order for me to perform all the different tests and effectively use the equipments. Big thanks go to Robert Paquette, Helen Campbell, Monique Riendeau, Ray Langlois, and Alain Gagnon. Special thanks have to go to Florence Paray, who has provided me with her wisdom and many important suggestions and opinions on various aluminum topics. I am also tremendously grateful to Keith Dennis for his previous work that motivated this project, and in helping me familiarize with the topics and the testing equipments.

Fellow students are definitely a big part of university life, and here I have a chance to thank them for their companionship and camaraderie, and also wish them the best of all. To Juan, Mathieu, Claudia, and basically the whole ceramic and aluminum group, thank you so much sharing your time and space with me. Extra special credits have to go to Juan for his tremendous help in this project.

Finally, I have to extend my greatest respect and appreciation to my family, Mom, Dad and my sister Pui Wai for their unconditional love and support. My proudest accomplishments, which include this work, have all been results of their infinite encouragement. I love you Mom and Dad. I would also like to take this opportunity to remind my families back in Hong Kong and overseas that I always have them in my mind. And last but not least, my love and my dedication to Angela.

TABLE OF CONTENTS

ABSTRACT	ii
RESUME	iii
ACKNOWLEDGEMENTS	iv
TABLE OF CONTENTS	v
LIST OF FIGURES	vii
LIST OF TABLES	xii
1. INTRODUCTION	1
2. LITERATURE REVIEW	3
2.1 Oxidation of metals	3
2.2 Oxidation Problems	5
2.3 Oxidation Uses	6
2.4 Oxidation Mechanisms and Kinetics	7
2.4.1 Temperature Effects on Oxidation	
2.5 High Temperature Aluminum Oxidation	
2.6 Aluminum-Magnesium Alloy Oxidation	
2.5.1 A356-A357 Alloy Oxidation	
2.5.2 5000 Series Alloy Oxidation	
2.5.3 Effects of Strontium	
2.7 Summary	
3. EXPERIMENTAL PROCEDURE	25
3.1 Raw Materials	
3.2 Melting and Casting	
3.3 Sample Preparation and Fabrication	28
3.4 Alumina Crucible Fabrication	29
3.5 Oxidation Experiments - TGA Tests	31
3.6 Sample Analysis	
3.6.1 Emission Spectrometry	35
3.6.2 Optical Microscopy	
3.6.3 Scanning Electron Microscopy (SEM)	
3.6.4 X-Ray Diffraction (XRD)	

4. RESULTS	38
4.1 Alloy Compositions	39
4.2 5182 Alloy	39
4.3 5182 Alloy Containing Sr	
4.4 A356 Alloy	
4.5 A356 Alloy Containing Sr	
4.6 A357 Alloy	56
4.7 A357 Alloy Containing Sr	
5. DISCUSSION	63
5.1 Oxidation of 5182 Alloy	
5.1.1 Weight Gain Data	65
5.1.1.1 Effects of Temperature	68
5.1.1.2 Effects of Strontium	68
5.1.2 Microscopy and XRD	69
5.1.2.1 Additional Emission Spectrometry	72
5.1.3 Breakaway Oxidation Behavior and Hypothesis and Model of	
Depletion	
5.2 Oxidation of A356 and A357 Alloys	
5.2.1 Weight Gain Data	
5.2.1.1 Effects of Magnesium Content	
5.2.1.2 Effects of Strontium	
5.2.2 Microscopy	
5.2.2 X-Ray Diffraction	
5.2.3 Protective Behavior Hypothesis	82
5.3 Practical and Industrial Relevance	84
6. CONCLUSIONS	86
7. SUGGESTED FUTURE WORK	88
REFERENCES	89

List of Figures

Figure 2.1:	Schematic representation of processes that are involved in the gaseous oxidation at a metal surface
Figure 2.2:	Oxide stresses according to P-B Ratios8
Figure 2.3:	Graphical depiction of the various general kinetics10
Figure 2.4:	Model for breakaway oxidation14
Figure 2.5:	High magnification micrograph of the surface oxide on commercial 356 alloy samples
Figure 2.6:	Micrographs showing the modification of the silicon phase in a commercial 356 alloy due to the presence of 250 ppm Sr
Figure 2.7:	Heat-treated and quenched aluminum magnesium alloy samples20
Figure 2.8:	SEM pictures 26 of top oxide formed at 740°C for 24 hours22
Figure 2.9:	Weight gain curves of the commercial 356 alloy without strontium at three different temperatures
Figure 2.10:	Weight gain curves for the commercial 356 alloy containing 250 ppm Sr at three different temperatures
Figure 3.1:	Graphite mold used for casting of the aluminum alloys26
Figure 3.2:	Actual picture of the graphite mold and the riser27
Figure 3.3:	The graphite mold and a piece of the cast aluminum alloy27
Figure 3.4:	A machined and polished sample
Figure 3.5:	Schematic illustration 30 of the drain-casting process30
Figure 3.6:	Sample in a crucible ready for oxidation experiment31
Figure 3.7:	Diagram 30 of TGA set-up to measure the oxidation weight gains33
Figure 3.8:	Picture of TGA set-up in the lab
Figure 4.1:	Averaged weight gain curve for 5182 alloy at 700°C40

Figure 4.2:	Averaged weight gain curve for 5182 alloy at 750°C40
Figure 4.3:	Averaged weight gain curve for 5182 alloy at 800 ^o C41
Figure 4.4:	Low magnification image of the top surface of 5182 alloy oxidized at 750°C
Figure 4.5:	Low magnification image of the top surface of 5182 alloy oxidized at 800°C
Figure 4.6:	Intermediate magnification image of the top surface of 5182 alloy oxidized at 800°C
Figure 4.7:	Intermediate magnification image of top surface of 5182 alloy oxidized at 700°C
Figure 4.8:	Intermediate magnification image of top surface of 5182 alloy oxidized at 750°C
Figure 4.9:	Intermediate magnification image of top surface of 5182 alloy oxidized at 800°C
Figure 4.10:	XRD pattern for the 5182 alloy in as-oxidized powder form45
Figure 4.11:	Averaged weight gain curve for 5182 alloy containing Sr at 700 ⁰ C46
Figure 4.12:	Averaged weight gain curve for 5182 alloy containing Sr at 750 ^o C46
Figure 4.13:	Averaged weight gain curve for 5182 alloy containing Sr at 800°C47
Figure 4.14:	Intermediate magnification image of top surface of 5182 alloy containing Sr oxidized at 700 ⁰ C
Figure 4.15:	Intermediate magnification image of top surface of 5182 alloy containing Sr oxidized at 750 ^o C
Figure 4.16:	Intermediate magnification image of top surface of 5182 alloy containing Sr oxidized at 800°C
Figure 4.17:	XRD pattern for the 5182 alloy containing Sr in as-oxidized powder form
Figure 4.18:	Averaged weight gain curves for A356 alloy at 7000C, 7500C and 800°C

Figure 4.19:	Low magnification image of top surface of A356 alloy oxidized at 700°C
Figure 4.20:	Intermediate magnification image of top surface of A356 alloy oxidized at 700°C
Figure 4.21:	Intermediate magnification image of top surface of A356 alloy oxidized at 750°C
Figure 4.22:	Intermediate magnification image of top surface of A356 alloy oxidized at 800°C
Figure 4.23:	XRD pattern for the A356 alloy in as-oxidized form53
Figure 4.24:	Averaged weight gain curves for A356 alloy containing Sr at 700 ^o C, 750 ^o C and 800 ^o C.
Figure 4.25:	Intermediate magnification image of top surface of A356 containing Sr oxidized at 700°C
Figure 4.26:	Intermediate magnification image of top surface of A356 containing Sr oxidized at 750°C
Figure 4.27:	Intermediate magnification image of top surface of A356 containing Sr oxidized at 800°C55
Figure 4.28:	XRD pattern for the A356 alloy containing Sr in as-oxidized form56
Figure 4.29:	Averaged weight gain curves for A357 alloy at 700°C, 750°C and 800°C
Figure 4.30:	Intermediate magnification image of top surface of A357 oxidized at 700°C58
Figure 4.31:	Intermediate magnification image of top surface of A357 oxidized at 750°C58
Figure 4.32:	Intermediate magnification image of top surface of A357 oxidized at 800°C
Figure 4.33:	XRD pattern for the A357 alloy in as-oxidized form
Figure 4.34:	Averaged weight gain curves for A357 alloy containing Sr at 700°C, 750°C and 800°C

Figure 4.35:	Intermediate magnification image of top surface of A357 containing Sr oxidized at 700°C
Figure 4.36:	Intermediate magnification image of top surface of A357 containing Sr oxidized at 750°C
Figure 4.37:	Intermediate magnification image of top surface of A357 containing Sr oxidized at 800°C
Figure 4.38:	XRD pattern for the A357 alloy containing Sr in as-oxidized form62
Figure 5.1:	An example of initial 30-hour experiments for the 5182 alloy64
Figure 5.2:	A weight gain curve depicting the three distinct stages of breakaway oxidation
Figure 5.3:	Comparison of weight gain curves of 5182 with and without strontium at 700°C
Figure 5.4:	Comparison of weight gain curves of 5182 with and without strontium at 750°C
Figure 5.5:	Comparison of weight gain curves of 5182 with and without strontium at 800°C
Figure 5.6:	Example of an oxidized 5182 alloy sample and its cross-section69
Figure 5.7:	Low magnification image of internal porosity70
Figure 5.8:	Intermediate magnification image of internal porosity70
Figure 5.9:	High magnification image of internal porosity70
Figures 5.10:	High magnification images of common micro-morphology of 5182 samples
Figure 5.11:	Schematic of the proposed model for the effects of strontium73
Figure 5.12:	Schematic of the proposed model without strontium74
Figure 5.13:	Summary of oxidation curves for the A356 alloy samples77
Figure 5.14:	Summary of oxidation curves for the A357 alloy samples77
Figure 5.15:	Micrographs at different magnification of the surface oxide morphology of A356/A357 alloy

Figure 5.16:	Example of a surface layer and localized eruption of A356/A357 alloy samples containing Sr					
Figure 5.17:	Example of coherent surface oxide formed on A356/A357 alloy samples containing Sr					

List of Tables

Table 2.1:	The effect of temperature on the oxidation behavior of various metals1	1
Table 4.1:	Average composition (in weight %) of the alloys used	9
Table 5.1:	Average incubation/inductions periods	58
Table 5.2:	Average chemical compositions of samples with strontium after oxidation experiments	
Table 5.3:	Tabulated average weight gain data comparing A356 and A357 alloy samples	8
Table 5.4:	Tabulated average weight gain data comparing A356 and A357 alloy samples with and without Sr	9

1. INTRODUCTION

In today's aluminum foundry business, molten metal losses during processing stages are often the result of rapid oxidation. In the presence of air, oxidation of the molten aluminum alloy will easily take place. Most of the commercial applications of aluminum involve magnesium-containing alloys. In melt preparation, significant amounts of oxidation occur in these melts as many melt holding furnaces in the industry are exposed to the oxygen containing atmosphere. These melt losses contribute significantly to the inefficiency of molten aluminum alloy processing. In today's competitive metals industry, process efficiency is a critical element in a successful operation. The oxidation not only harms the operation by contributing to melt losses, but the processing of the oxides present in the melt and refractory is also costly in time and money. In addition, oxide inclusions contribute to casting porosity and a deterioration of the mechanical properties.

Usually, pure solid aluminum oxidizes to form a protective oxide layer. Molten aluminum alloys exhibit a similar behavior, but this protection is only effective when there is no physical disturbance of the melt. In this liquid/solid system, the oxide layer forms as a solid barrier to reduce further transport of oxygen ions to react with the melt.

Aluminum alloys containing magnesium are known to oxidize much more easily and rapidly. In some alloys, where the magnesium content is quite high, the result of the oxidation can be quite dramatic and catastrophic as a very large portion of the melt could be oxidized and lost. In previous studies of oxidation of aluminum alloys, it has been found that strontium additions to the alloy reduce the amount of oxidized layer in an undisturbed melt ^{1,2}.

The effects of strontium on the oxidation behavior of aluminum silicon alloy containing magnesium has proven to be very interesting and may be very helpful in the processing stages of the molten alloy. This thesis presents a more detailed investigation of this phenomenon in low and high magnesium containing alloys.

2. LITERATURE REVIEW

2.1 Oxidation of metals

Oxidation of metals is a chemical reaction that takes place in the presence of oxygen in contact with the metal. It usually involves the removal of one or more electrons from an atom. In a normal atmospheric environment, the oxygen present affects almost all metals. The process of oxide layer formation is an electro-chemical one, depicted in Figure 2.1 and can be expressed by the following reactions:

$$M + \frac{1}{2} O_2 \rightarrow MO$$

Where M is a divalent metal,

The oxidation reaction is composed of these half-reactions:

$$M \rightarrow M^{2+} + 2e^{-}$$

$$\frac{1}{2} O_2 + 2e^- \rightarrow O^{2-}$$

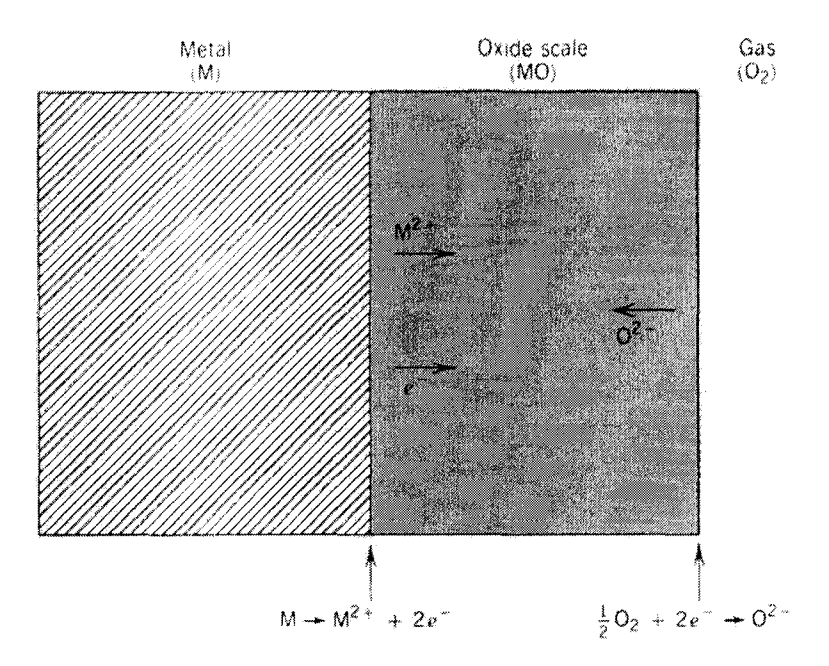


Figure 2.1: Schematic representation of processes that are involved in the gaseous oxidation at a metal surface.³

The basic form of oxidation for pure aluminum can be represented by the following reactions:

$$2 \text{ Al} \rightarrow 2 \text{ Al}^{3+} + 6e^{-}$$

$$3/2 \text{ O}_2 + 6e^- \rightarrow 3\text{ O}^{2-}$$

The respective ions then combine to form the oxide:

$$2 \text{ Al}^{3+} + 30^{2-} \rightarrow \text{Al}_2\text{O}_3$$

The oxidation of pure magnesium would involve the following reaction:

$$2 \text{ Mg} + \text{O}_2 \rightarrow 2 \text{ MgO}$$

For the oxidation reaction to take place, the presence of oxygen in contact with the metal is essential. In the initial stages of oxidation, this condition is met when the metal is in direct contact with air/O₂. As this reaction takes place, an oxide is being formed continuously at the metal/air interface. For this oxidation reaction to continue, there are many other factors that would combine to either facilitate or impede the reaction.

The study of oxidation then becomes a study of the oxidized layer, or coating, that formed on the metal. An important parameter of the layer formed is its protectiveness.

2.2 Oxidation Problems

As in almost every situation, oxidation can present itself as a major problem for a metal, as a form of corrosive loss of materials, which can render the material either useless or out of specification. In aluminum melt processing, oxidation mainly presents itself as melt losses that contribute to process inefficiency and inconsistency. The metal entrapped within the oxide layer is lost when the melt surface is skimmed and the dross discarded as per industrial practice. In the foundry, oxidation of molten aluminum-magnesium alloy is more prominent than that of pure aluminum. Magnesium has a higher affinity for oxygen, hence causing it to oxidize more easily than aluminum. Theoretically, this suggests that in an aluminum-magnesium melt, the oxidation of magnesium in the melt may predominate over that of aluminum.

This selective oxidation of each element presents another problem for the melt processing of the alloy. As different amounts and concentrations of the elements are consumed by the oxidation from the melt, the chemistry of the melt changes and becomes inconsistent with the calculated and predicted composition.

In the case of high magnesium-containing alloys such as the 5000 series, oxidation also presents additional problems over and above what has been mentioned. The interactions between the oxides formed and the refractories used in industrial furnaces can lead to severe accretions along the walls. Costly labor and materials expenditures to remove these accretions and repair/replace refractories are then necessary.

2.3 Oxidation Uses

A better understanding of oxidation behavior can also lead to useful applications. As ceramics and ceramic metal matrix composites become more widely used, specific applications of controlled oxidation as steps in manufacturing processes are noteworthy, and results from academic research further enhance the understanding of the fundamentals behind such processes.

For example, M. Guermazi et al. ⁴ has noted that, a new process, the DIMOXtm process ⁵, for making ceramic matrix and metal matrix composites was developed and commercialized by Lanxide Corporation. This technology is based on the use of a unique

directed-metal oxidation process to grow ceramic matrices around pre-placed composite fillers or reinforcements. The research was performed where metal-ceramic matrix composites were grown into different SiC powders by the directed oxidation of aluminum alloys in air at various temperatures.

2.4 Oxidation Mechanisms and Kinetics

In order to determine the kinetics of the chemical reactions taking place in the system, one has to understand the mechanisms of the reaction. The oxidation occurs at the metal-oxide interface. For the oxide layer to increase in thickness (or grow), there must be a continual feed of metal and oxygen to the interface. In the liquid metal system, the metal atoms will be continuously fed to the interface since it is liquid, but the oxygen atoms will have to come from the atmosphere, to which the oxide layer formed remains a barrier. The oxide layer may protect the metal from further oxidation as it acts as a barrier to the transport or diffusion of the oxygen atoms to the interface from the atmosphere. The rate of oxidation and the tendency of the oxidized layer to protect the metal from further oxidation then depend on the relative volumes of the oxide and the metal. The ratio of these volumes is referred to as the Pilling-Bedworth ratio ⁶:

$$P - B Ratio = \frac{A_O \rho_M}{A_M \rho_O}$$

Where A is the molecular weight, ρ is the density, and the subscripts O and M represent the oxide and metal, respectively. The use of the P-B ratio is mostly associated with a metal in the solid phase. Since the present study is focused on oxidation in the liquid system, the use of the P-B ratio to explain the oxide layer may not be very pertinent. It is nevertheless a good indication of a specific metal's tendency to form a protective layer. For example, as depicted in Figure 2.2, the ideal P-B ratio for an oxide layer formed would be unity. For metals having P-B ratios less than unity, the oxide film tends to be porous and un-protective as it is insufficient to fully cover the exposed metal surface. If the ratio is greater than unity, compressive stresses result in the oxide layer as it forms and may cause it to be unstable and crack and flake off.

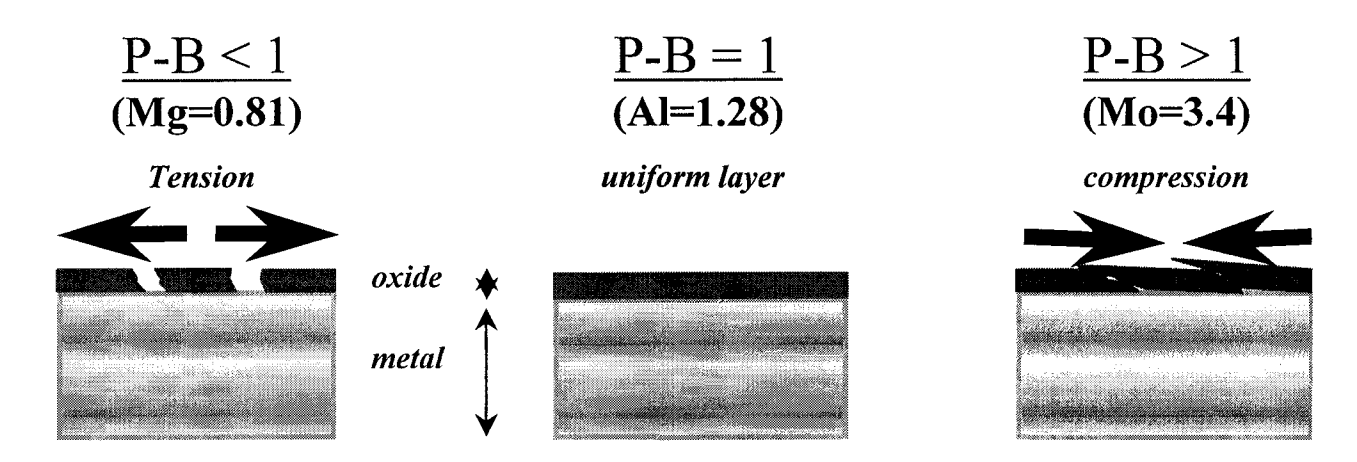


Figure 2.2: Oxide stresses according to P-B Ratios⁷

For the study of the kinetics of oxidation, the analysis of weight gain versus time exposed to oxidizing atmosphere is generally employed. Often, as with many other chemical processes, the graphical representation of this relationship can indicate the

mechanism of the reaction. Some basic oxidation kinetics have been found experimentally, such as: ⁸

Linear $\xi = k_l \cdot t$

Parabolic $\xi^2 = k_p \bullet t$

Cubic $\xi^3 = k_c \bullet t$

Logarithmic $\xi = k_e \cdot \log(a \cdot t + t_o)$

Inverse Logarithmic $\frac{1}{\xi} = A - k_i \bullet \log(t)$

Where ξ is the oxide thickness as a function of time, and a, A and k are constants. The theoretical curves shown in Figure 2.3 are often used as a way to describe the reaction kinetics in a simpler form. A metal can undergo much more complex kinetics, and this would be an indication of many different forms and stages of kinetics present.

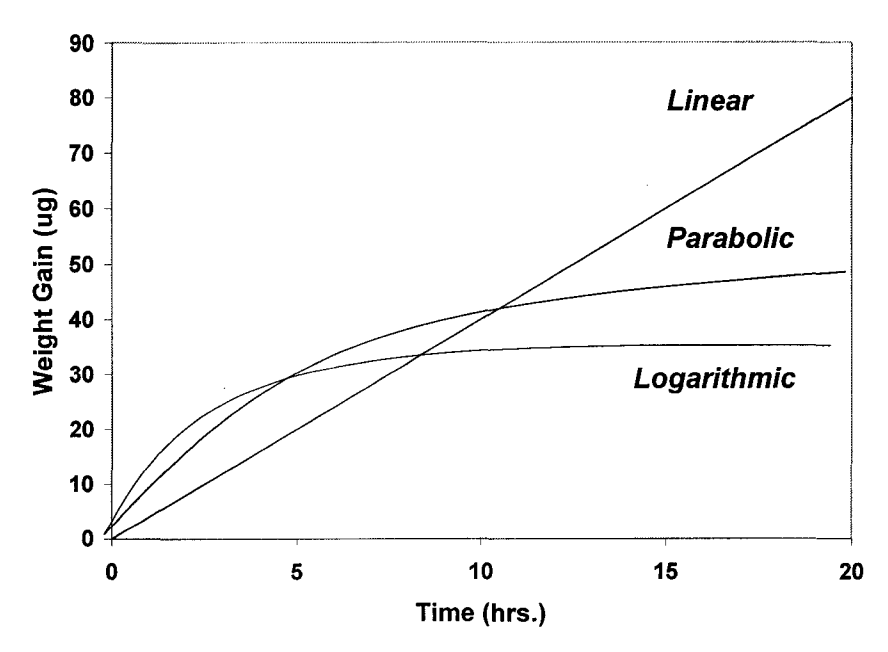


Figure 2.3: Graphical depiction of the various general kinetics.9

For example, a linear curve would most probably represent an un-protective oxidation; a parabolic or logarithmic curve would indicate more complex protective kinetics.

2.4.1 Temperature Effects on Oxidation

The temperature affects oxidation, like any other chemical reaction and diffusion related phenomenon. Oxidation rates are dependent on temperature because of the fact that the kinetic energy of the atoms in the reaction is dependent on temperature. Another important consideration for the temperature effect on oxidation is that when an oxide layer offers protectiveness, oxidation is also a diffusion dependent process. Diffusion is a thermally dependent transport mechanism, thus temperature effects are obvious. It is noteworthy that the viscosity of molten aluminum alloys decreases with increasing

temperature, allowing more molten metal to penetrate/to be transported to the oxidizing front. An increase in temperature also increases reaction kinetics and the supply of fresh, un-oxidized metal to the oxide.

The Arrhenius equation has been used to describe the oxidation process; and the diffusion process can also be described by an Arrhenius type relationship:

$$k=A \bullet e^{\frac{-Q}{RT}}$$
 and $D=D_O \bullet e^{\frac{-Q_d}{RT}}$

Where k is the rate constant, A is a constant, Q is the activation energy, R is the gas constant, T is the temperature, and D is the diffusion coefficient, D_0 is a diffusion constant. Table 2.1 briefly summarizes the relationship between the temperature and the oxidation kinetics of selected metals.

Table 2.1: The effect of temperature on the oxidation behavior of various metals ¹⁰ (log=logarithmic, lin=linear, para=parabolic, inv=inverse, cub=cubic, accel=accelerated, asym.=asymptotic)

Temp	100) 20	00 30	00 40	500	60	00 700	800	900	1000	1100	1200
(°C)						1						
Mg	log		para	para	-lin	lin						
Ti			lo	og cub		cub	para-lin		pa	ara-lin		
Zr			log	cub		cub			cub	cub-li	n	
Nb			para	para	para-li	n	lin		lin		accel	asym.
Mo			para	para	a-lin p	ara-lin	lin		lin			
W				para	pa	ara	para-lin		para-lin	p	ara-lin	
Fe	log	log		para	para		para		para		para	
Ni		log	lo	g cubic	para				para		para	
Cu	log	cub	para		para		para	para				
Zn			log	log para	para							
Al	log	inv.log	log	para	asym	lin						

2.5 High Temperature Aluminum Oxidation

Oxidation of aluminum above the melting point is different from oxidation in the solid state. Impey et al. 11 conducted experiments that involved the oxidation of commercial purity aluminum at molten temperatures, and he proposed the following theories on the mechanism of oxide scale growth on liquid aluminum. At 750 °C, an initial oxide, γ-Al₂O₃, forms on the surface of the liquid aluminum. Within the γ-Al₂O₃ film, crystallites of α-Al₂O₃ (corundum) then nucleate and grow. This transformation produces a 24% reduction in oxide volume and generates a tensile stress that cause scale failure. Breakaway oxidation kinetics is also observed. Localized failure of the oxide film is accompanied by the exudation of liquid metal that is a consequence of the wetting of alumina by liquid aluminum. An oxidized surface composed of oxide nodules containing metal can result from increased exposure time causing growth of the exudations.

In a pure aluminum system, even after prolonged exposure of air at molten temperatures, oxides formed can be considered to be protective. Many high temperature experimentations have been performed to characterize the oxidation kinetics of pure liquid aluminum. Bachrach ¹², Cabrera ¹³, Mott ¹³ and Cochran ¹⁴ et al. all found that a parabolic relationship seemed to be the closest fit to the overall oxidation process of pure aluminum at high temperatures.

2.6 Aluminum-Magnesium Alloy Oxidation

Alloying elements present can have very significant effects on the oxidation of the metal. In aluminum alloys containing magnesium, oxidation would take a different route. The presence of magnesium in aluminum alloys has been found to accelerate and increase the amount of oxidation in the molten system.

In order to grasp the basis for the effects of magnesium on oxidation of aluminum alloys, some basic properties of magnesium should be noted. First of all, magnesium has a higher affinity for oxygen than aluminum. Oxidation will usually deplete magnesium from the bulk of the metal. Then magnesium will preferentially oxidize to form MgO and spinel. Secondly, magnesium is a metal with a very high vapor pressure. This would usually result in a significant amount of magnesium loss at high temperatures due to vaporization and build-up of gaseous magnesium.

According to a study by Gregg and Jepson ¹⁵, the oxidation of magnesium is different from that of aluminum. A protective film is always formed initially and then a "breakaway" occurs and the oxidation becomes linear. In a molten system, at the breakaway, the film ruptures and the cracks penetrate to the underlying metal. The oxidation rate then becomes proportional to the area of metal exposed without any effects of protective oxidation behavior.

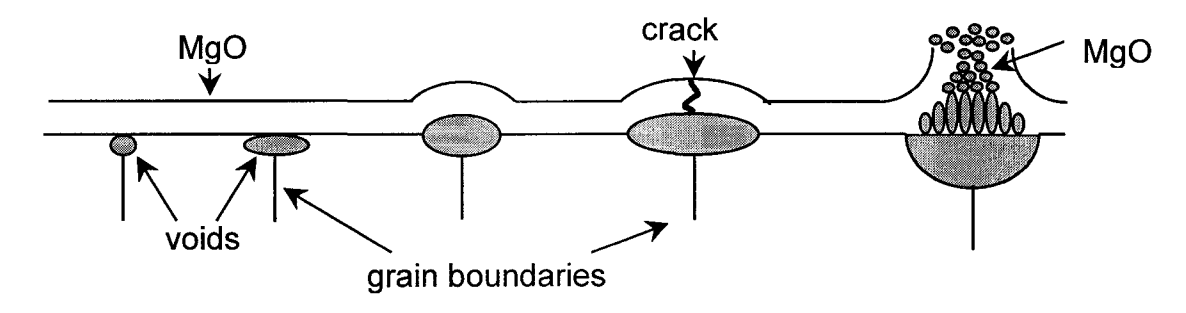


Figure 2.4: Model for breakaway oxidation ¹⁶

In the breakaway oxidation model shown in Figure 2.4, voids are present at the metal/oxide interface. In the presence of Mg, Mg vapor diffuses into these voids and cracks the oxide layer, exposing fresh molten alloy. Further oxidation occurs, resulting a in a "mushroom"-like growth.

De Brouckere et al. ¹⁷ showed that aluminum-magnesium alloy oxidation would result in an oxide film with a duplex structure. The inner film was thin and continuous and consisted of alumina, spinel, or magnesium aluminates, while the thick outer layer was porous and consisted largely of magnesia.

Hine et al. ¹⁸ stated that the oxidation characteristics of aluminum-magnesium alloys would be expected to depend on the relative rates of diffusion of the ions of the two metals, the rate being higher for magnesium than aluminum. During oxidation, the outer layers of oxide become progressively enriched in magnesium oxide because of the preferential diffusion of magnesium ions and vapor to the oxide/air interface. The aluminum alloy immediately adjacent to the oxide becomes denuded of magnesium.

Smeltzer et al. ¹⁹ also drew attention to the importance of the high vapor pressure of magnesium in determining that the oxidation of magnesium became the rate-controlling factor. He also deduced that a thin layer of magnesium aluminates was always present at the inner interface that controlled the diffusion to the porous oxide interface.

Noteworthy studies have been carried out by Impey et al. ²⁰ and Silva et al. ²¹ and Dennis et al. ¹ where their hypotheses all lead to several common observations. A primary oxide layer is formed, and it provides a significant amount of protection during the initial period of oxidation. Then the breaking of the oxide layer associated with the presence of magnesium in the system will promote the continual oxidation of the metal and growth of the oxide layers present. The continuation of the oxide layers, as in the attributed to the continuous feeding of liquid aluminum through the oxide layers, as in the mechanism termed "wicking," due to the wetting of the oxide and the capillary forces.

2.6.1 A356-A357 Alloy Oxidation

Dennis et al. ¹ conducted oxidation experiments above the melting point of A356 aluminum alloy. The commercial 356 and 357 alloys both contained 0.35% Mg and 0.55% Mg respectively; they represent low magnesium content aluminum silicon alloys commonly used in the industry.

It has been observed that oxidation is characterized by a steady growth rate that continually decreases with time. Figure 2.5 depicts an image of the oxide surface

observed. The growth of the oxide layer is controlled by the formation of MgO from magnesium, and where magnesium is depleted, the MgO available will react with aluminum to form spinel. As the magnesium content of these alloys is quite low, it is expected that magnesium becomes less and less readily available to form MgO as the magnesium level becomes depleted. The availability of the MgO to form spinel also decreases with time, thus the exhaustion of magnesium and MgO slows down the oxidation rate and weight gains become negligible.

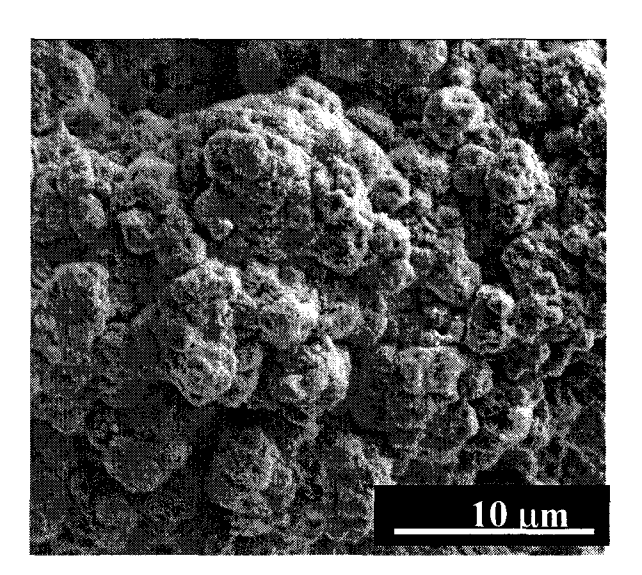


Figure 2.5: High magnification micrograph of the surface oxide on commercial 356 alloy samples. 22

2.6.2 5000 Series Alloy Oxidation

The 5000 series aluminum alloys is a good model alloy to verify the effects of magnesium on the oxidation behavior of aluminum silicon alloys, as the 5000 series alloys contain a high concentration of magnesium (4.5-5.5%). Dennis et al. performed a detailed study into the oxidation of a synthetic 5000 series alloy in the temperature range of 700 to 800 °C ²³. Several interesting theories have been proposed concerning the oxidation behavior of this alloy. The oxidation can be characterized into three distinct stages: a) an initial slow oxidation stage, b) followed by a stage of rapid oxidation and c) subsequent continuation or discontinuation of rapid oxidation. Temperature also has an important effect on the oxidation behavior, as increased temperature accelerates the oxidation rate because an increase in temperature usually results in faster kinetics.

- Initial oxidation, or the induction period, is defined as the time required to initiate breakaway oxidation. This stage can be best described with a parabolic relationship controlled by diffusion kinetics. The reaction taking place is that of magnesium oxidizing to form MgO. Stresses caused by the volume decrease associated with the oxidation of magnesium to MgO, or the nucleation of large spinel crystals, can then cause the oxide layer to crack. This induction period is affected significantly by the temperature; since an increase in temperature would decrease the induction period.
- Rapid oxidation is defined as the period after the induction period in which the growth rate of the oxide layer is increased dramatically. The oxidation in this stage is so fast that sometimes all of the magnesium can be depleted from the

sample within the experimental period (45 hours). Breakaway oxidation is the main mechanism responsible for this accelerated oxidation behavior. Initial breaking of the oxide is caused by the reaction of the MgO oxide layer with the walls of the alumina container to form spinel crystals that are less cohesive than MgO. The build-up of magnesium gas and molten metal is released through the cracks and results in the accelerated oxidation. This rapid oxidation stage will continue until all of the available magnesium has been oxidized.

2.6.3 Effects of Strontium

Strontium is a common addition element used in aluminum-silicon alloys as a eutectic modifier ²⁴. The Sr-modified structure has a less acicular shape and the resulting mechanical properties are improved, as shown in Figure 2.6. Some disadvantages also exist for the addition of Sr, such as an increase in the presence of micro-porosity.

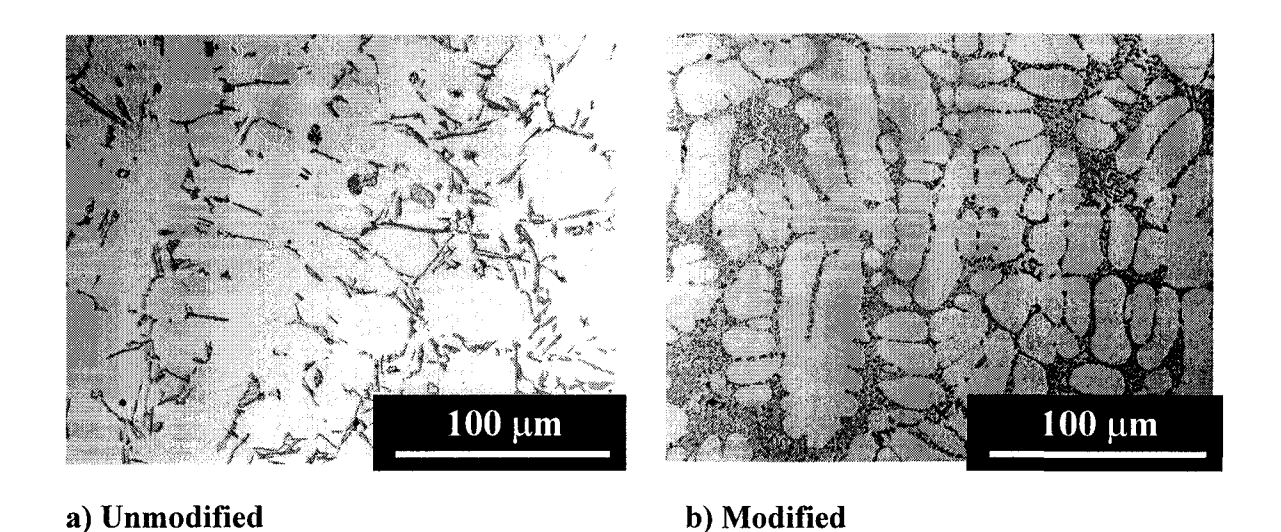


Figure 2.6: Micrographs showing the modification of the silicon phase in a commercial 356 alloy due to the presence of 250 ppm Sr. ²⁵

In a previous study at McGill by Emadi et al. ²⁶, it has been shown that for Al - 7% Si alloy, the addition of strontium resulted in differing oxidation kinetics, such as a more rapid initial oxidation (first 7 hours), followed by the formation of a long term protective oxide layer. The 356 alloy containing strontium displayed completely different oxidation characteristics from the 356 alloy without strontium. The weight gains observed were in the order of about ten times less with the addition of strontium.

It has been proposed that a strontium-containing phase forms underneath the initial MgO layer. The oxide containing strontium is protective and very thin. Thus, the addition of strontium effectively reduced the oxidation by establishing a more stable or coherent top oxide.

Effects of strontium on the oxidation of Al-Si-Mg alloys in a non-molten state have always been commonly noted with researchers or foundrymen who have dealt with such alloys in high temperature heat treatment. The presence of an "orange peel" oxide has been often associated with strontium-modified alloys compared with non-modified alloys. This indicates that even below molten temperatures, in the solid-state, strontium does have a noticeable effect on surface oxidation and does probably play a role in the formation of an oxide layer with a different chemical composition, hence the different color and appearance. Figure 2.7 depicts examples of this surface oxide difference in high temperature (540 °C) solution heat-treated and quenched samples.

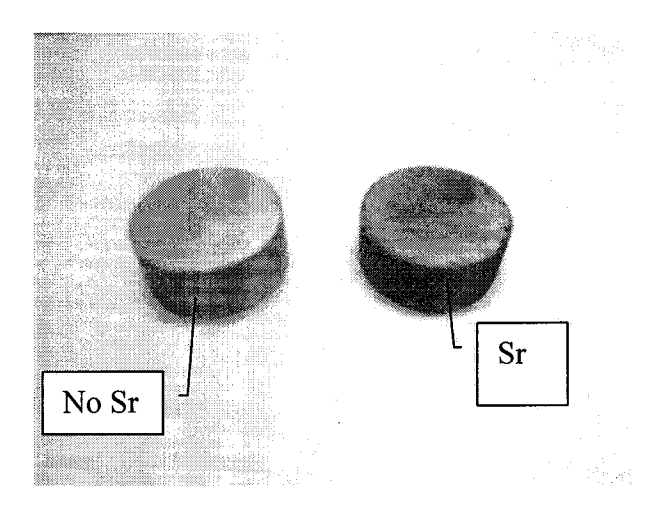
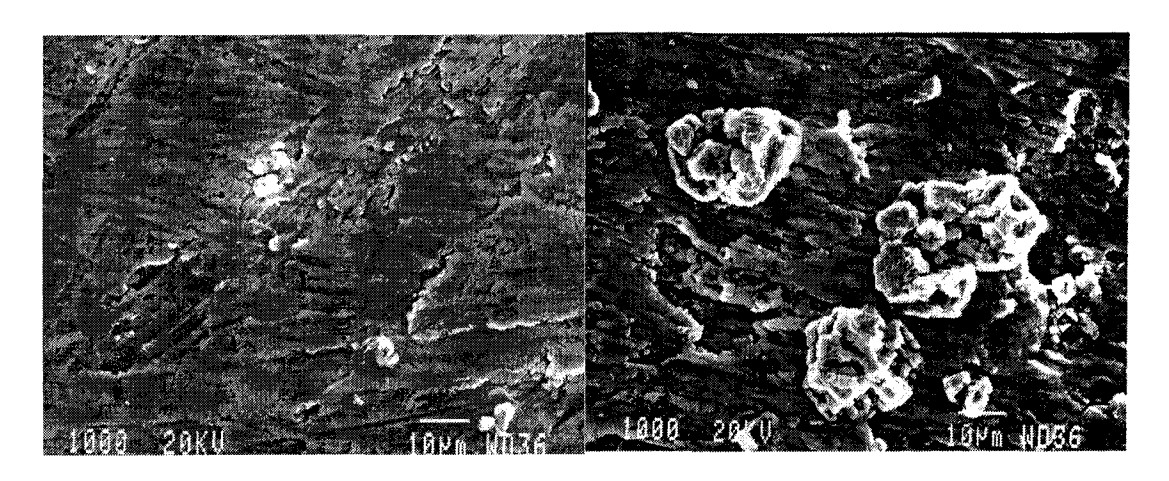


Figure 2.7: Heat-treated and quenched aluminum magnesium alloy samples.

Dennis et al. ²⁷ provided several interesting hypotheses for the effects of strontium on aluminum magnesium alloy in the molten state. Experiments with 250 ppm. strontium addition to A356 alloy were the basis for the findings. The strontium can affect the oxidation in that it can oxidize to form an oxide of its own, such as SrO or SrO₂; and it can also combine with other elements in the melt in order to form more complex oxides such as SrAl₂O₄. The following are the theories proposed by Dennis et al.:

• An initial oxide of the Al-Si-Sr-O species is formed very quickly on the top of the melt. This oxide is extremely protective, but further formation of this oxide is not feasible because of the limited amount of strontium available in the melt. Additional oxidation occurs only through the slow diffusion of metallic ions through this layer and they then react with the oxygen in the air to form MgO. If this hypothesis is correct, the transition from one type of oxidation behavior to another should be observed in the weight gain curves.

- MgO is formed on the surface, but it is stabilized by a solid solution of strontium within the crystal structure. A solid solution of Sr within the MgO layer is possible since MgO and SrO share the same electron valence number, and they both form a similar rock salt cell crystal structure. A difficulty exists for this hypothesis since the P-B ratio of strontium (0.69), compared with that of magnesium (0.83), will render the resultant oxide layer less protective as the overall P-B ratio deviates more from unity.
- An initial layer of MgO is formed at room temperature, but as the temperature rises to the molten range, strontium oxidizes preferentially with aluminum and silicon to form SrAl₄O₇ below the layer of MgO. The combination of these layers is protective and further oxidation occurs only when there are small-localized eruptions caused by build-up of magnesium vapor below the oxide. The gas build-up below the oxide occurs because of the high vapor pressure of magnesium and the fact that there is little growth of the MgO oxide layer and thus minimal consumption of magnesium.



A) Al-7%Si showing oxide nodules

B) Al-7%Si with 250ppm Sr

Figure 2.8: SEM pictures ²⁶ of top oxide formed at 740°C for 24 hours.

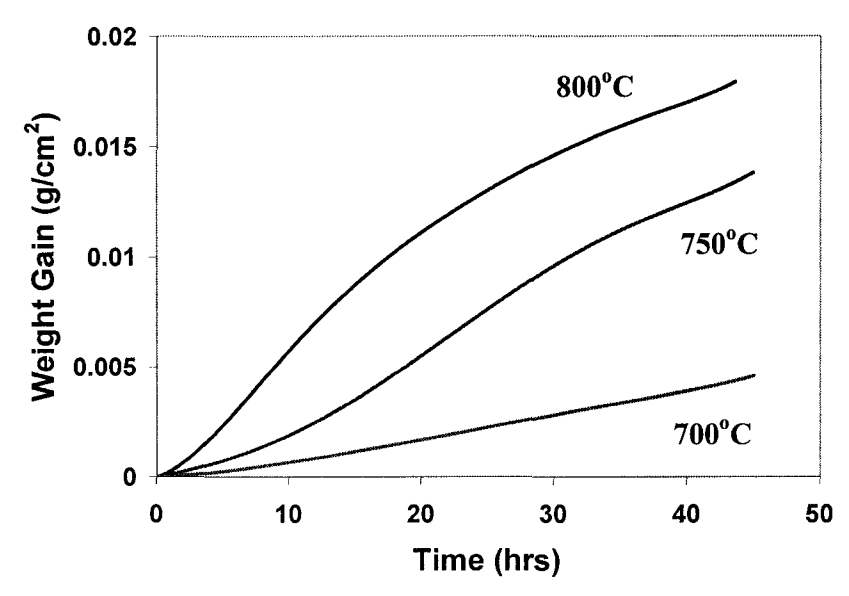


Figure 2.9: Weight gain curves of the commercial 356 alloy without strontium at three different temperatures. 28

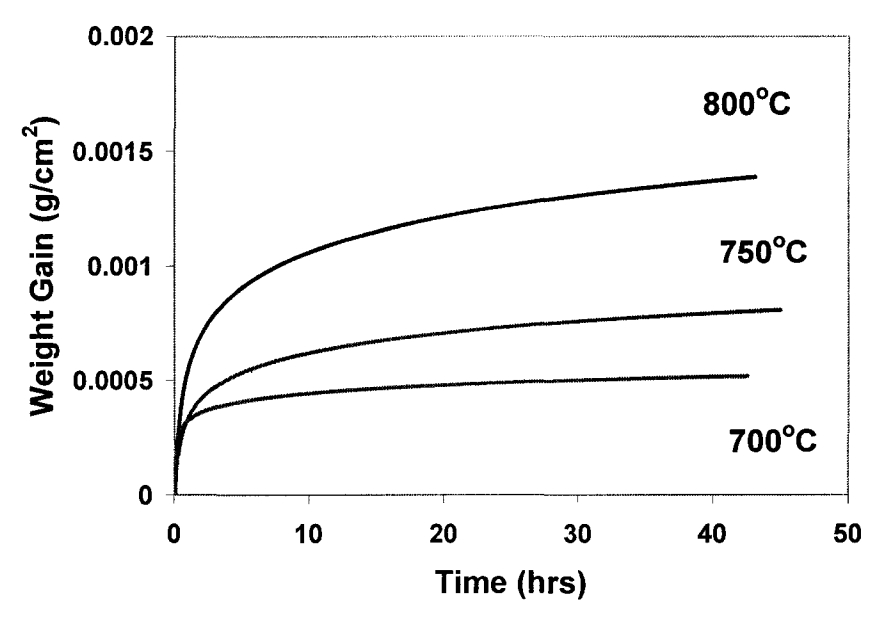


Figure 2.10: Weight gain curves for the commercial 356 alloy containing 250 ppm Sr at three different temperatures.²⁹

In Figure 2.8, an example of a coherent oxide layer and an oxide nodule are shown. In Figures 2.9 and 2.10, one can notice the differing kinetics; the curves for the alloy containing Sr indicate parabolic relationships that suggest a decelerated or protective oxidation. There is also a significant decrease in magnitudes of weight gain in the Sr-containing alloys data; for example, at 800 °C: 0.018 g/cm² compared to 0.0013 g/cm².

2.7 Summary

The oxidation of aluminum silicon alloys containing magnesium in the liquid state is significant in the processing of the alloys. The literature reviewed shows a basic scope of the oxidation process of aluminum-magnesium alloys and the effects of strontium in the liquid melt processing state.

The oxidation behavior of aluminum magnesium alloys is notably different but also comparable to that of pure aluminum because of the intense effects that the presence of magnesium can have in the alloy system. Properties of magnesium such as its high vapor pressure and higher affinity for oxygen to promote accelerated oxidation are key to the understanding of the overall oxidation behavior. The combination of the basic properties of both aluminum and magnesium can often explain some of the phenomena observed.

The effects of strontium on the oxidation of the aluminum alloys in the liquid state have not been studied in depth to date, and information is very scarce. Interesting results have been shown for strontium addition effects, and further study can become a topic of interest to the industry if the observed effects of decreased oxidation can be confirmed and understood.

3. EXPERIMENTAL PROCEDURE

3.1 Raw Materials

Three different alloys were chosen and used for the oxidation experiments in this research project. All the alloys were in the form of commercial ingots, A356, A357, and 5182 (to represent high Mg 5000 series). For strontium modification, a 90% aluminum – 10% strontium master alloy was used. The alloy compositions, as verified, are presented in the results section. For the fabrication of the alumina crucibles, A17SG alumina powder was used.

3.2 Melting and Casting

Initially, the commercial ingots had to be pre-cut into smaller useful pieces using a band saw. SiC crucibles were used for melting and casting. Melting small amounts of the alloy to be used and then casting them as scrap was the process used to clean the crucibles. A gas-fired furnace was used and casting was performed in the range of 730-750 °C. The temperatures were monitored using chromel-alumel K-type thermocouples and a hand-held display. For strontium addition, small pieces of the master alloy were cut

and then wrapped in aluminum foil as the addition package. The addition package was then submerged with a graphite plunger into the melt, and held for 20 minutes. Stirring of the melt was carried out with the graphite plunger. The melt was then stirred, skimmed, and finally cast into the graphite mold setup shown in Figures 3.1, 3.2 and 3.3.

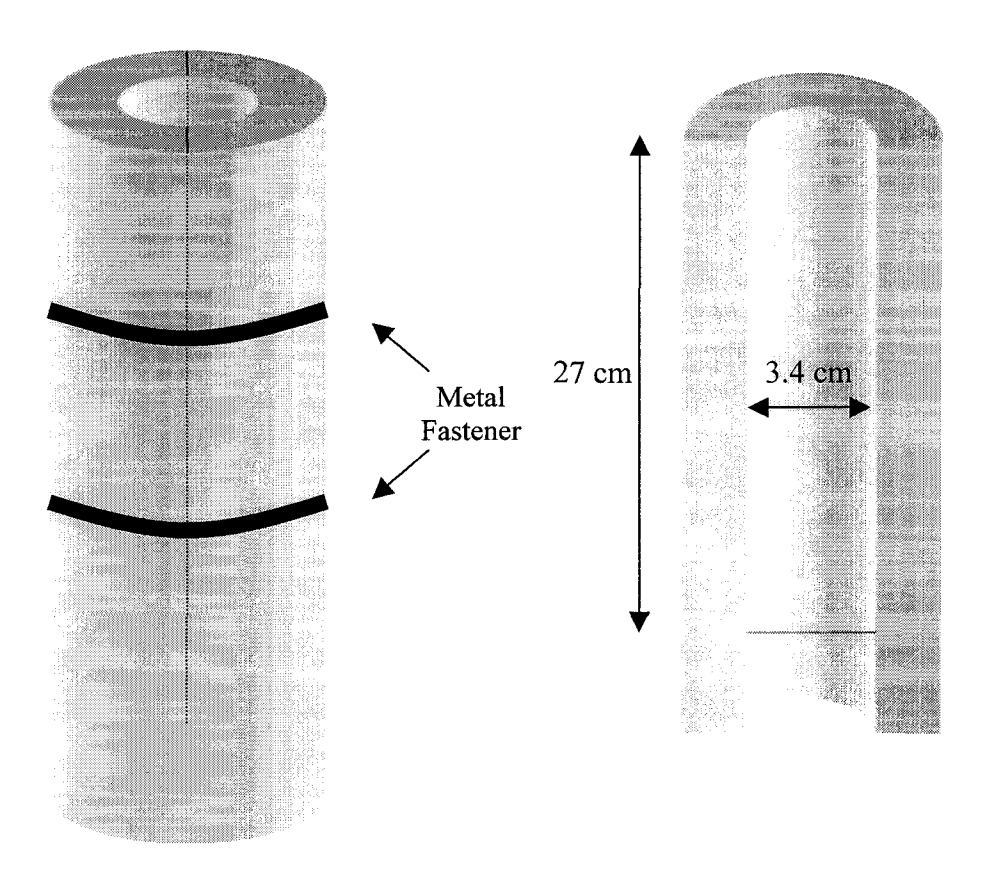


Figure 3.1:Graphite mold used for casting of the aluminum alloys ³⁰.

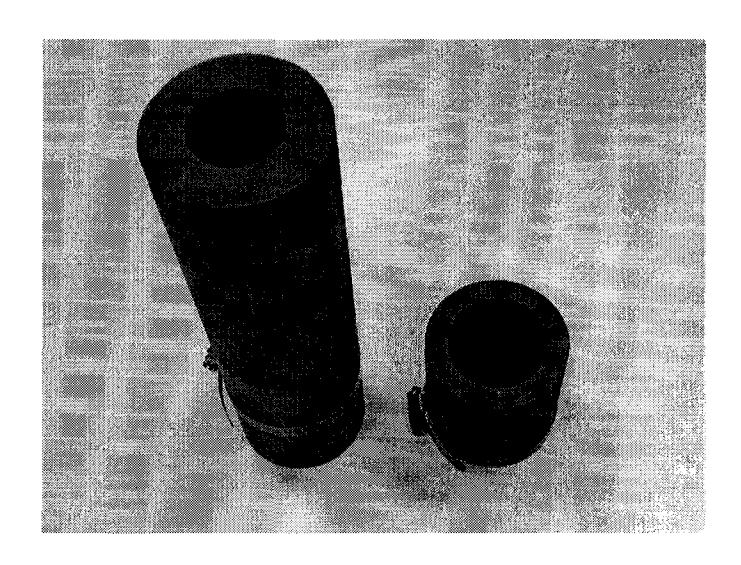


Figure 3.2: Actual picture of the graphite mold and the riser

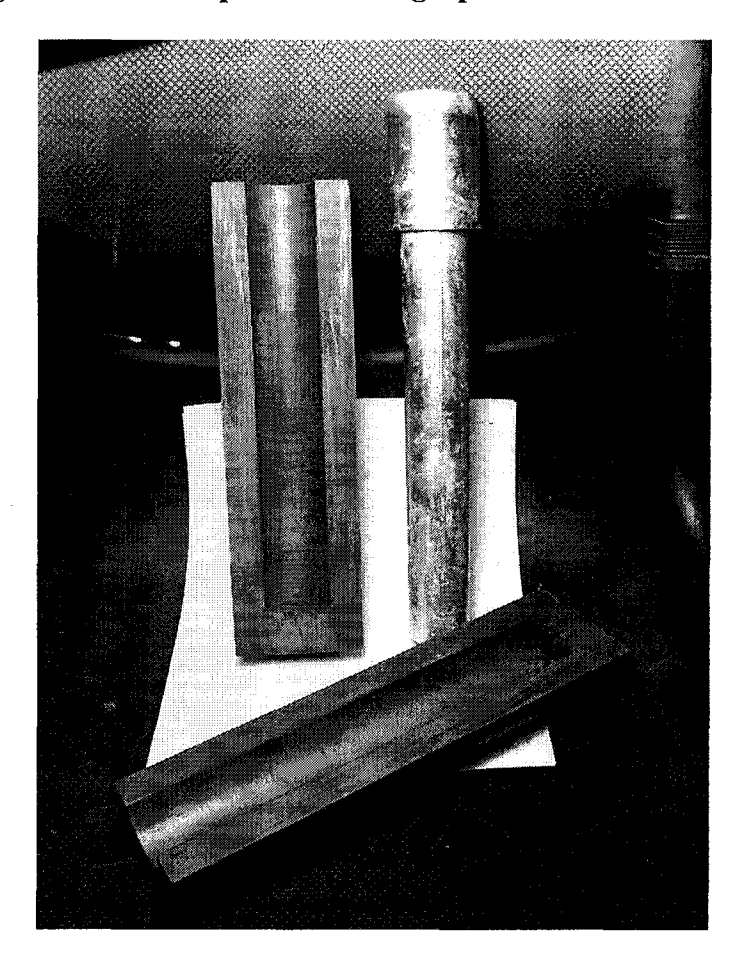


Figure 3.3: The graphite mold and a piece of the cast aluminum alloy.

3.3 Sample Preparation and Fabrication

From the cast cylinders, the aluminum samples were machined to approximate dimensions of 1.4cm in height and 3.2cm in diameter, and with average weights of 30 grams. This size was chosen with respect to the crucible size used and the TGA equipment. Before subjecting the samples to the oxidation experiments, all faces of the samples were ground to a 600-grit finish using abrasive SiC grinding paper. Figure 3.4 shows an example of a machined sample.

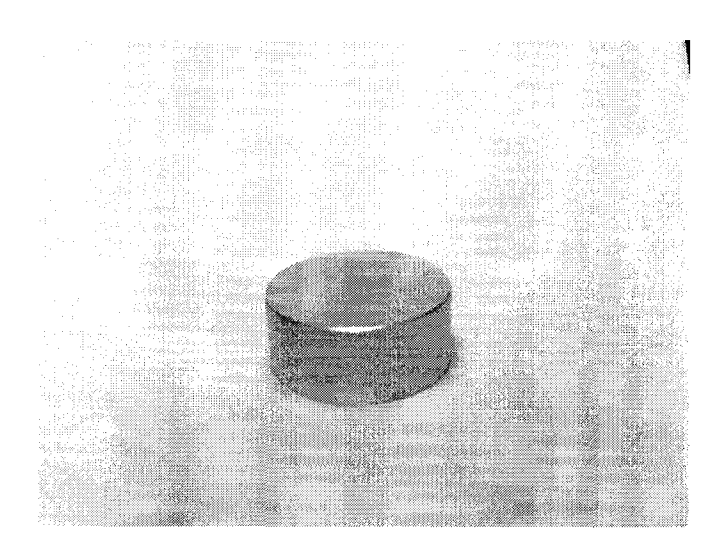


Figure 3.4: A machined and polished sample.

3.4 Alumina Crucible Fabrication

As the oxidation experiments take place with the aluminum samples in alumina crucibles, pure alumina crucibles were fabricated in the ceramic lab using a slip casting procedure. The molds used to slip cast the alumina crucibles were made with Plaster of Paris. With a weight ratio of 70:30, plaster and water were mixed respectively. In order to shape the mold into the useful shape, a glass beaker with outer diameter of 4.1cm was used as the crucible shape, and a larger plastic container of approximately 10 cm in diameter was used as the outer cup. With the mixture shaped and solidified, the mold was air dried for at least 48 hours and then sectioned in half so that upon opening this allowed for the removal of the slip cast crucibles.

The alumina slip was prepared using a mixture of the A17SG alumina powder, water and the Darvan 821A deflocculant; with weight ratios of 70:30:0.3 respectively. This slip mixture was then ball milled for 1 hour.

The procedure for slip casting was as presented in Figure 3.5. The prepared slip was poured into the plaster mold and left there for approximately 4.5 minutes. The remaining slip was then poured out, and the partially dried cast shape (crucible) was left to dry for 1 hour before being carefully extracted from the plaster mold. This crucible was air-dried for at least one day prior to firing.

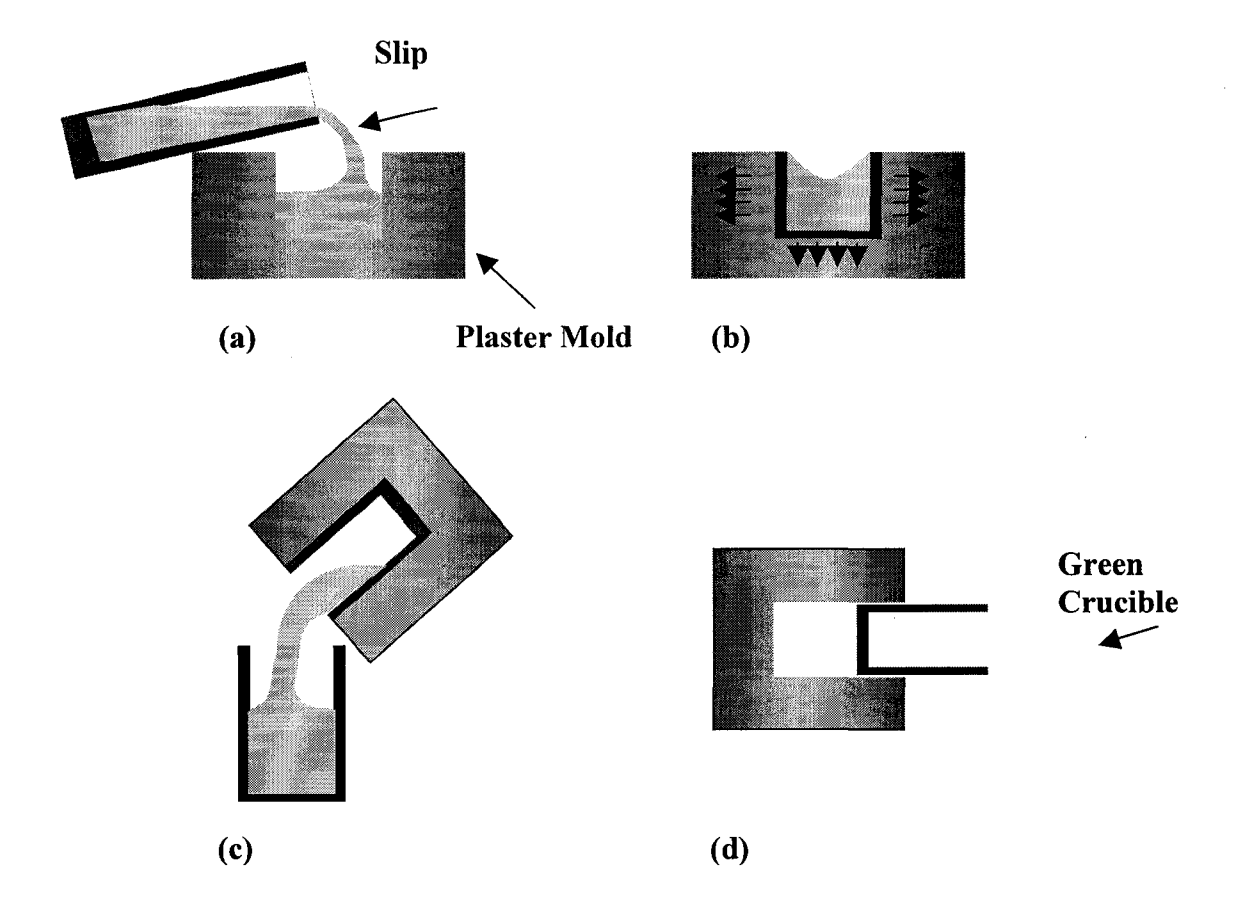


Figure 3.5: Schematic illustration ³⁰ of the drain-casting process, (a) fill mold with slip, (b) liquid extracted through mold leaving compact layer along walls, (c) excess slip drained, and (d) casting removed after partial drying.

Sintering was performed in a two-step process to allow for ease of machining and modifications. The first sintering step was performed for 1.5 hours at 1200 0 C to achieve partial sintering. Anomalies were now removed and holes were drilled into the sides of the crucible to allow it to be hung from a wire. Second sintering was performed for 2 hours at 1400 0 C to improve the properties and strength. The final diameter of the crucibles was approximately 3.3-3.4 cm. A picture of the crucible along with a sample is shown in Figure 3.6.

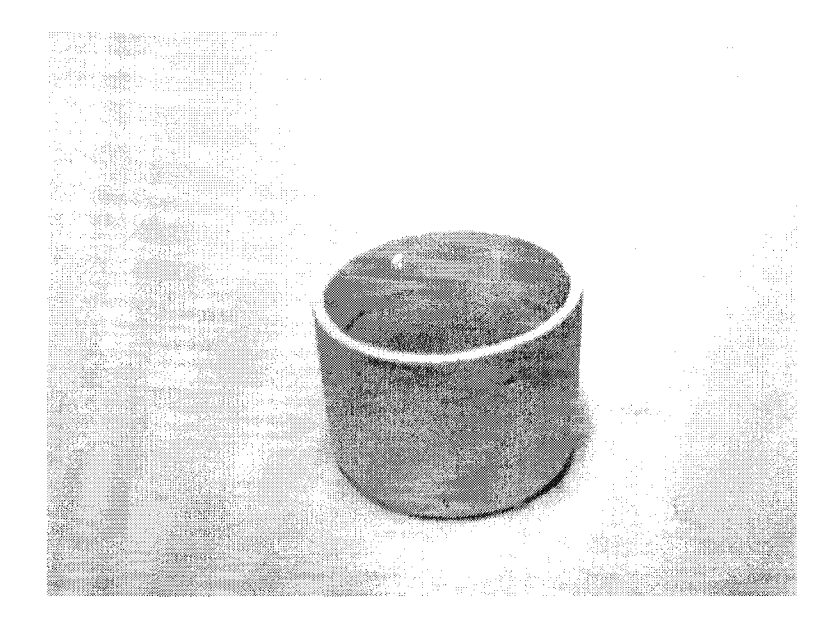


Figure 3.6: Sample in a crucible ready for oxidation experiment.

3.5 Oxidation Experiments – TGA Tests

The laboratory oxidation experiments were conducted in a special setup consisting of a thermo-gravimetric balance connected to a vertical, dense mullite tube furnace, as shown in Figures 3.7 and 3.8. The furnace was equipped with a B-type thermocouple, with an accuracy of $\pm 1\%$, connected to a Gultan West 2050 temperature controller. Six SiC GLOBAR heating elements, arranged in a circular manner, were used as the heating source. The furnace was calibrated with another B-type thermocouple to establish a hot zone, where the sample would be located.

The machined aluminum samples were placed inside the fabricated alumina crucible and suspended from the nickel-chromium wire connected to the thermo-

gravimetric balance inside the tube furnace. A visual examination from the bottom of the furnace was performed to ensure that the crucible was suspended correctly and centered with respect to the mullite tube. A simple routine of vacuum and evacuation of the system using argon was performed each time before a test was started to ensure that the system was free from air and contaminants. First the furnace was evacuated to a vacuum of approximately 200 mTorr, and then it was refilled with argon. This was repeated 3 to 4 times. A continual flow of argon was introduced, as controlled by a flowmeter; this was flowed from the top of the TGA frame and out through the vacuum tubing at the bottom of the system. The furnace was then set to heat up to the test temperature, with a 2 hours ramp time. When the furnace had reached the test temperature, controlled air flow from a cylinder was then introduced into the furnace and sample weight gain data acquisitions commenced.

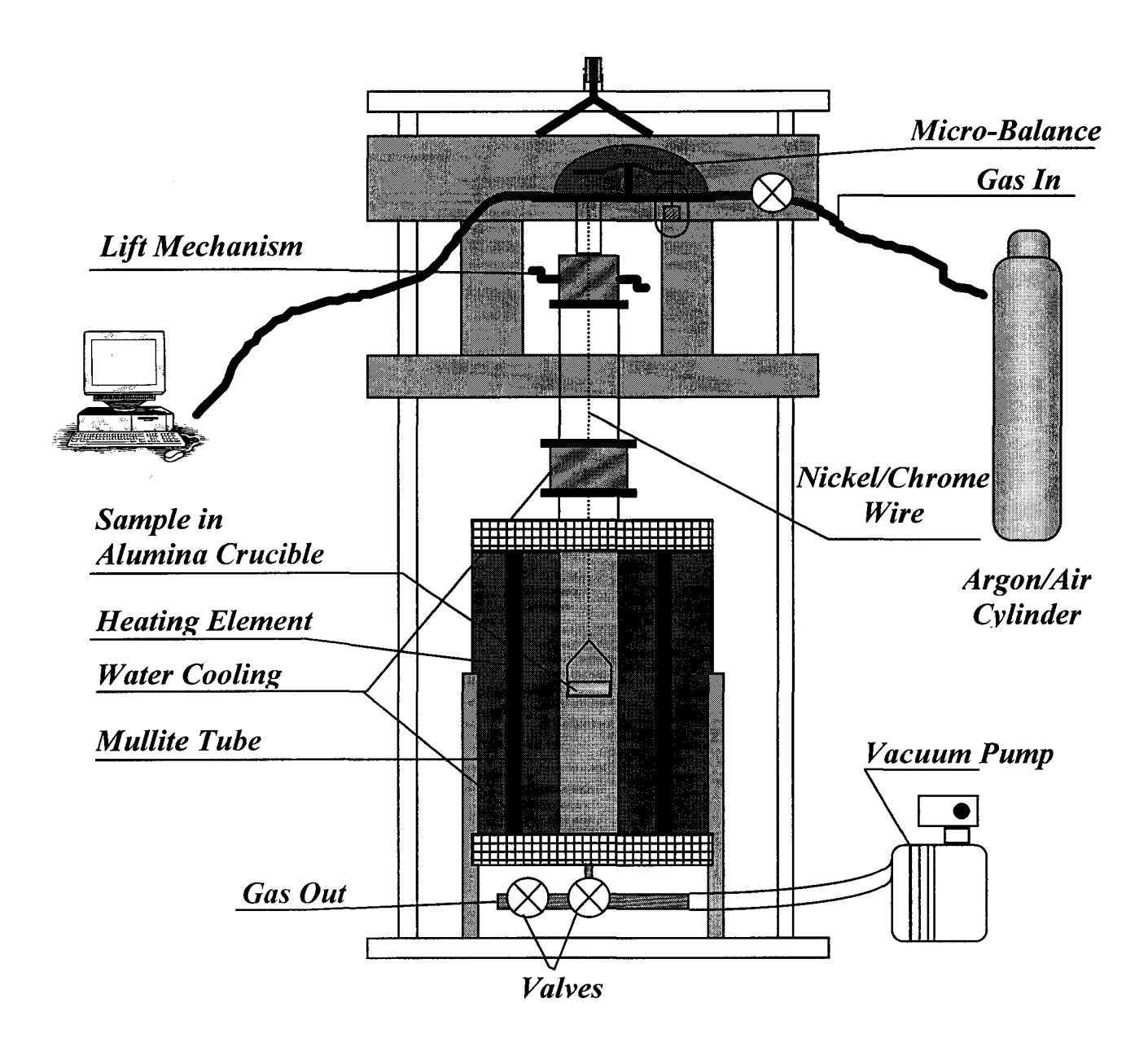


Figure 3.7: Diagram ³⁰ of TGA set-up to measure the oxidation weight gains.

The weight change data was monitored with respect to time for a period of 30 hours (356 & 357) and 60 hours (5000). Initially, 30 hours was the test duration for all the alloys, but over the course of theresearch, it was decided that extending the 5000 series test time to 60 hours would prove to be more useful. Three test temperatures were

chosen for this study, 700, 750 and 800 0 C. The Thermo-Gravimetric Analyzer (TGA) data acquisition was performed using the package and software called CAHN D-100. The data files generated were then analyzed using the Microsoft Excel spreadsheet program.

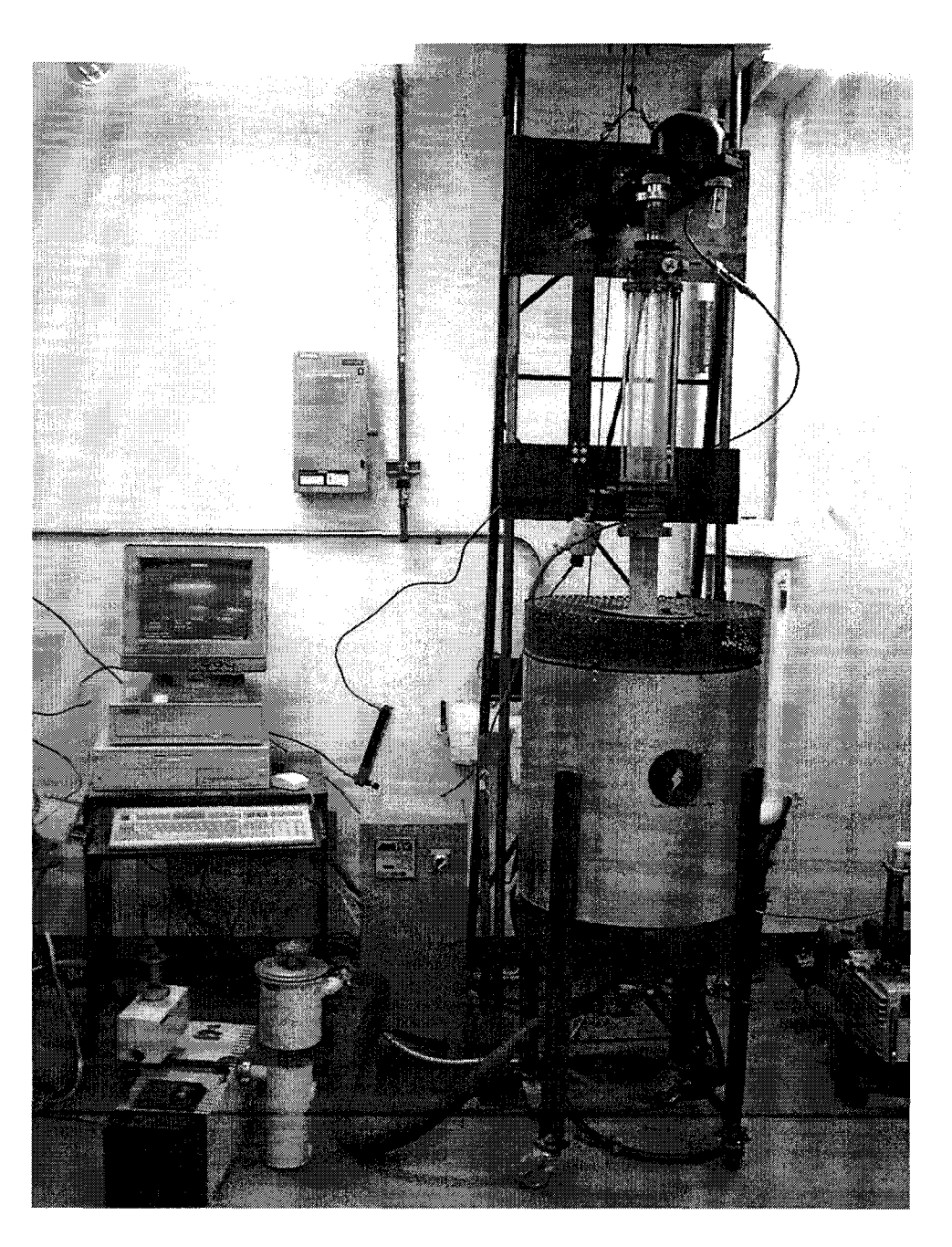


Figure 3.8: Picture of TGA set-up in the lab.

In order to produce data that would represent only the oxidation of the alloy sample, trial experiments were performed without an alloy sample in the crucible. These were done in order to quantify oxidation occurring from outside sources, mainly from the wires used to suspend the crucible. It was found that wire weight gains were negligible when the wires were re-used after being oxidized beforehand with these trial experiments. For all the oxidation experiments performed in this study, the same two suspending wires were used and re-used.

3.6 Sample Analysis

3.6.1 Emission Spectrometry

Chemical analysis of the alloys was quantified using an emission spectrometer, Spectrovac 1000, with an MC20 data processing system. Analyses were performed on cast spectro samples and the actual machined oxidation samples. All alloy compositions and strontium modification were verified with this method.

3.6.2 Optical Microscopy

Optical microscopy was only performed to verify strontium modification in alloy samples and used as a pre-check before the preparation of oxidized samples for further analysis such as electron microscopy and XRD. Standard cutting, grinding and polishing procedures for the aluminum alloys were followed. Grinding stage: surfaces were ground down to an 800 Grit finish using SiC grinding media; polishing stage: 1 micron diamond paste was initially used, followed by 0.5 micron colloidal silica.

3.6.3 Scanning Electron Microscopy (SEM)

Oxide surface morphologies and qualitative chemical analysis of the surface were examined using the JEOL JSM 840A scanning electron microscope. Energy dispersive spectroscopy was used for the chemical analyses. Samples that were prone to problems of charging with the electron microscope were either coated, or that one section of the sample piece was ground off so that the underlying metallic layer was exposed and could be electrically grounded to the sample holder.

3.6.4 X-Ray Diffraction (XRD)

The oxide layers formed throughout the oxidation experiments were examined using X-Ray diffraction. The diffractometer, Philips APD 1700, utilized a scan rate of 0.1 ⁰/sec with filtered Cu-Kα radiation at an accelerating voltage of 40 kV and a beam current of 20mA.

Two methods were used to examine the samples. With relatively smooth surfaces and thin oxide layers, it was possible to analyze the surface directly. On samples that had very rough surfaces, or highly oxidized samples, powder analyses were performed by preparing the samples using the following manner. The samples were submerged into a 5% HF solution for 24 hours so that the majority of the metals would have been leached

out. The remaining bulk of the oxides were then put into a shatterbox for approximately 10 seconds. After this separation of oxides from the metal, the oxide powder was screened for acceptable sizes, sub-200 mesh, and tested in the diffractometer.

Since the oxides are not highly crystalline, and as-oxidized samples were not smooth, X-Ray diffraction peaks obtained had high background and the peaks were shifted.

4. RESULTS

In this chapter, results are presented in different sections corresponding to each alloy investigated. More in-depth analysis and explanation will be presented in the discussion chapter, where more comprehensive results will also be presented. Results presented in this section consist mainly of averaged weight gain curves from the oxidation experiments, images from SEM microscopy of various oxidized specimens, and XRD results and phase identification. Results for the 5000 series alloy refer to samples oxidized over a period of 60 hours; while results for the A356 and A357 alloys refer to samples oxidized over a period of 30 hours. The weight gain is in terms of mass/unit area (g/cm²), which represents the weight gain per oxidizing surface area. An averaged weight gain curve would represent and best fitted from the combined and averaged data for three oxidation experiments for each set of test parameters.

4.1 Alloy Compositions

As outlined in the experimental procedure, emission spectrometry was performed on samples in order to verify the chemistry of the alloys used for the oxidation experiments. The levels of strontium were aimed at 250 ppm for all the strontium containing alloys. The results are shown in Table 4.1.

Table 4.1: Average composition (in weight %) of the alloys used.

% Composition	Si	Mg	Cu	Fe	Sr
A356	6.8	0.35	0.028	0.12	<0.001
A357	6.7	0.52	0.030	0.13	<0.001
5182	<0.2	4.50	0.035	0.16	<0.001
With Sr					
A356 /w Sr	6.9	0.34	0.030	0.13	0.024-0.026
A357 /w Sr	6.7	0.51	0.031	0.13	0.024-0.026
5182 /w Sr	<0.2	4.40	0.034	0.16	0.024-0.026

4.2 5182 Alloy

The oxidation experiments for this high Mg-containing alloy showed significant weight gain and demonstrated the presence of a breakaway oxidation mechanism. The weight gain curves at the three temperatures are depicted in Figure 4.1-4.3.

39

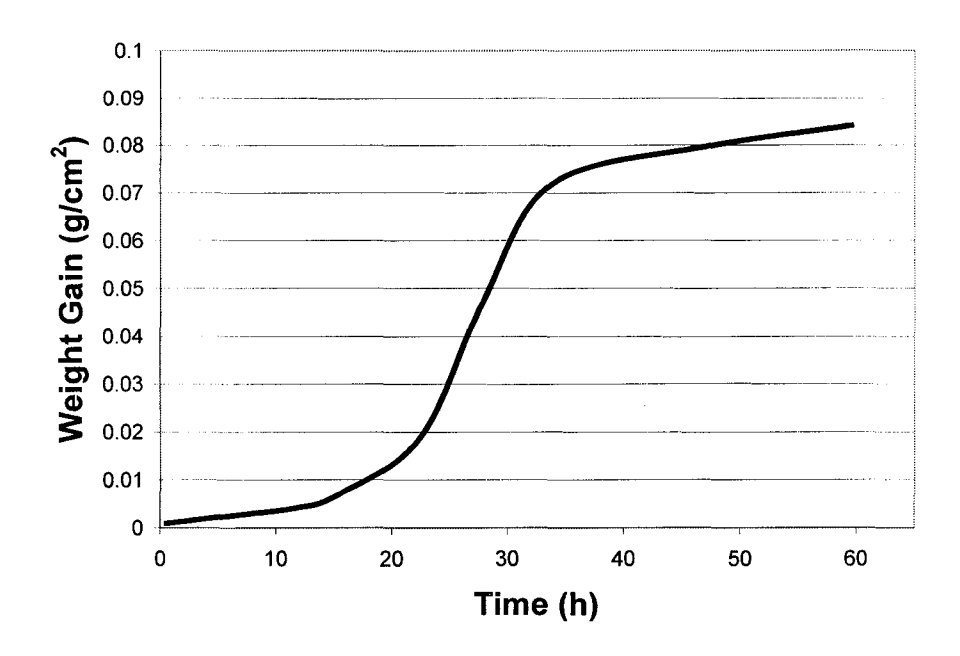


Figure 4.1: Averaged weight gain curve for 5182 alloy at 700°C.

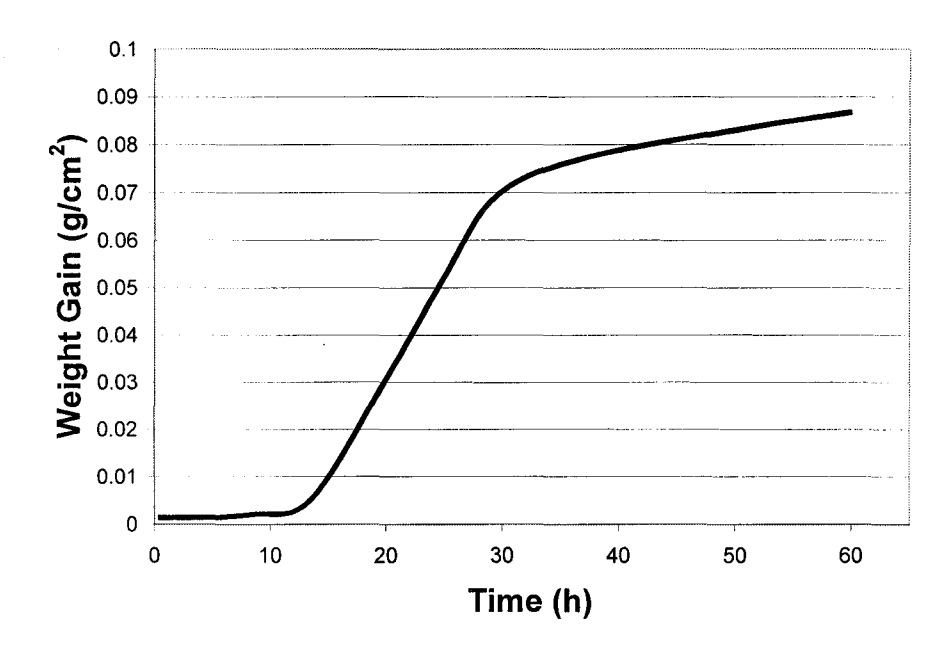


Figure 4.2: Averaged weight gain curve for 5182 alloy at 750°C.

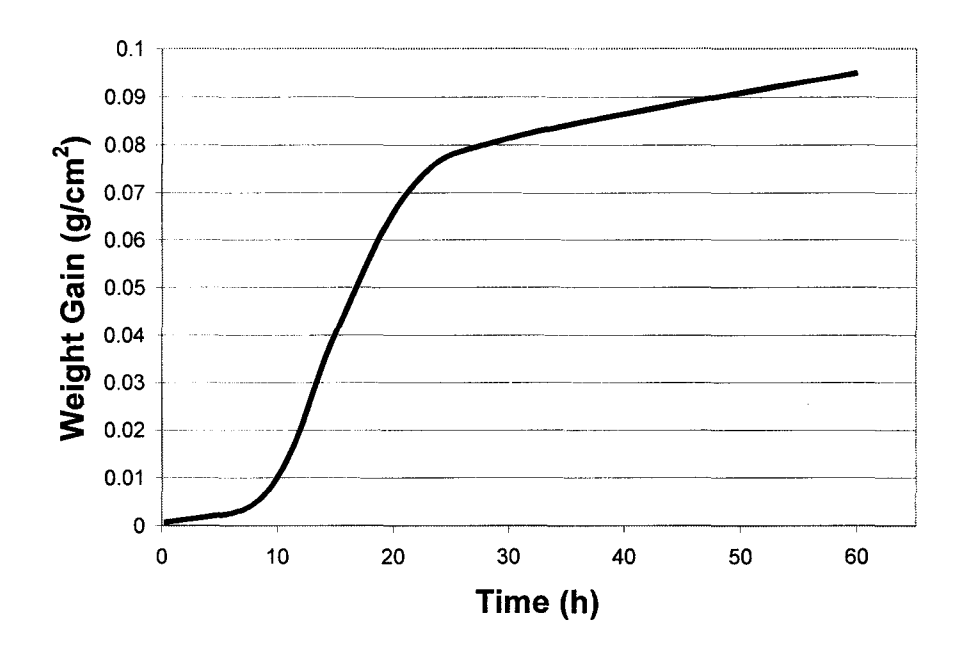


Figure 4.3: Averaged weight gain curve for 5182 alloy at 800°C.

The oxide surfaces formed were very rough in nature, and the colors of the surfaces could be described as a combination of gray, dark gray and even blackish. The oxide layer and the associated formation after the experiment could be best described as "bloated" and crumpled, with the presence of many folds, spikes, peaks and eruptions. Sample surfaces were mostly irregular and abnormal. The final shapes of the samples were also very irregular and inconsistent. The following figures show examples of SEM images of the oxide surface at selected magnifications.

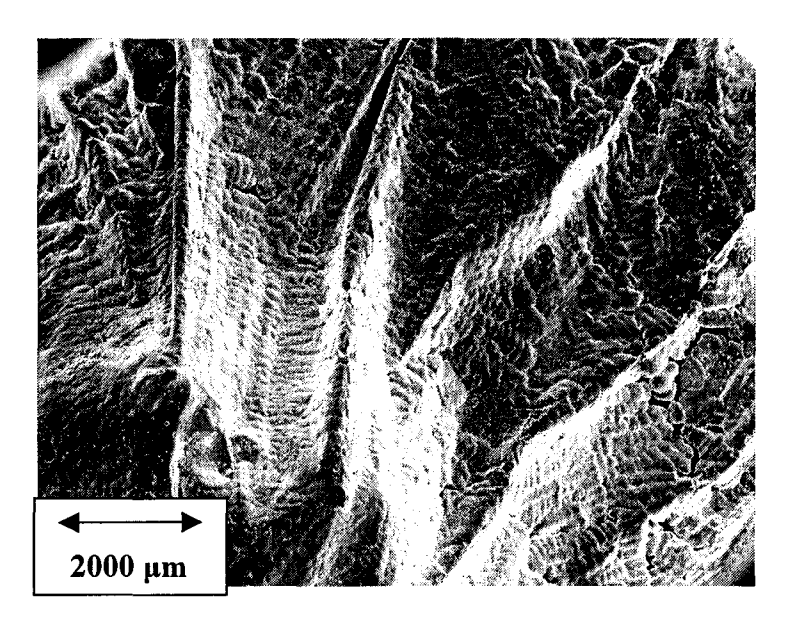


Figure 4.4: Low magnification image of the top surface of 5182 alloy oxidized at 750°C.

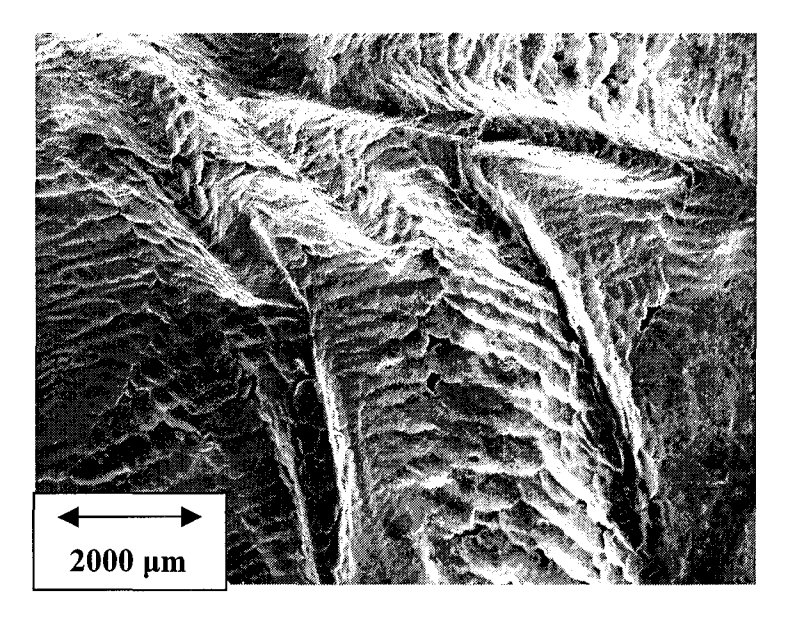


Figure 4.5: Low magnification image of the top surface of 5182 alloy oxidized at 800°C.

In Figures 4.4 and 4.5, one can clearly see the presence of violent oxidation behavior and eruptions by the multi-faceted and fold-like morphology and topography. Figure 4.6 provides a slightly higher magnification image of the folding behavior.

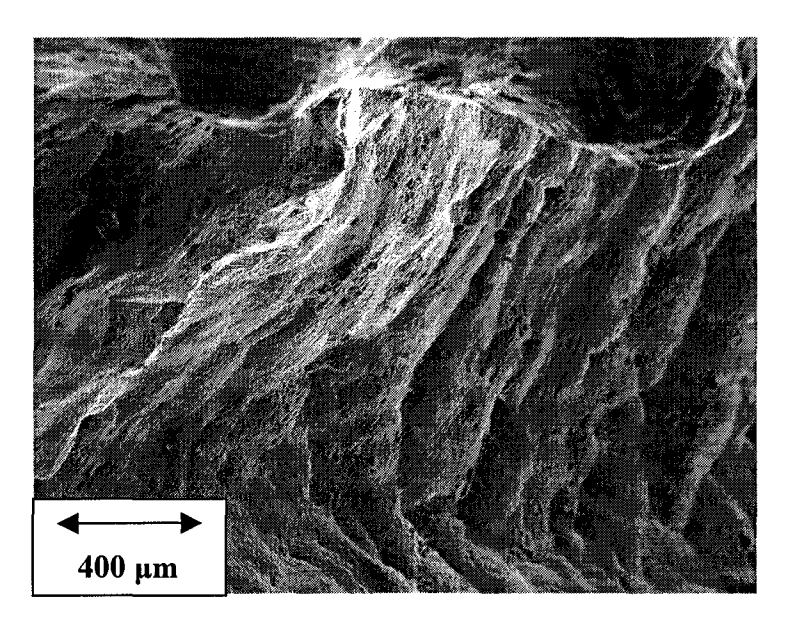


Figure 4.6: Intermediate magnification image of the top surface of 5182 alloy oxidized at 800°C.

Due to the abnormal oxidized surfaces of all 5182 samples at the different temperatures, it became very difficult to compare them. Figures 4.7-4.9 are slightly higher magnification sample images of the surfaces oxidized at the three different experimental temperatures.

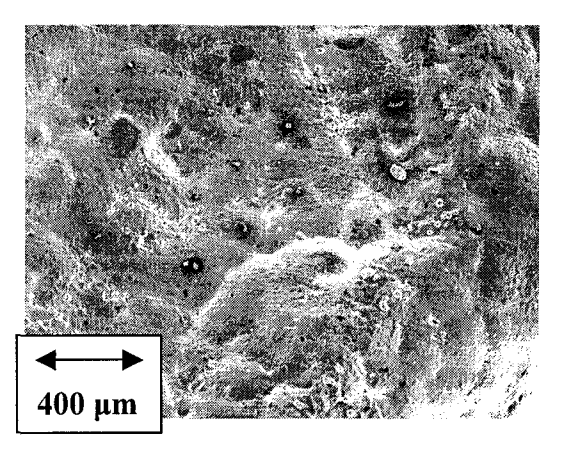


Figure 4.7: Intermediate magnification image of top surface of 5182 alloy oxidized at 700°C.

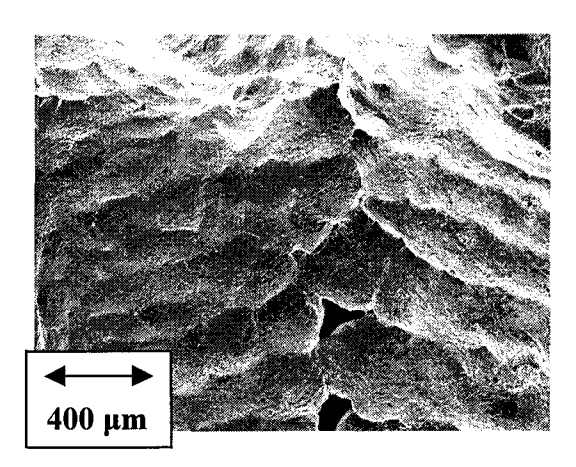


Figure 4.8: Intermediate magnification image of top surface of 5182 alloy oxidized at 750°C.

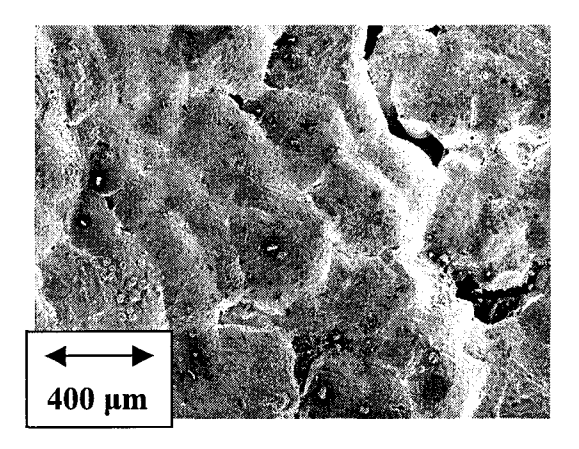


Figure 4.9: Intermediate magnification image of top surface of 5182 alloy oxidized at 800°C.

Examination of the top oxide through EDS confirmed the presence of aluminum, magnesium and oxygen.

Since the nature and shapes of the as-oxidized samples were extremely rough and irregular, X-ray diffraction was only performed on powder samples that were prepared by leaching the as-oxidized samples and pulverizing them. X-ray diffraction results showed only the presence of spinel-MgAl₂O₄. Figure 4.10 gives a typical example of a XRD pattern generated. It is of note, that due to the nature and small quantity of the sample, a significant background noise was present.

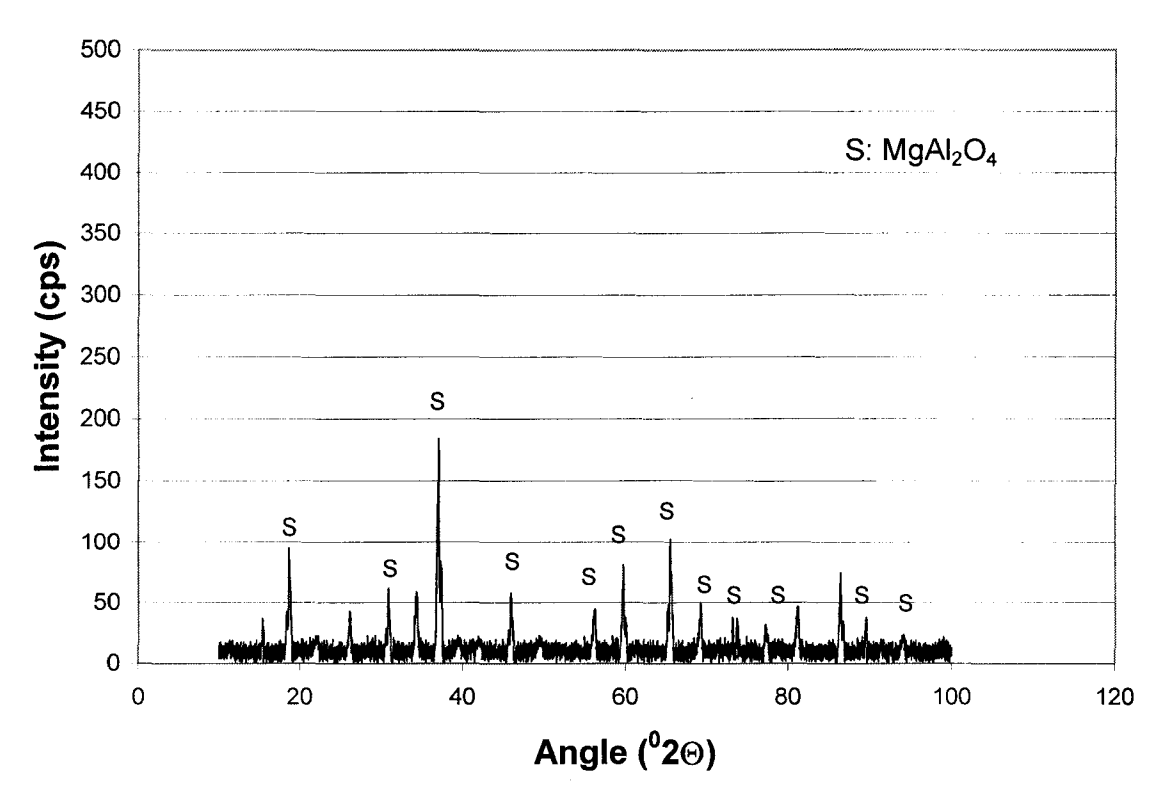


Figure 4.10: XRD pattern for the 5182 alloy in as-oxidized powder form.

4.3 5182 Alloy Containing Sr

The oxidation experiments for this high Mg-containing alloy with strontium showed significant weight gain and demonstrated the presence of a breakaway oxidation mechanism. The weight gain curves at the three temperatures are depicted in Figures 4.11-4.13.

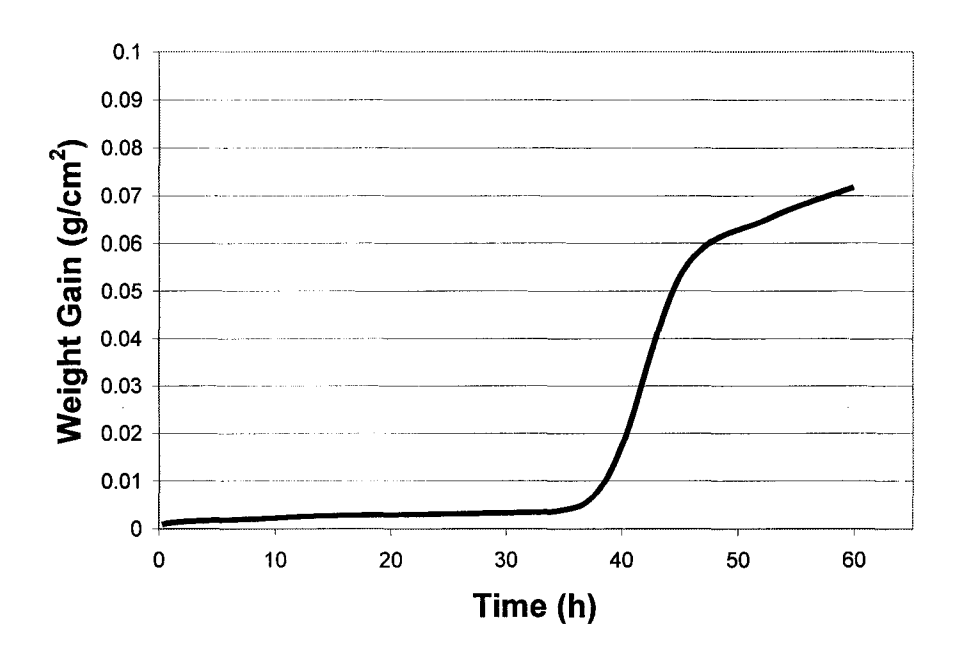


Figure 4.11: Averaged weight gain curve for 5182 alloy containing Sr at 700°C.

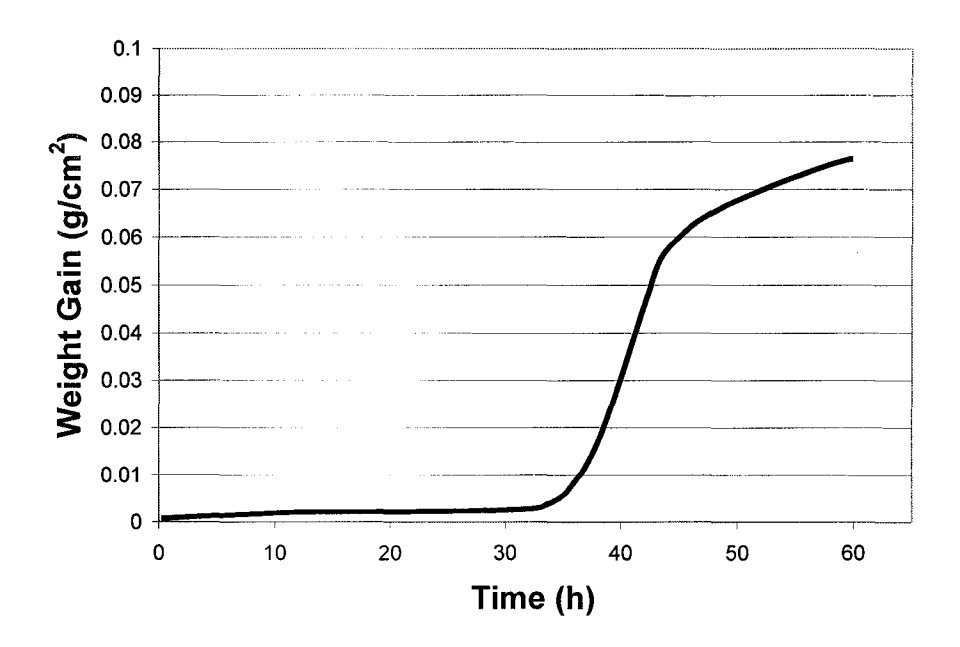


Figure 4.12: Averaged weight gain curve for 5182 alloy containing Sr at 750°C.

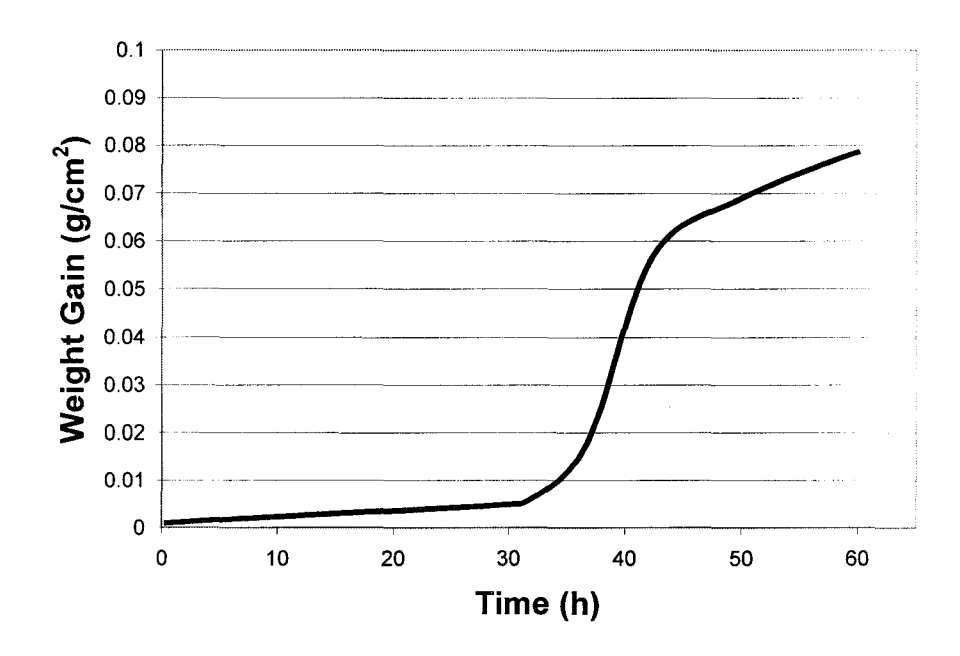


Figure 4.13: Averaged weight gain curve for 5182 alloy containing Sr at 800°C.

Compared to the samples without strontium, the oxide surfaces formed were relatively similar. Naked eye observations of the overall sample shape and the top oxide layer could discern some small differences, such as slightly less bloating and slightly less crumpling, but overall as it was very difficult to confirm this in a quantitative way. Figures 4.14-4.16 are examples of SEM images of the oxide surface at selected magnifications.

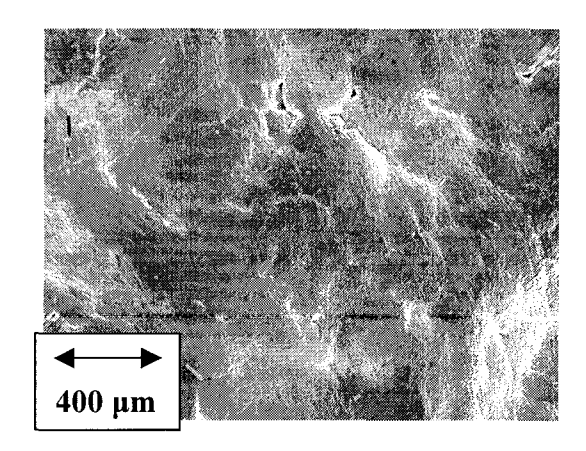


Figure 4.14: Intermediate magnification image of top surface of 5182 alloy containing Sr oxidized at 700°C.

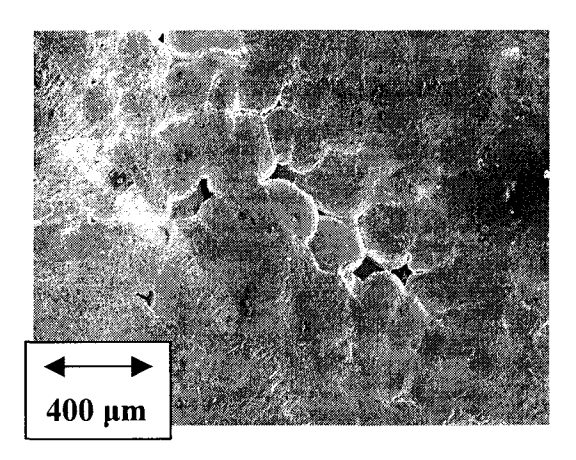


Figure 4.15: Intermediate magnification image of top surface of 5182 alloy containing Sr oxidized at 750°C.

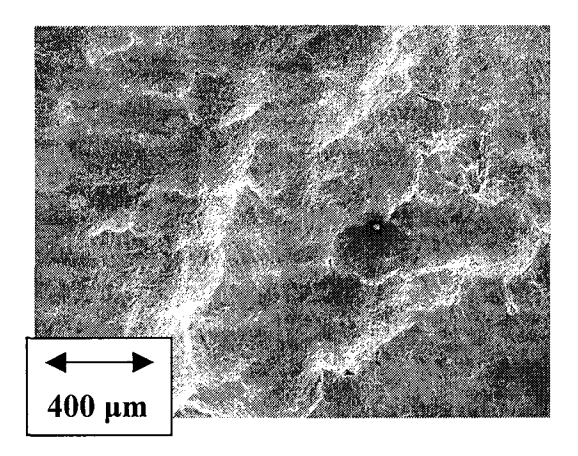


Figure 4.16: Intermediate magnification image of top surface of 5182 alloy containing Sr oxidized at 800°C.

Examination of the top oxide through EDS confirmed the presence of aluminum, magnesium and oxygen. But the presence of strontium could not be detected.

The same methodology for these strontium containing samples was used for XRD sample preparation. X-ray diffraction results (Figure 4.17) confirmed only the presence of MgAl₂O₄. Again, a significant background noise was present due to the nature of the powder sample. Searches for any possible strontium containing phases were unsuccessful.

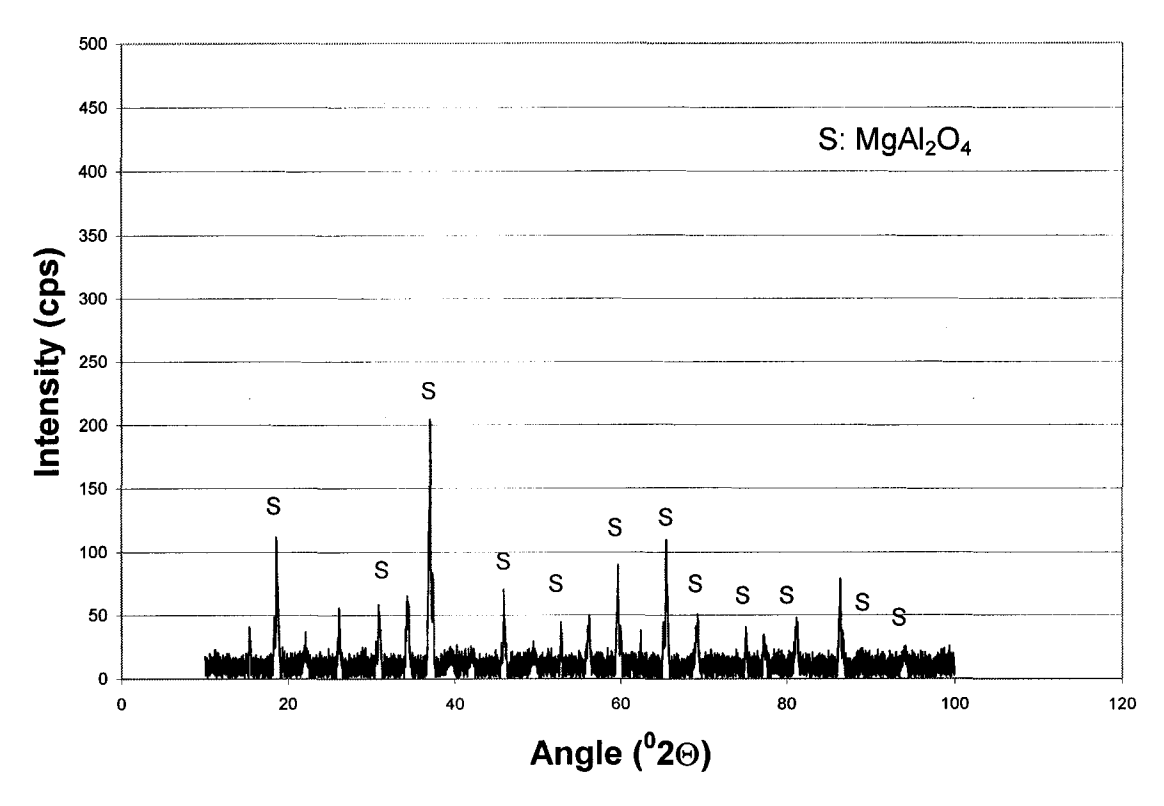


Figure 4.17: XRD pattern for the 5182 alloy containing Sr in as-oxidized powder form.

4.4 A356 Alloy

The oxidation behavior of A356 alloy was as expected from the literature. The weight gains increased steadily throughout the 30 hours period at each of the selected temperatures.

The summarized and averaged weight gain curves at the three temperatures are depicted in Figure 4.18. The curves could be best fitted and treated as a linear

relationship, keeping in mind the curves presented also contain the noise inherent in the data acquisition. Higher temperatures brought about increased weight gains.

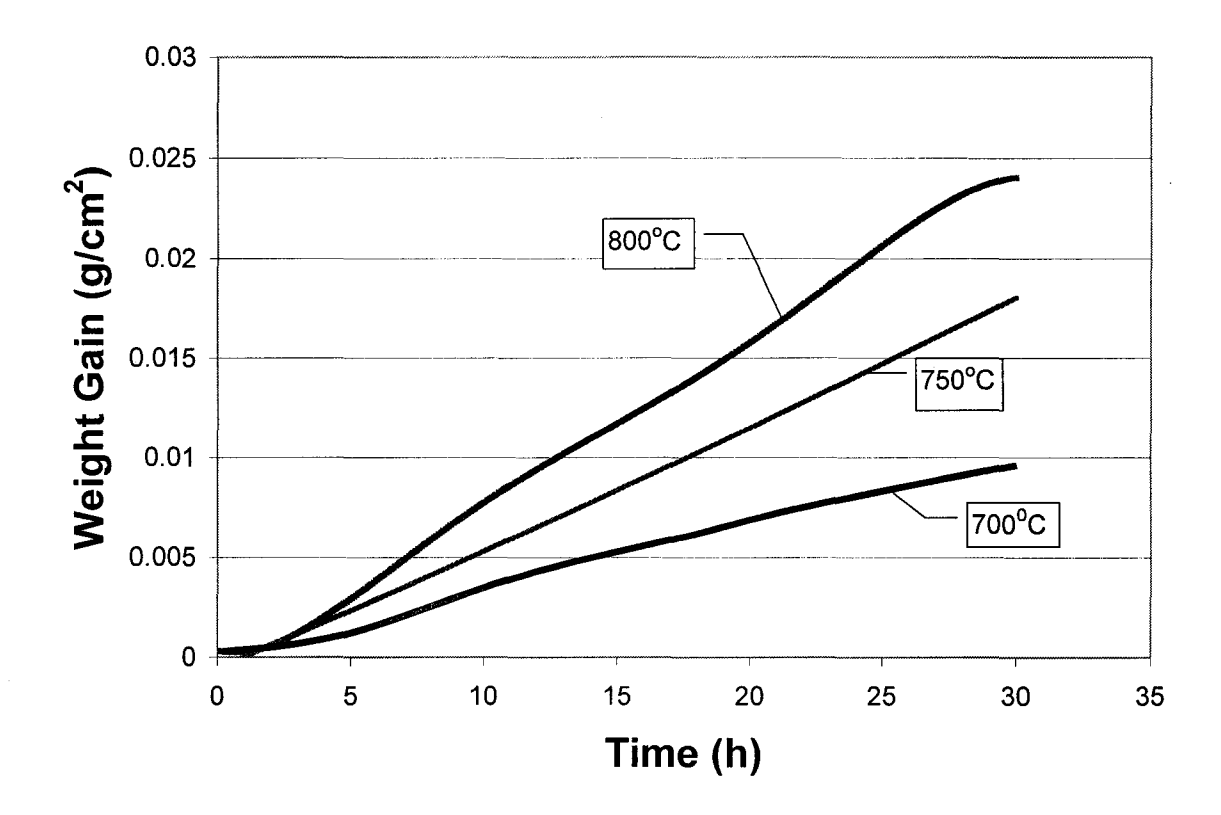


Figure 4.18: Averaged weight gain curves for A356 alloy at 700°C, 750°C and 800°C.

All the samples tested exhibited oxide surfaces that were crumpled and gray colored top surfaces, and substantial visible oxidation could be observed. An example of the crumpled and cauliflower-like morphology is shown in the very low magnification image of Figure 4.19.

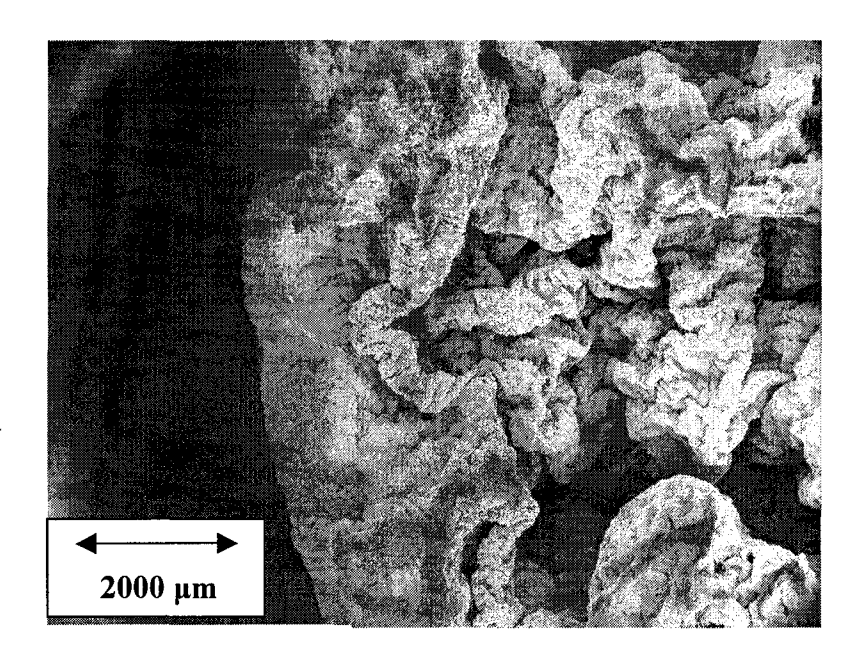


Figure 4.19: Low magnification image of top surface of A356 alloy oxidized at 700°C.

The oxidized surfaces of the samples at different temperatures are seem at higher magnification in the sample images of Figures 4.20-4.22.

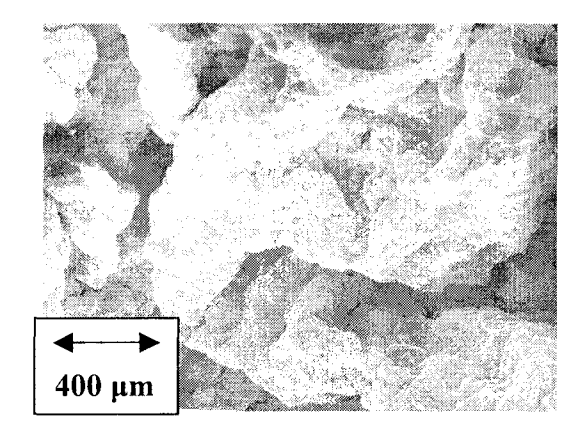


Figure 4.20: Intermediate magnification image of top surface of A356 alloy oxidized at 700°C.

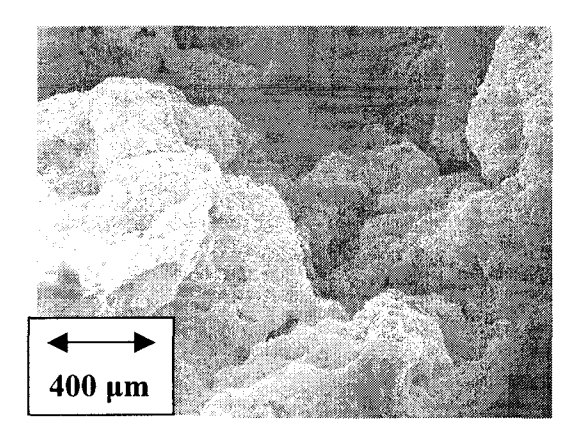


Figure 4.21: Intermediate magnification image of top surface of A356 oxidized at 750°C.

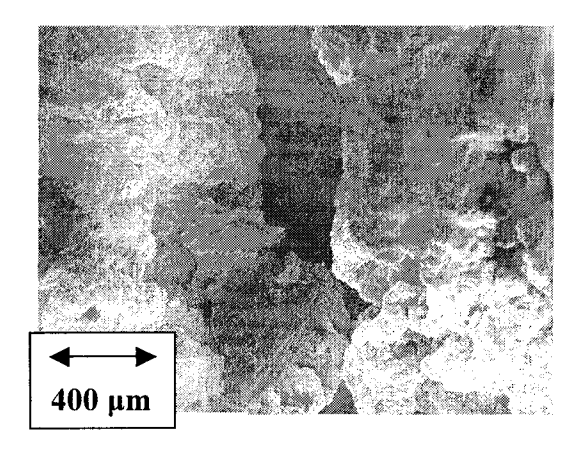


Figure 4.22: Intermediate magnification image of top surface of A356 alloy oxidized at 800°C.

The oxidized samples had the same exterior color representing the oxide layer, which ranged from light gray to gray. Examination of the top oxide through EDS confirmed the presence of aluminum, magnesium, silicon and oxygen. Due to the roughness of the top oxidized surface, the bottoms of the samples were used to obtain X-ray diffraction patterns. Results of the XRD confirmed the expected presence of elemental aluminum, silicon and spinel. It is of note that some A and S peaks can overlap each other and they are depicted as A/S. Figure 4.23 is an example of a pattern obtained.

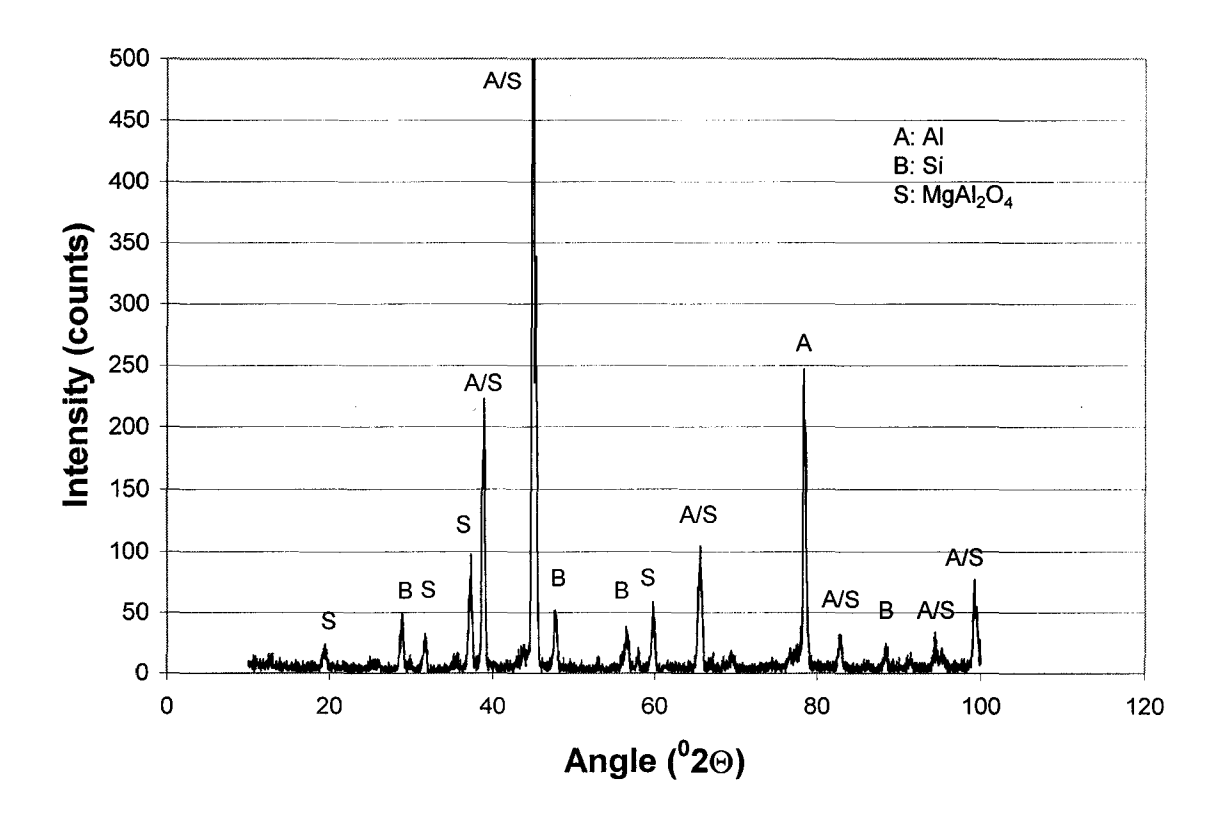


Figure 4.23: XRD pattern for the A356 alloy in as-oxidized form.

4.5 A356 Alloy Containing Sr

The A356 alloy containing strontium exhibited a significant difference in oxidation characteristics both visibly and quantitatively, from the non-strontium-containing A356 alloy samples. Weight gains could be easily noted to be about four to six times less with the presence of strontium. Visibly, the top oxide layers of the strontium-containing samples did not have the same dull gray color of the plain A356 alloy samples; but instead exhibited a shinier, multi-colored and more metallic oxide. The summarized and averaged weight gain curves at the three temperatures are given in

Figure 4.24. The curves could be best described with a logarithmic relationship. Increased temperatures brought about higher amounts of weight gain.

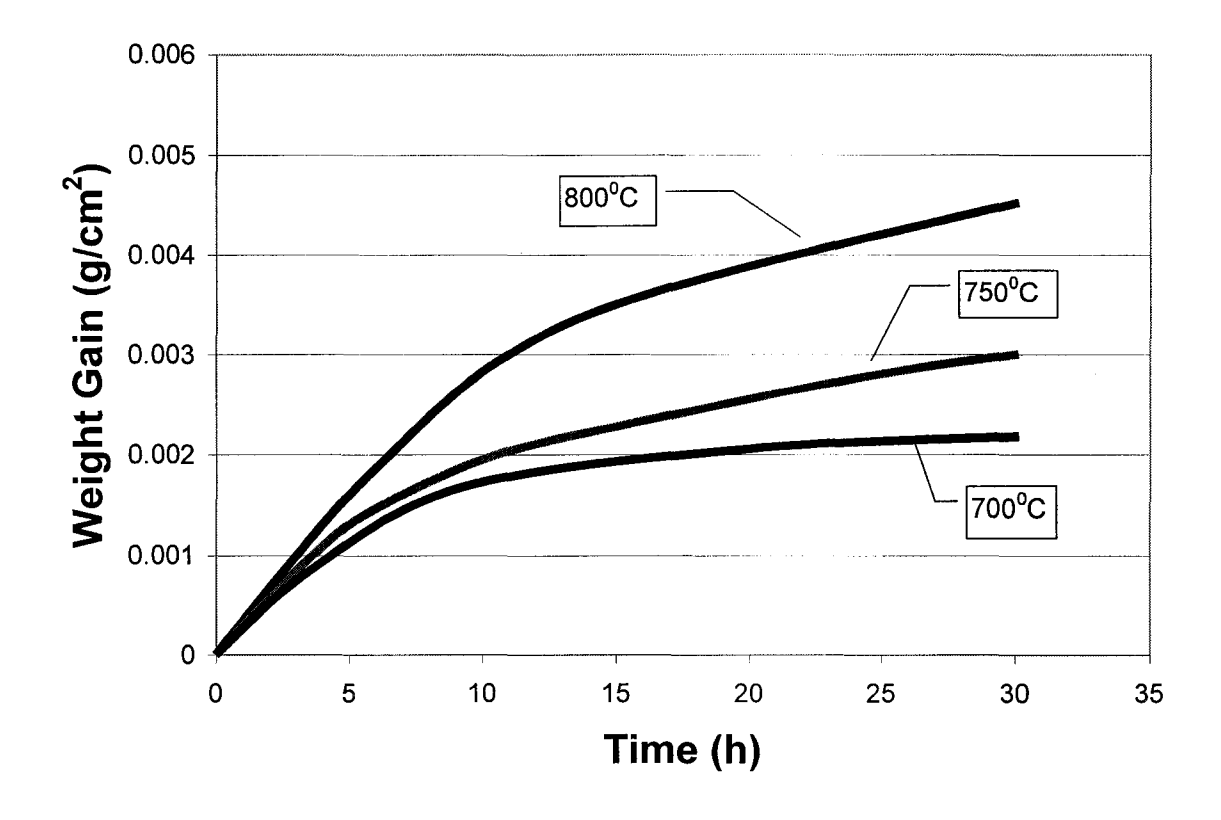


Figure 4.24: Averaged weight gain curves for A356 alloy containing Sr at 700°C, 750°C and 800°C.

Examination of the top oxide revealed very little sign of heavy oxidation. Basically, the observations on these A356 samples could be best expressed as concurring exactly with the observations of Dennis et al. ²⁹, "All surfaces exhibited a dense, coherent surface oxide with the presence of sporadic and randomly distributed oxide 'extrusions.' An increasing number of these localized areas of oxidation were found with increasing temperature."

Medium magnification micrographs of the oxidized surfaces of the samples at different temperatures are given in the sample images, Figures 4.25-4.27.

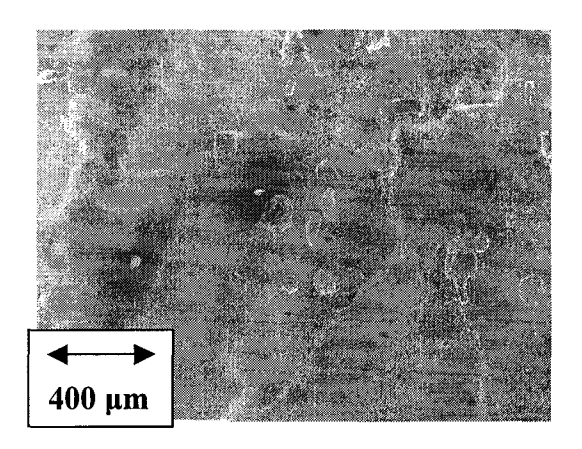


Figure 4.25: Intermediate magnification image of top surface of A356 containing Sr oxidized at 700°C.

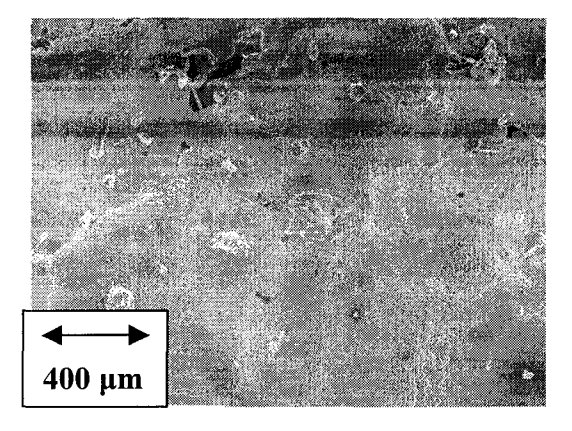


Figure 4.26: Intermediate magnification image of top surface of A356 containing Sr oxidized at 750°C.

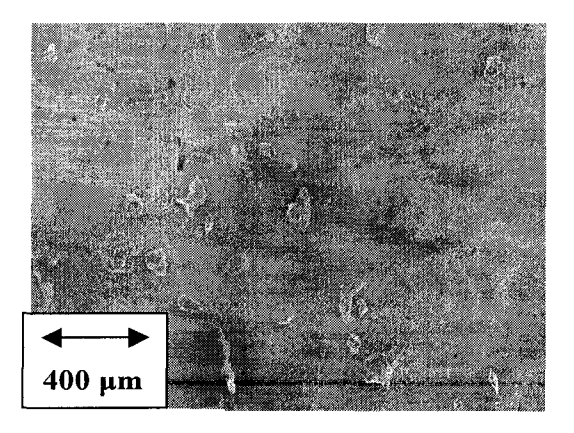


Figure 4.27: Intermediate magnification image of top surface of A356 containing Sr oxidized at 800°C.

Results

Examination of the top oxide through EDS confirmed the presence of aluminum, magnesium, silicon and oxygen, but did not confirm the presence of strontium. Results of the XRD confirmed the presence of aluminum, silicon, and small peaks associated with a Sr-containing species. Figure 4.28 is an example of a spectrum obtained.

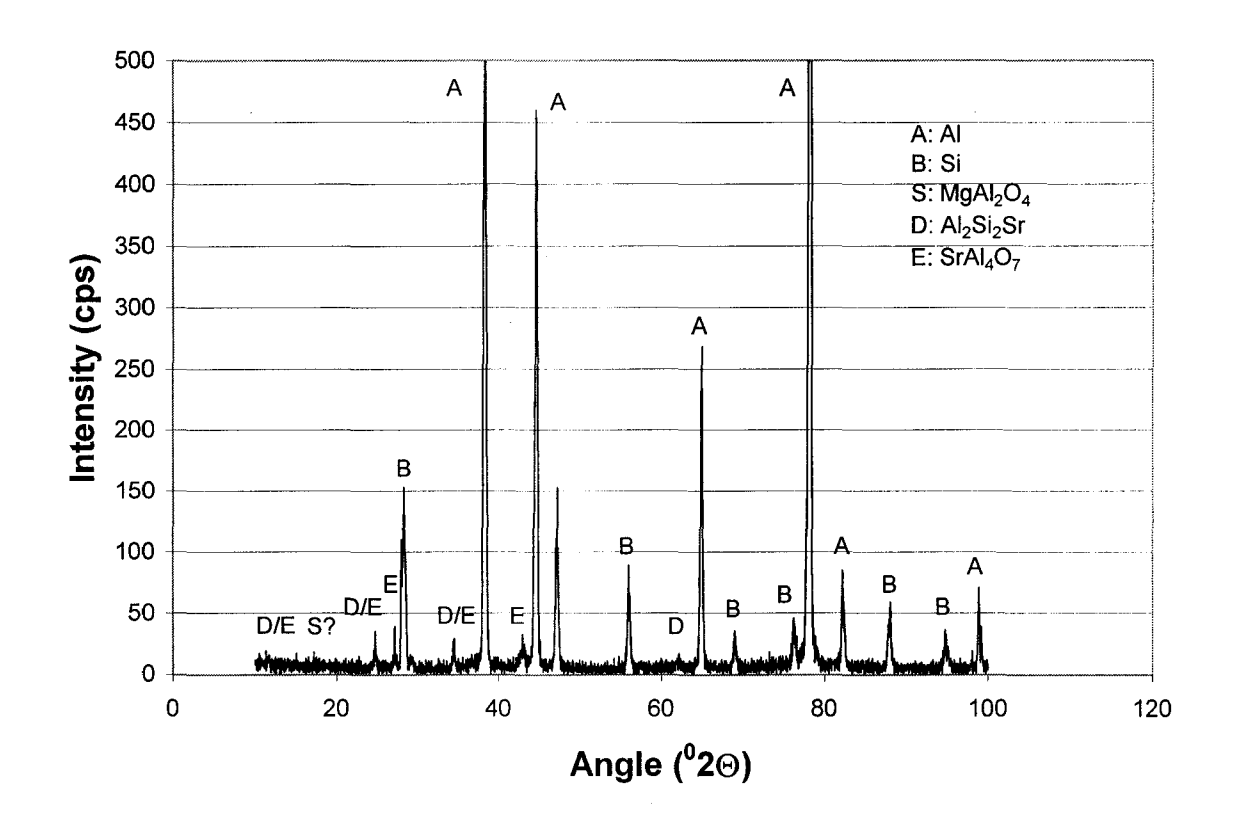


Figure 4.28: XRD pattern for the A356 alloy containing Sr in as-oxidized form.

4.6 A357 Alloy

The composition of the A357 alloy was very similar to that of A356 in that only its magnesium content was slightly higher at 0.52% compared to 0.35%. As expected, almost all the results and observations were similar to those of the A356 alloys. The averaged weight gains were slightly higher compared to that of A356. The summarized

and averaged weight gain curves at the three temperatures are given in Figure 4.29. The curves could best be fitted and treated as a linear relationship, keeping in mind the curves presented also contain the noise inherent in the data, which can contribute to the non-linearity observed. Increased temperatures brought about higher weight gains.

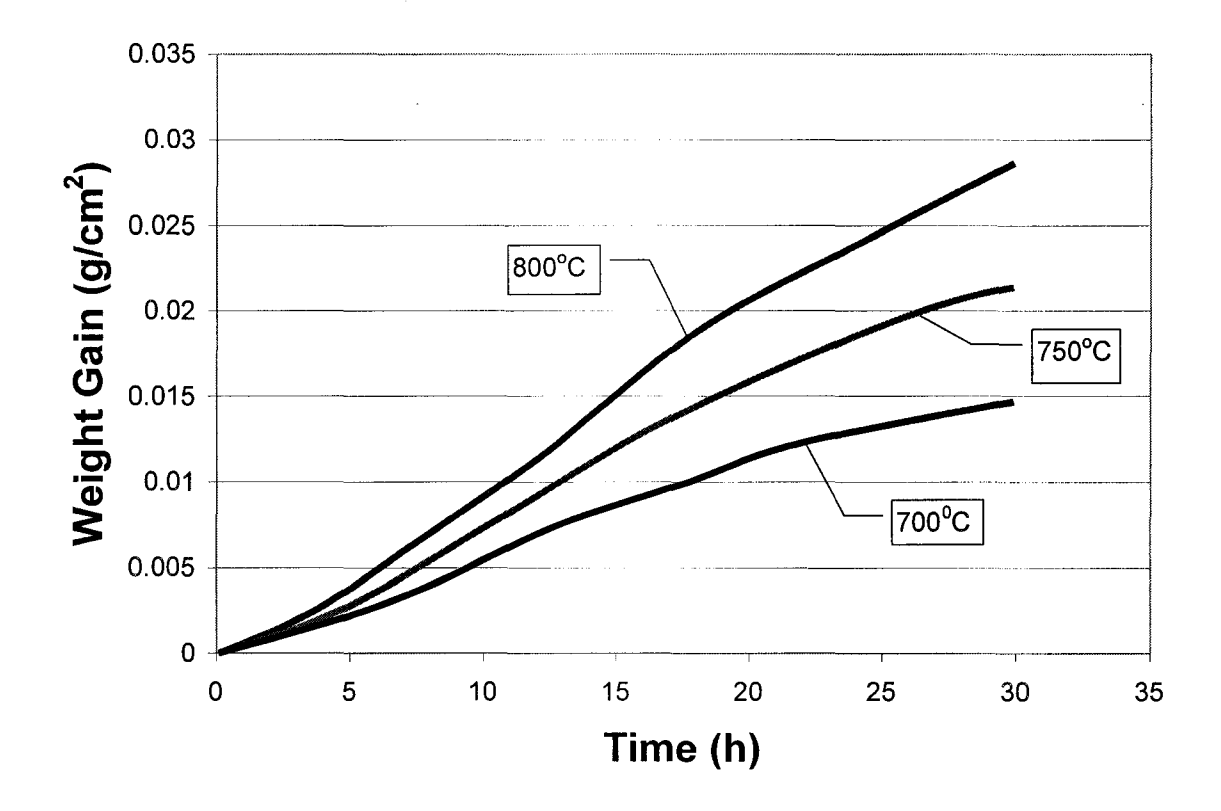


Figure 4.29: Averaged weight gain curves for A357 alloy at 700°C, 750°C and 800°C.

Micrographs of the oxidized surfaces of the samples at different temperatures are shown in the sample images of Figures 4.30-4.32.

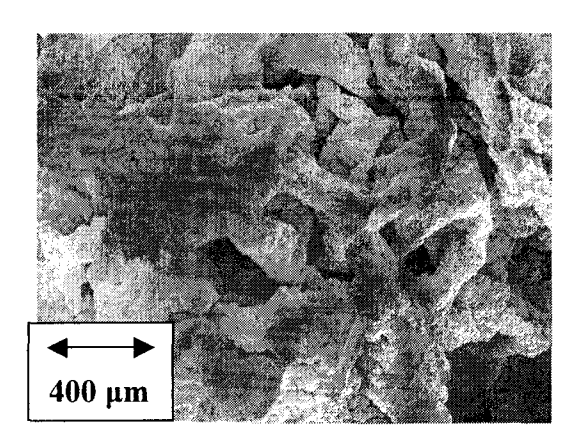


Figure 4.30: Intermediate magnification image of top surface of A357 oxidized at 700°C.

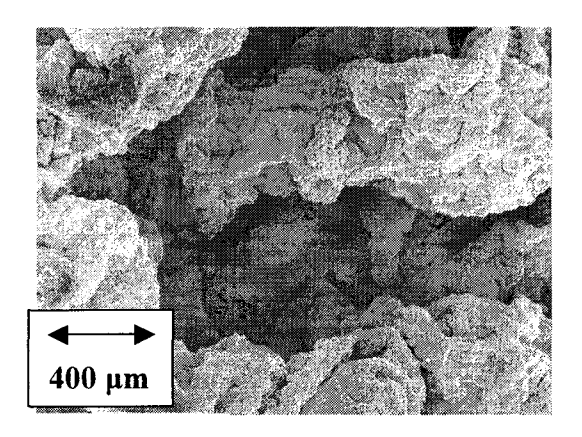


Figure 4.31: Intermediate magnification image of top surface of A357 oxidized at 750°C.

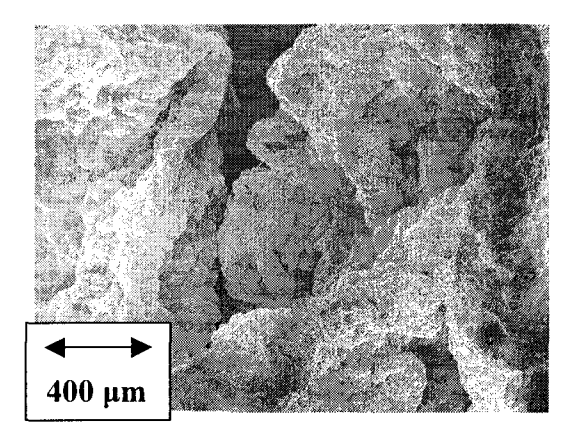


Figure 4.32: Intermediate magnification image of top surface of A357 oxidized at 800°C.

Examination of the top of the oxide through EDS confirmed the presence of aluminum, magnesium, silicon and oxygen. Results of the XRD confirmed the expected

presence of aluminum, silicon and spinel. Figure 4.33 is an example of a typical spectrum obtained.

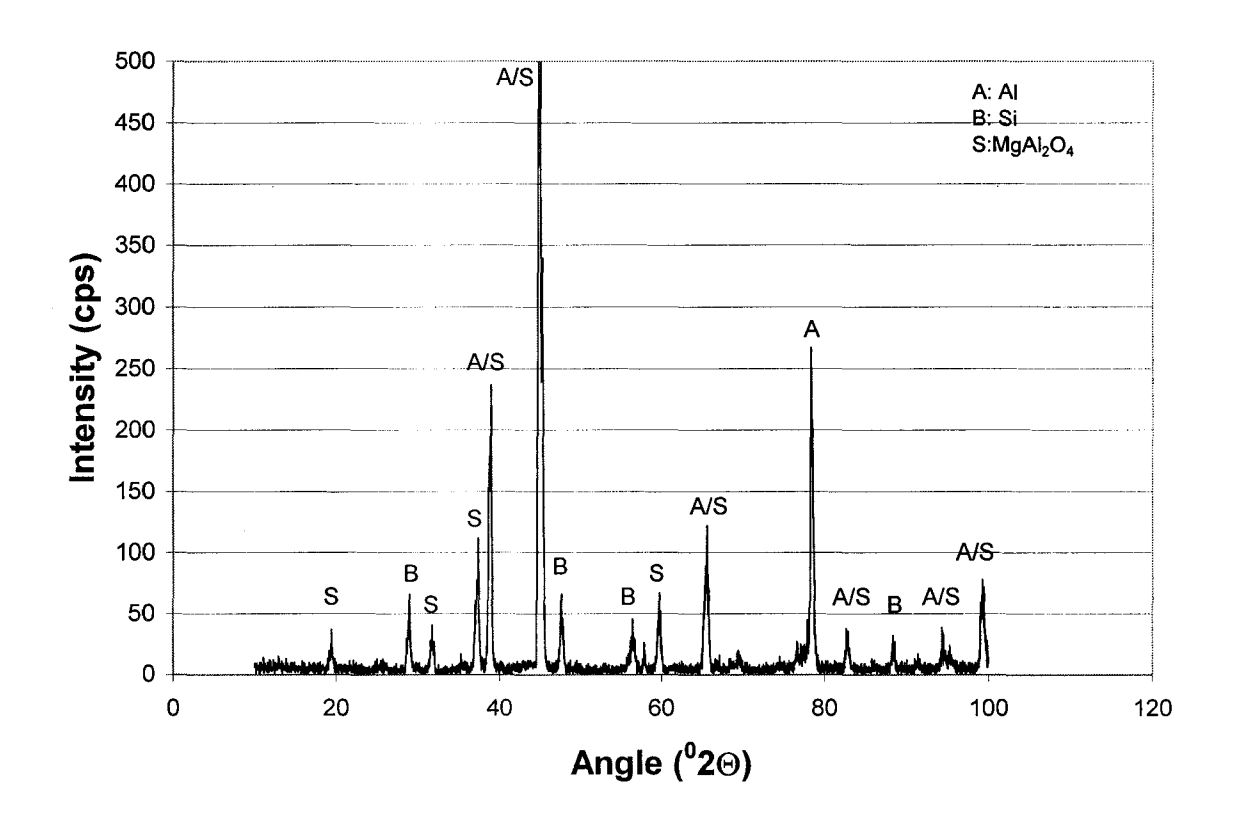


Figure 4.33: XRD pattern for the A357 alloy in as-oxidized form.

4.7 A357 Alloy Containing Sr

Again, the results and observations for the A357 alloy containing strontium were similar to those of the strontium containing A356 alloy. Weight gains were noted to be four to six times less with the presence of strontium. Visibly, the top oxide layers of the strontium-containing samples did not have the same dull gray color of the plain A357 alloy samples; but instead, were shinier, multi-colored and more metallic in nature. The

summarized and averaged weight gain curves at the three temperatures are depicted in Figure 4.34. The curves could be best fitted with a logarithmic relationship. Increased temperatures brought about greater weight gains.

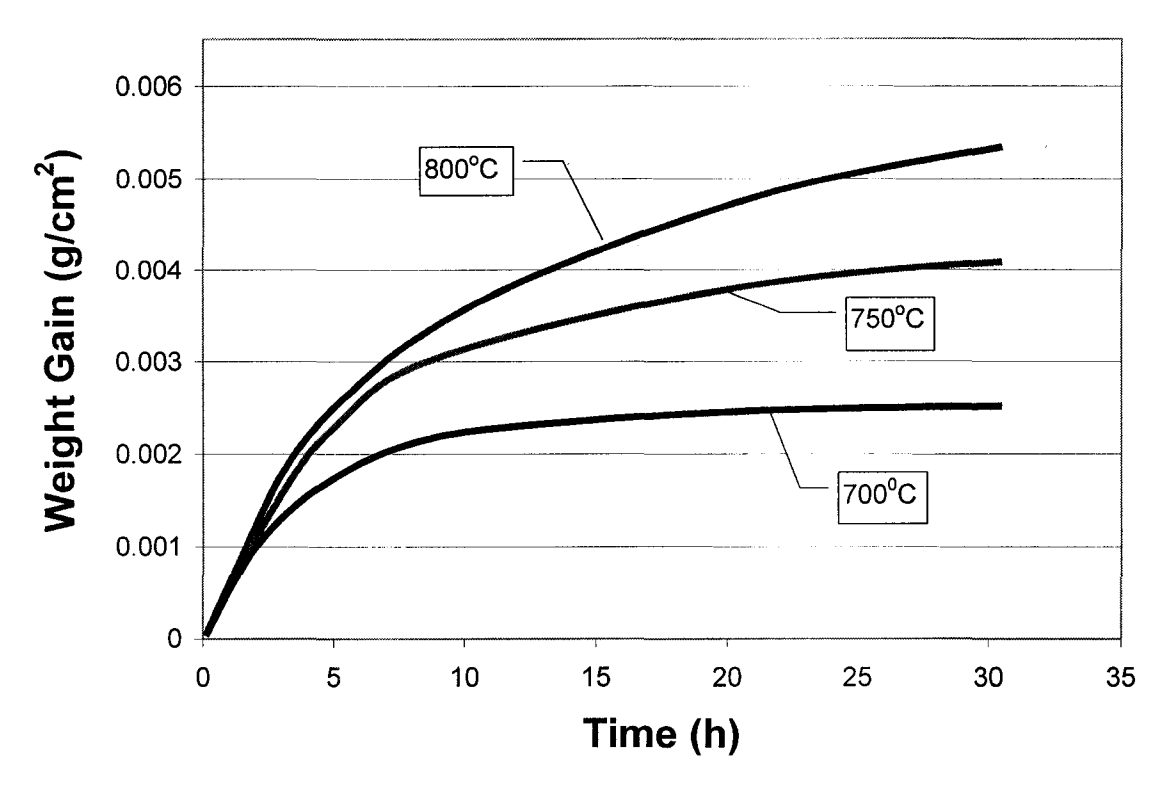


Figure 4.34: Averaged weight gain curves for A357 alloy containing Sr at 700°C, 750°C and 800°C.

Micrographs of the oxidized surfaces of the samples at different temperatures are seen in the sample images of Figures 4.35-4.37.

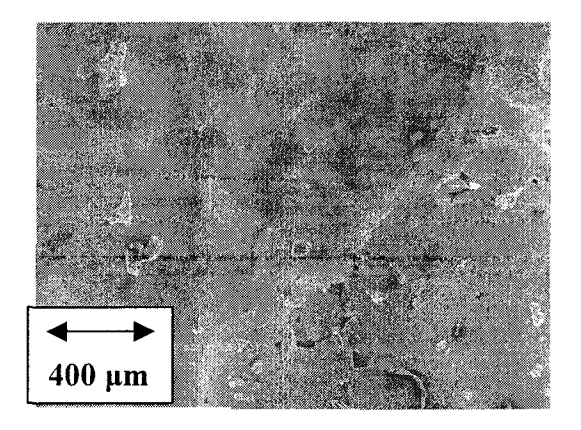


Figure 4.35: Intermediate magnification image of top surface of A357 containing Sr oxidized at 700°C.

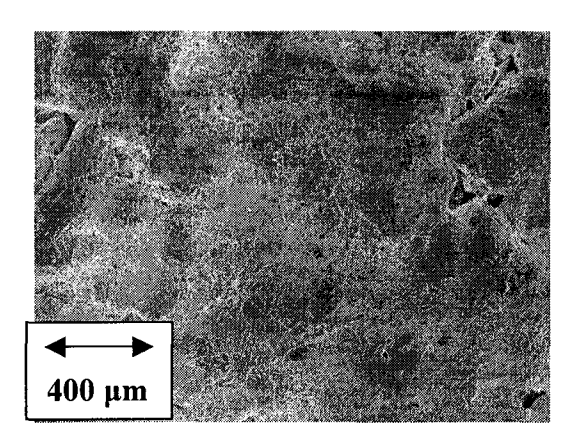


Figure 4.36: Intermediate magnification image of top surface of A357 containing Sr oxidized at 750°C.

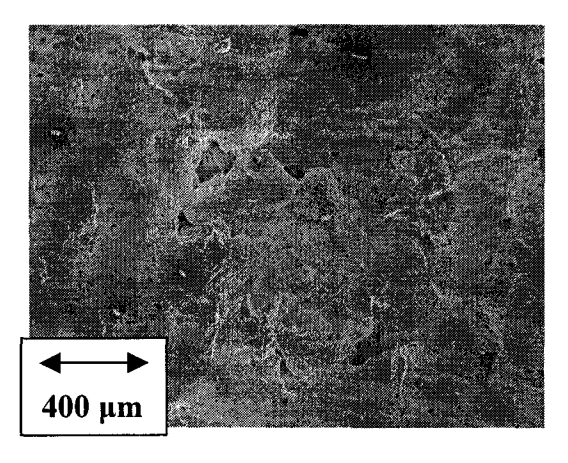


Figure 4.37: Intermediate magnification image of top surface of A357 containing Sr oxidized at 800°C.

Examination of the top oxide through EDS confirmed the presence of aluminum, magnesium, silicon and oxygen, but there was no presence of strontium. Results of the XRD confirmed the presence of elemental aluminum, silicon and small peaks associated with two possible Sr-containing species, Al₂Si₂Sr and SrAl₄O₇. Figure 4.38 gives an example of a typical spectrum obtained.

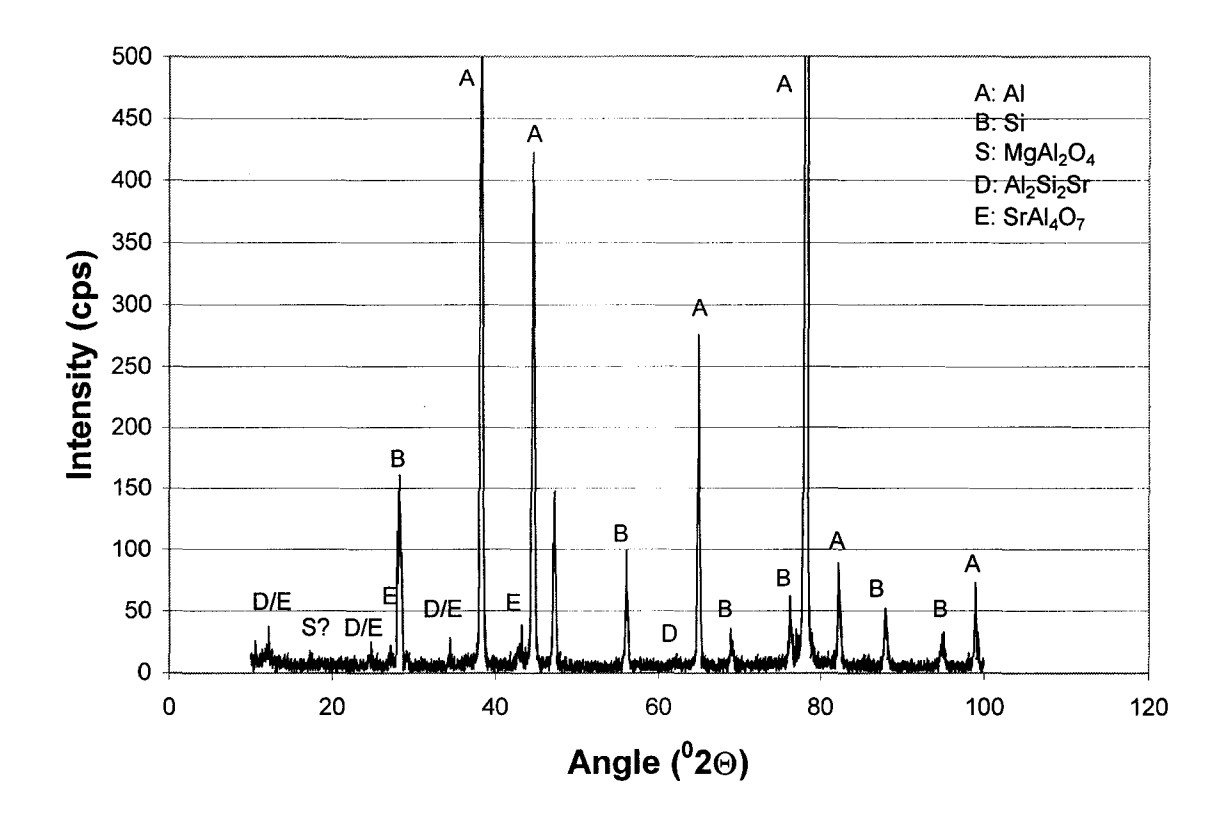


Figure 4.38: XRD pattern for the A357 alloy containing Sr in as-oxidized form.

5. DISCUSSION

This section is organized as such to present and discuss the significance of the results obtained, and the theories and hypotheses behind the observations. Although three alloy systems were studied, it is clear that discussion can be divided into two different sections: the high magnesium-containing 5182 wrought alloy; and the A356 and A357 casting alloys. Since A356 and A357 exhibited very similar results they can be treated together. As the title of this study suggests, the main focus of this thesis should lead to a better understanding of the effects of strontium on the oxidation behavior of these alloy systems in the molten state.

Initially, all three alloy systems were to be studied with an oxidation period of 30 hours, and this was chosen because of its relevance to industrial furnace practice and typical melt holding periods. But, during the course of experimentation, it was found that this 30 hour period was actually insufficient to study the oxidation behavior of the 5182 alloy and the effects of strontium on that alloy.

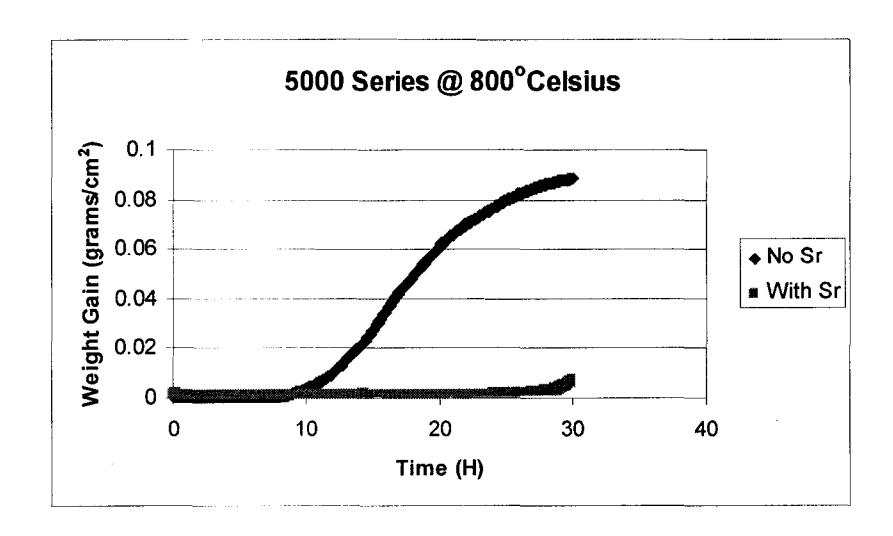


Figure 5.1: An example of initial 30-hour experiments for the 5182 alloy.

Figure 5.1 gives some of the results of the initial 30 hours tests conducted, and as depicted, one can easily see that a significant amount of oxidation occurs around the 30-hour mark. It is also suggested that significant data and events occur after the initial 30-hour holding time. Thus, for the 5182 alloy system, the oxidation experiments were all extended to 60 hours. As for the A356 and A357 alloy systems, previous data from Dennis et al. ¹, and the results from this study confirmed that the 30 hour experiments were sufficient to examine the oxidation behavior and the effects of strontium.

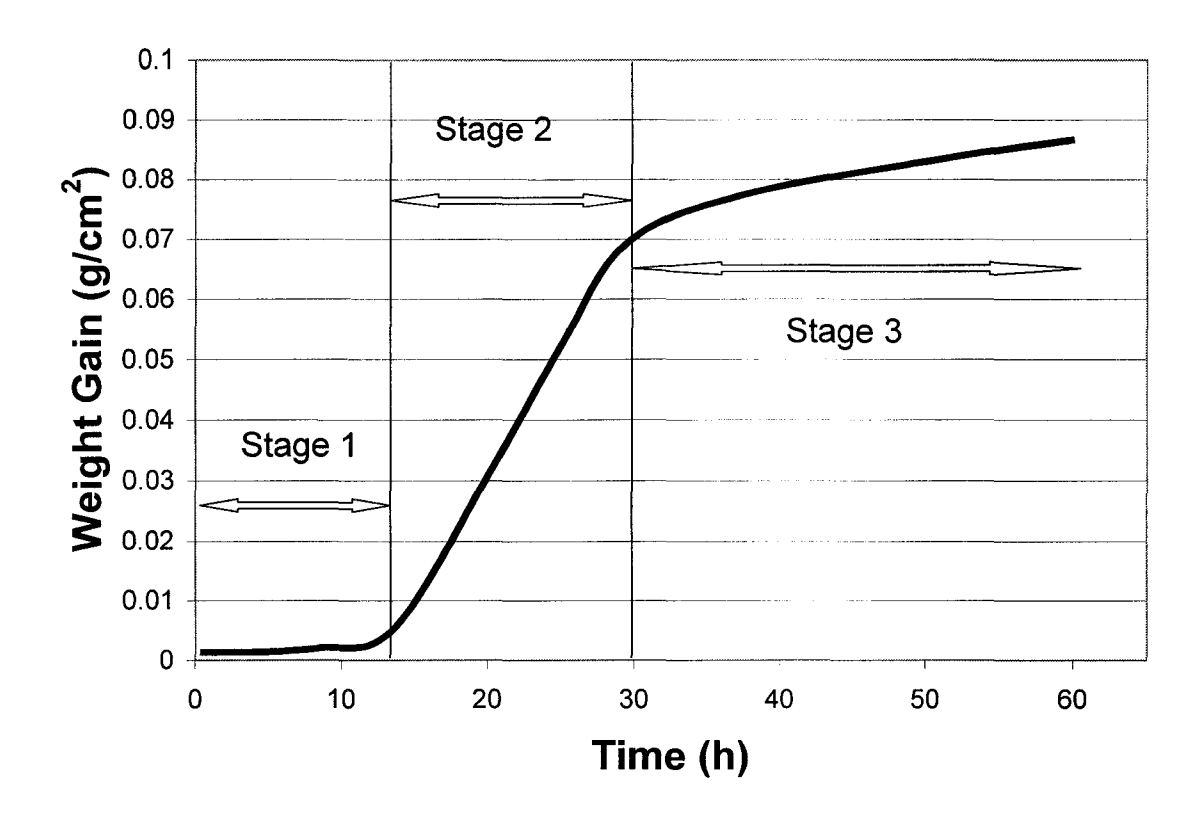
It is also of note that direct comparison of oxidation behavior and the results of the oxidation experiments between the 5182 alloy and A356/A357 alloy is not appropriate. The chemical compositions were significantly different in that A356/A357 both contained relatively high levels of silicon with much lower levels of magnesium; whereas 5182 alloy did not contain any silicon but had high levels of magnesium.

5.1 Oxidation of 5182 Alloy

Results from the oxidation experiments of the commercial 5182 alloy are significant in several areas. The effects of strontium are mainly seen in the weight gain data. One of the main factors governing the oxidation of the 5182 alloy was the high level of magnesium, as high weight gains and heavy oxidation observed had been associated with the presence of magnesium in aluminum-magnesium alloys. The highly preferential oxidation of magnesium could also be observed.

5.1.1 Weight Gain Data

The results obtained corresponded well with the previous study of synthetic 5000 series alloys conducted by Dennis et al. ¹ It can be noted that the characteristics of oxidation and weight gain data followed the proposed model for breakaway oxidation behavior. The proposed three distinct stages could be observed: stage 1, an initial slow oxidation stage – incubation/induction; followed by stage 2, rapid oxidation; and stage 3, subsequent continuation and discontinuation of rapid oxidation. An example of the three distinct stages is shown in Figure 5.2, which is the averaged weight gain curve of 5182 alloy at 750 degrees Celsius.



Stage 1: Incubation/Induction. Stage 2: Rapid Oxidation. Stage 3: Continuation

Figure 5.2: A weight gain curve depicting the three distinct stages of breakaway oxidation.

All weight gain data obtained followed these series of kinetics, including the samples containing strontium. One important feature that could be clearly distinguished when the data were examined was the time span of stage 1 – the incubation/induction period.

Figures 5.3-5.5 and Table 1 demonstrate the effects of strontium and temperature effects on the oxidation behavior.

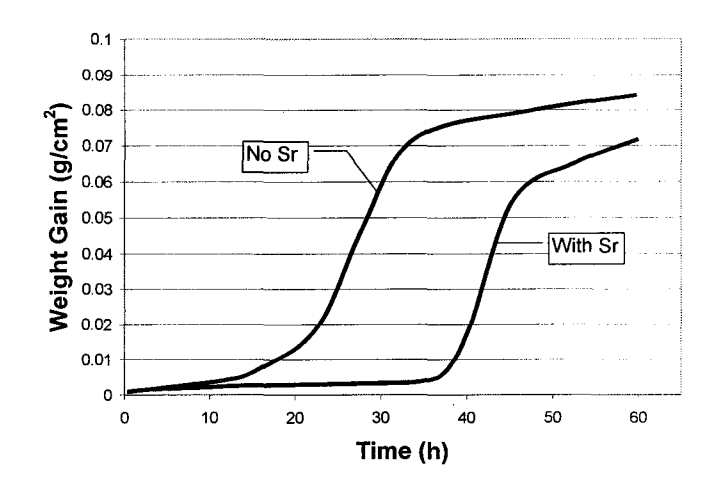


Figure 5.3: Comparison of weight gain curves of 5182 with and without strontium at 700°C.

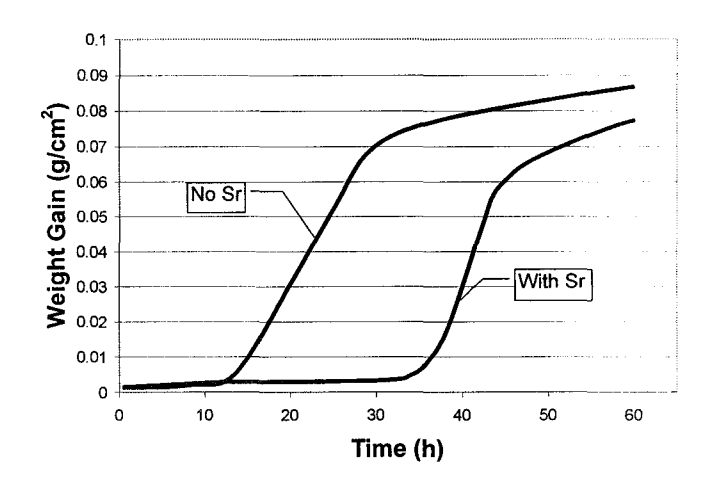


Figure 5.4: Comparison of weight gain curves of 5182 with and without strontium at 750°C.

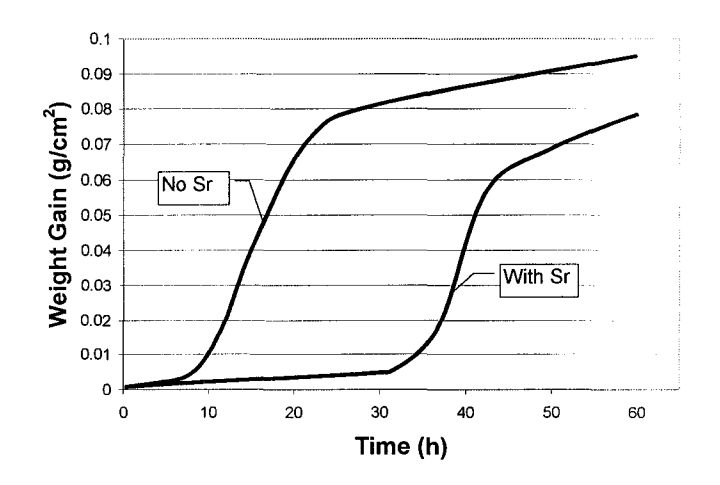


Figure 5.5: Comparison of weight gain curves of 5182 with and without strontium at 800°C.

Table 5.1: Average incubation/inductions periods.

Temperature (⁰ C)		700 °C	750 °C	800 °C
Incubation/Induction period	5182 alloy	17	13	8
(approx. hours)	5182 alloy with Sr	37	34	31

5.1.1.1 Effects of Temperature

The effects of temperature on the weight gain data agree with those of Dennis et al. ¹ in their study on synthetic 5000 series alloy. Increased temperature brings about a shortening of the incubation/induction period. This had been linked to the effects that higher temperatures have on the formation of the initial oxide and the build-up of pressure and stresses leading to the rapid oxidation stage.

5.1.1.2 Effects of Strontium

The effects of strontium on the weight gain data are briefly summarized as follows. The presence of strontium prolonged the incubation/induction period of the breakaway oxidation behavior for over 25 hours at each of the temperatures used. As pertaining to the final weight gain readings at the end of the 60 hours oxidation period, the effects of strontium could contribute to slightly lower total weight gained as the curves were more shifted to the right (prolongment of stage 1 – Incubation/Induction period) and the initial protectiveness was offered by the presence of strontium.

5.1.2 Microscopy and XRD

Unfortunately, both microscopy and XRD were unable to reveal significant differences between 5182 samples with and without strontium. Low magnification (10X-50X) up to very high magnification (1000X-1500X) SEM analyses were performed in order to determine if any quantifiable differences existed between samples with and without strontium. Due to the fact that most samples were irregular and abnormal in shape and surface characteristics, the results of low magnification microscopy were not very consistent. Figure 5.6 presents actual photographs of a typical highly-oxidized 5182 sample and its cross-section.

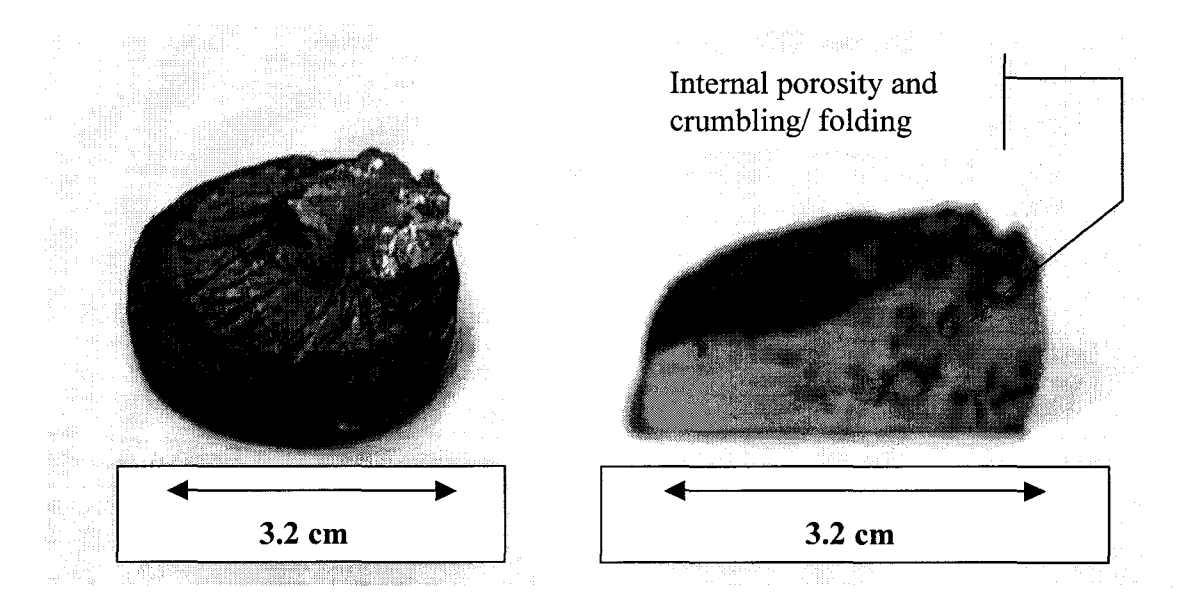


Figure 5.6: Example of an oxidized 5182 alloy sample and its cross-section.

Internal porosity and voids were present in many samples and Figures 5.7-5.9 show the results of a cross sectional examination of an example of the crumbling, spikes, peaks and folding present in the samples.

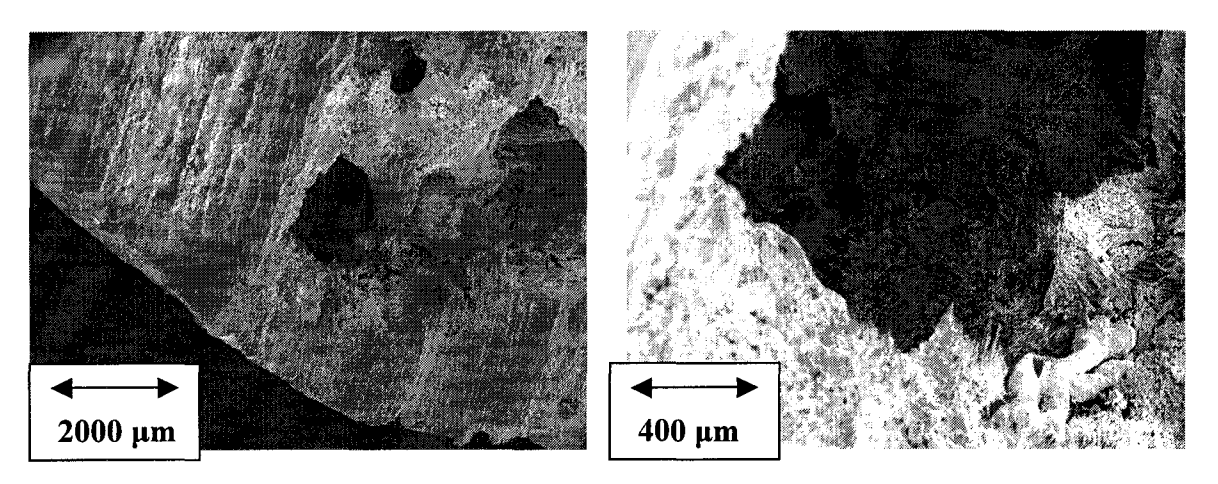


Figure 5.7: Low magnification image of internal porosity / Figure 5.8: Intermediate magnification image of internal porosity

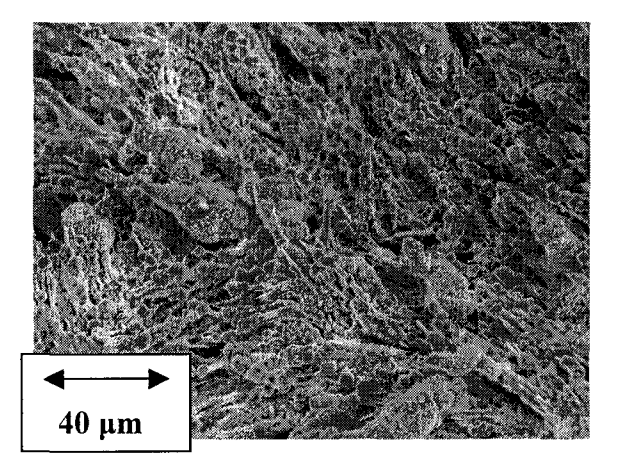
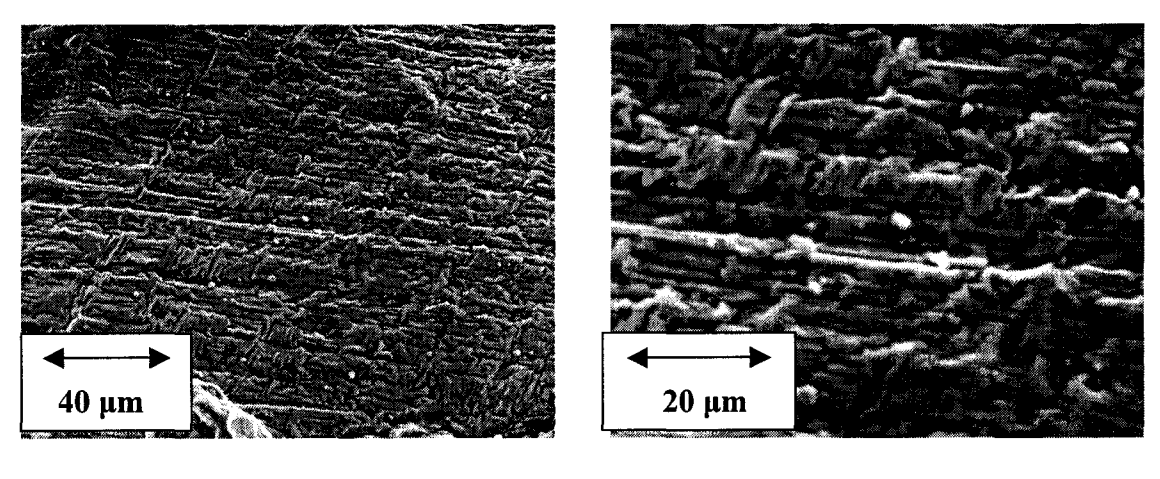


Figure 5.9: High magnification image of internal porosity.

High magnification microscopy yielded slightly more consistent images by demonstrating the same surface morphologies between all the samples, with and without strontium. Figures 5.10a and 5.10b are high magnification micrographs from the SEM depicting the similar micro-morphology commonly found in samples with and without strontium.



a) High magnification

b) Higher magnification

Figures 5.10: High magnification images of common micro-morphology of 5182 samples.

Results of XRD could only confirm the presence of spinel-MgAl₂O₄, thus supporting the expected mechanism of breakaway oxidation and the consumption of magnesium, aluminum and possibly MgO, leading to the final spinel-MgAl₂O₄ formation. No significant differences could be derived from the spectra obtained from samples with and without strontium. Any strontium containing species, if they are indeed present, could have been easily masked by the noise and the abundance of the heavily oxidized spinel.

5.1.2.1 Additional Emission Spectrometry

In order to shed some light into the mechanisms involved, additional analyses, not originally planned, were performed on some oxidized samples. The samples containing strontium with relatively regular shapes were ground on the bottom so that a small flat metallic surface would remain and be suitable for analysis using emission spectrometry. It is of note that, due to the presence of porosity and the irregular shapes, it was actually very difficult to obtain a good spot for the analysis. In Table 5.2, the results are tabulated along with the initial compositions of the alloy. The important elements to pay attention to here are magnesium and strontium.

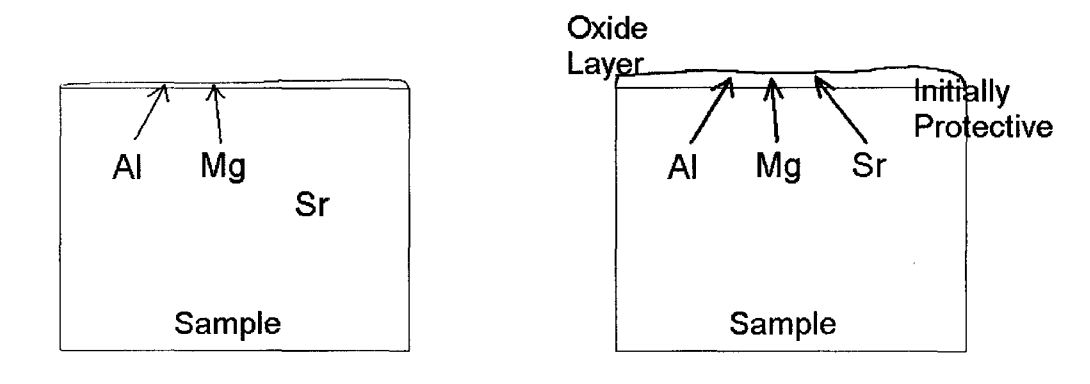
Table 5.2: Average chemical compositions of samples with strontium after oxidation experiments.

% Composition	Si	Mg	Cu	Fe	Sr
5182 /w Sr Before	<0.2	4.40	0.034	0.16	0.024-0.026
Average after 60 hrs	<0.2	0.30-1.30	0.032	0.11	0.004-0.012

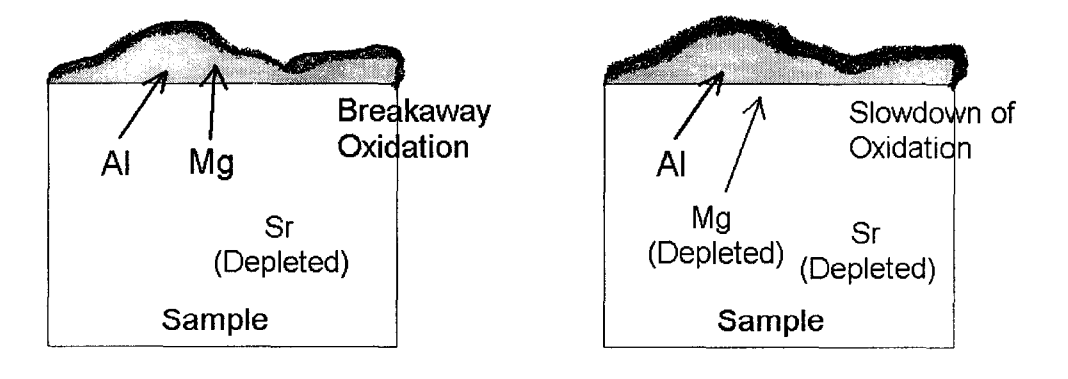
These results confirm many of the previously proposed hypotheses that magnesium is consumed during the oxidation process. A very interesting result was also the fact that the spectro-composition showed that, indeed, a significant amount of strontium was also lost (average of 250 ppm went down to average of 80 ppm) and presumably had been consumed during oxidation.

5.1.3 Breakaway Oxidation Behavior and Hypothesis and Model of Depletion

The results presented here clarify the oxidation behavior of 5182 alloy, with and without strontium. A schematic of a proposed mechanism for breakaway oxidation and the effects of strontium is presented in Figure 5.11, and can be compared to the mechanism of breakaway oxidation without strontium as shown in Figure 5.12.

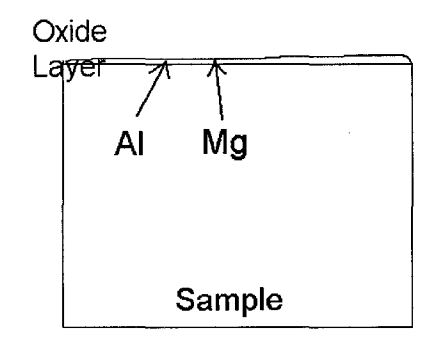


a) Stage 1: Incubation/Induction Period

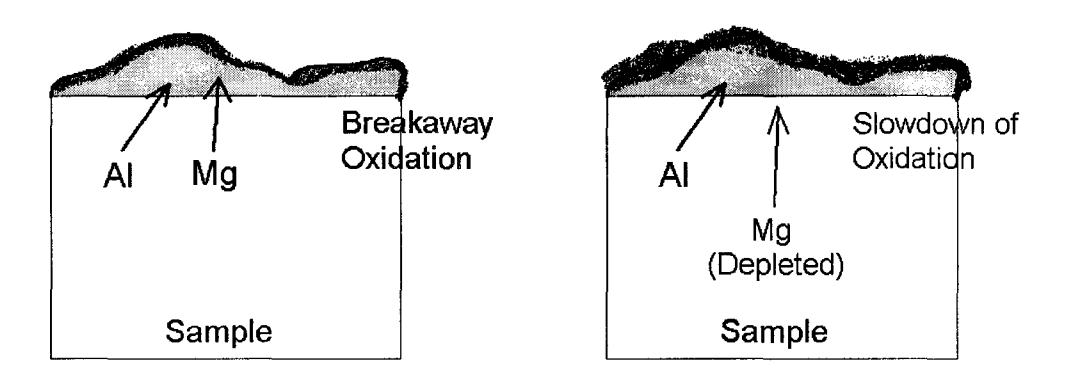


- b) Stage 2: Rapid Oxidation
- c) Stage 3: Continuation + Discontinuation

Figure 5.11: Schematic of the proposed model for the effects of strontium.



a) Stage 1: Incubation/Induction Period



b) Stage 2: Rapid Oxidation

Stage 3 : Continuation + Discontinuation

Figure 5.12: Schematic of the proposed model without strontium.

In this proposed mechanism, the strontium present has an effect on prolonging the incubation/induction period as it, and the oxide species that it may form, provide some form of protectiveness during this initial stage. As Dennis et al. proposed, strontium could initially oxidize preferentially with aluminum and silicon to form SrAl₄O₇ below the initial MgO layer formed. This strontium containing oxide is slightly protective, but

74

this protectiveness is not very resistant, and when the amount of strontium becomes depleted to a certain level and combined with stresses that are built-up due to the magnesium (vapor), the oxide can no longer offer significant protection. At this point, the onset of rapid oxidation takes place, driven by the high levels of magnesium, which results in breakaway oxidation. As the magnesium content is depleted, a slowdown of the oxidation process occurs and rapid oxidation ends, leading to the continuation of the slow oxidation process which is no longer magnesium-driven. The presence of strontium does not have any significant effects on the final stages of the mechanism, as they are characterized and dominated by the magnesium content.

Although 250 ppm was chosen because it was a benchmark in strontium modification in other alloy systems, it would be very interesting to see the effects of higher levels of strontium. At higher strontium levels, the depletion of available strontium should take longer to achieve or would be more difficult, possibly leading to more noticeable and significant effects, and a prolongment of the observed incubation period during oxidation.

5.2 Oxidation of A356 and A357 Alloys

Results from the oxidation experiments of the commercial A356 and A357 alloys were significant in several areas. The weight gain curves will first be examined closely, and the effects of strontium are easily demonstrated in the weight gain data. The commercial A356 and A357 alloys both contained 0.34 % and 0.52 % magnesium respectively, and one of the main factors governing the oxidation of aluminum magnesium alloys is the level of magnesium. Thus it was no surprise that the A357 samples exhibited slightly more oxidation with respect to their higher magnesium content compared to A356 samples.

5.2.1 Weight Gain Data

The results obtained corresponded well with the previous study on commercial 356 alloys conducted by Dennis et al. ¹ Oxidation behavior of A356 alloys without strontium could be described as a steady growth rate befitting a linear relationship. In Figures 5.13 and 5.14, the oxidation curves of A356 and A357 are summarized and compared respectively.

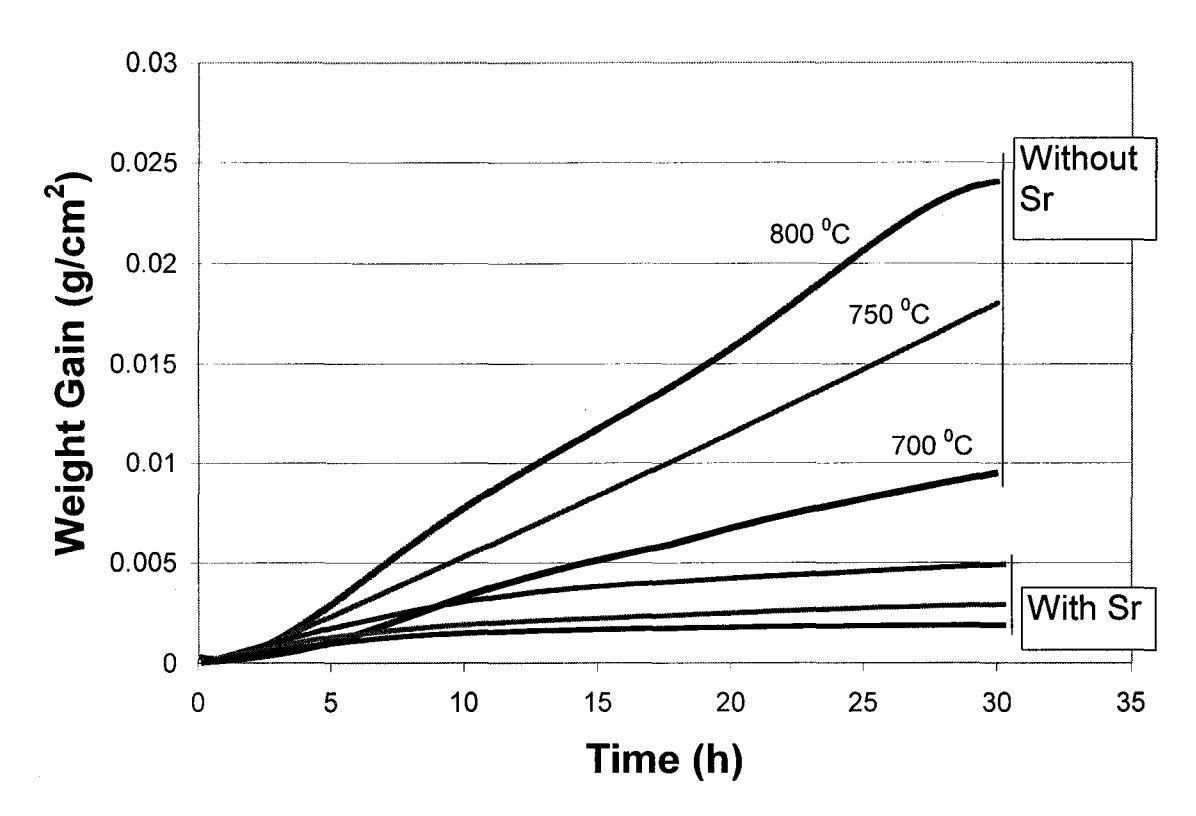


Figure 5.13: Summary of oxidation curves for the A356 alloy samples.

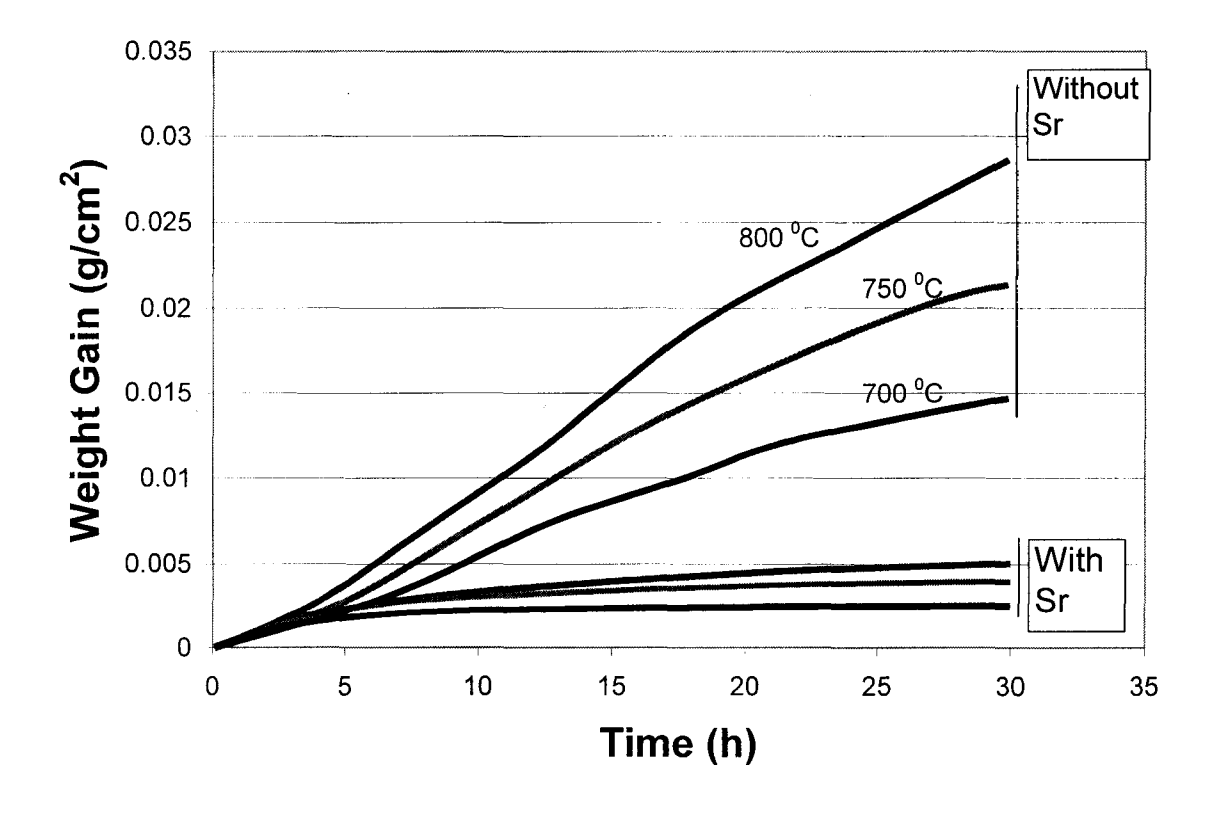


Figure 5.14: Summary of oxidation curves for the A357 alloy samples

It was evident that the effects of strontium were significant in the weight gain data. The presence of strontium led to significantly lower weight gains in both the A356 and A357 alloy samples; but it also affected the overall kinetic behavior, which changed to a more logarithmic fit, suggesting protective behavior.

The effects of temperature were also obvious as increased temperatures were associated with increases in weight gain. Interesting insights can be obtained from analyzing the weight gain curves in the manner presented in Tables 5.3 and 5.4.

5.2.1.1 Effects of Magnesium Content

Table 5.3: Tabulated average weight gain data comparing A356 and A357 alloy samples.

	Temperature (⁰ C)		
Weight gained @ 30 h	700	750	800
A356 0.35% Mg no Sr	0.009	0.018	0.024
A357 0.52% Mg no Sr	0.015	0.022	0.028
% Change with higher Mg	67%	22%	17%

In Table 5.3, the percentage change in the average total weight gained at the end of the 30 hour oxidation experiments provided by the increase in magnesium content from A356 and A357 are documented. The A357 samples contained approximately 50% more magnesium than the A356 samples. Keeping in mind that the data represents only average weight gains at only three temperatures, it is seen that the effects of magnesium

content were more apparent at 700 °C. Nevertheless, it is apparent that the effects of higher magnesium content are quite significant and sensitive in this alloy system.

5.2.1.2 Effects of Strontium

Table 5.4: Tabulated average weight gain data comparing A356 and A357 alloy samples with and without Sr.

	Temperature (⁰ C)		
Weight gained @ 30 h	700	750	800
A356 0.35% Mg no Sr	0.009	0.018	0.024
A356 w/ Sr	0.0022	0.003	0.0045
Factor of reduced weight gain w/ Sr	4.1	6.0	5.3

	Temperature (⁰ C)		
Weight gained @ 30 h	700	750	800
A357 0.52% Mg no Sr	0.015	0.022	0.028
A357 w/ Sr	0.0025	0.0041	0.0053
Factor of reduced weight gain w/ Sr	6.0	5.4	5.3

In Table 5.4, the magnitudes of the decrease in the average amounts of weight gain after the 30 hour oxidation experiments are tabulated. The factor indicates the number of times that the weight gains decreased with strontium; thus for both the A356 and A357 alloy samples, the total weight gains at the end of 30 hours were decreased by approximately four to six times with the presence of strontium.

The combined effects of decreased weight gains and changes in kinetics (linear to logarithmic relationship) leads to the conclusion that the presence of strontium does play an important role in the underlying oxidation mechanisms involved.

79

5.2.2 Microscopy

The sample surfaces from the A356/A357, with and without strontium were significantly different in color and morphology. Discussed here are the higher magnification analyses and the comparisons of the samples with and without strontium. As previously noted, samples without strontium yielded a cauliflower-like and cluster morphology of the oxide. Figures 5.15 demonstrates this morphology at higher magnification.

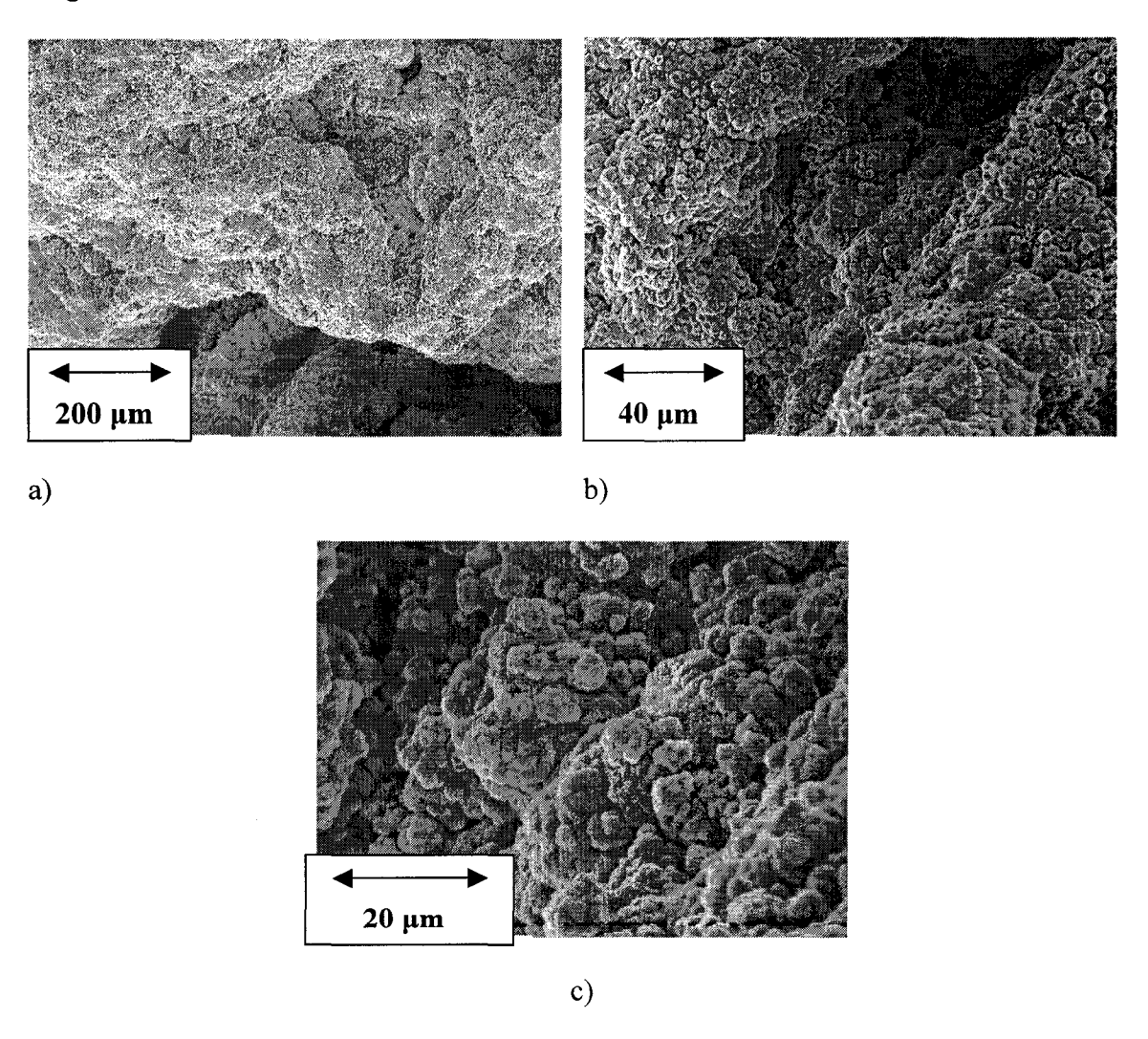
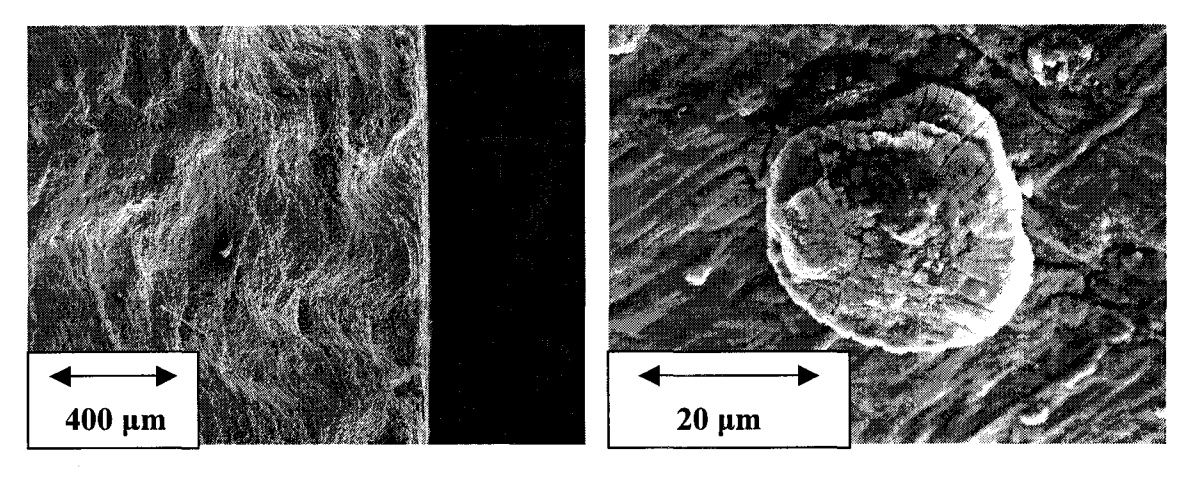


Figure 5.15: Micrographs at different magnification of the surface oxide morphology of A356/A357 alloy.

A356/A357 samples with strontium mostly exhibited a much different surface oxide layer, which was dense and coherent. On this coherent surface morphology, microscopic examination reveals the presence of sporadic and randomly distributed oxide extrusions, as also described by Dennis et al. ¹ In Figures 5.16a and 5.16b, examples of these localized extrusions are presented, and in Figure 5.17, a high magnification example of a typical coherent oxide layer associated with strontium containing samples is seen.



a) low magnification

b) high magnification

Figure 5.16: Example of a surface layer and localized eruption of A356/A357 alloy samples containing Sr.

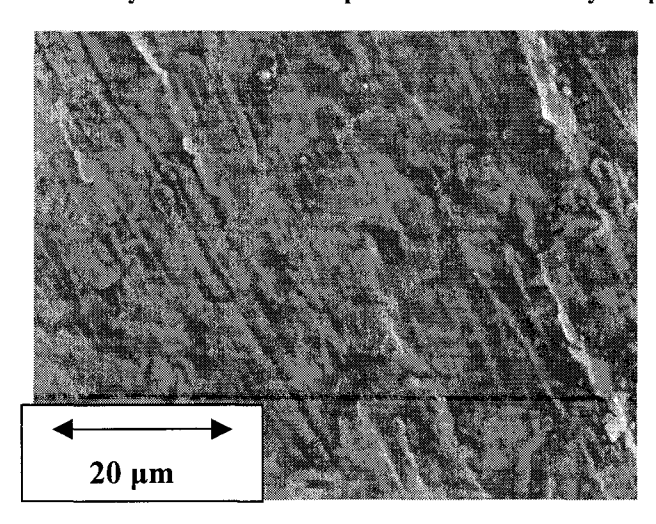


Figure 5.17: Example of coherent surface oxide formed on A356/A357 alloy samples containing Sr.

5.2.2 X-Ray Diffraction

A comparison of the XRD patterns from the results of A356/A357 samples, with and without strontium, leads to the following summary and suggestions. Without strontium, the presence of aluminum, silicon and spinel was confirmed; with strontium, the presence of aluminum and silicon was confirmed, but the presence of spinel could not be established. Additional, albeit, small peaks were found to be associated with certain strontium-containing species. The strontium-containing species, Al₂Si₂Sr and SrAl₄O₇, were determined from suggestions largely imparted by the study performed by Dennis et al. ¹ It is of note that the matches were incomplete and that some peaks were missing. The underlying importance of the XRD results is the confirmation of the presence of different species of surface oxide layer associated with the presence of strontium in these samples.

5.2.3 Protective Behavior Hypothesis

Although the results of this study are very interesting, the exact underlying mechanisms that govern the effects of strontium in the A356/A357 alloy system remain undetermined and unconfirmed. At this stage, the following hypothesis and propositions as suggested by Dennis et al. ³¹ best describe what can be deduced.

The mechanism which seems to prevail is one in which an initial layer of MgO forms before or during the heating cycle. When the alloy is heated, strontium oxidizes preferentially with aluminum and silicon to form SrAl₄O₇ or SrSiO₃ below the initial MgO layer formed. This strontium containing oxide is protective and prevents further oxidation, except for the occasional localized eruption. These eruptions are caused by

small, localized build-ups of magnesium vapor below the surface oxide. Since a protective oxide formed, a thickening of the initial MgO layer is prevented, but a concentration of magnesium vapor does build-up at the metal/oxide interface. This build-up does not occur in the non-strontium containing A356/A357 alloys because the continual thickening of the surface MgO layer prevents the build up of magnesium vapor on the surface of the sample. This hypothesis is supported by the fact that the weight gain curves for A356/A357 alloy samples with and without strontium followed a different kinetic law since they formed different initial oxides upon heating, and different species of the surface oxide layer were maintained throughout the oxidation process.

5.3 Practical and Industrial Relevance

Potential for improvements in dross/oxides treatment of molten A356/A357 in the industry could be useful and improve efficiency. Dross treatment is always a problem for the foundrymen, but it is important to note that this had not been a specific problem that demanded and sought after a solution. But on the other hand, 5000 series alloys had always been known to experience process and treatment problems in terms of accretions and dross/oxides formation in alumina-based holding furnaces. In order to look at the problem of accretions, it is essential to not only study the oxidation of the molten alloy itself, but also the interaction between the oxide species formed and alumina based refractories under industrial conditions. Judging from the results obtained, the effects of strontium on the oxidation behavior: the potential protectiveness offered, the reduction in breakaway oxidation behavior, and the formation of different species of oxides; could prove to be promising in suggesting a possible solution for the problems of accretion formation.

What is significant from this study from a practical point of view is the further understanding of the two common observations by foundrymen and process engineers alike. Fundamentals of fading of strontium modification in a molten alloy system after a certain period of time can be partly attributed to the depletion of strontium through its role and involvement in the underlying mechanisms of oxidation. Also, the concept and observations of the "orange peel" oxide observed in heat-treated alloys had led some people to believe that strontium would entail a higher degree/amount of oxidation. But, as discussed before, the occurrence of "orange peel" could easily be attributed to the fact

that a different species of oxide layer is formed, with a noticeable color difference, thus leading to the common perception of "more oxidation" in the presence of strontium. What is more likely is the formation of different surface oxide species, which in effect are actually more protective.

It is important to realize that all the oxidation experiments in the present study were performed in a highly controlled laboratory setting (and controlled TGA environment). The quantity of the metal was extremely small compared to any melting operations in the industry, and the molten metal environment was stagnant and well-controlled. In the industrial setting, significant convection, stirring, agitation are present. It must be appreciated that, it is possible that any observed effects and associated protectiveness in a stable and well-controlled laboratory setting can easily be canceled by the disturbances of the melt which can easily occur in an industrial setting.

6. CONCLUSIONS

Oxidation experiments were conducted on three alloy systems: 5182, A356 and A357; with and without 250 ppm of strontium. The oxidation behaviors were noted at three different temperatures: 700 °C, 750 °C and 800 °C.

- For the high magnesium containing 5182 alloy, the three distinct stages could be
 observed: stage 1, an initial slow oxidation stage incubation/induction; followed
 by stage 2, rapid oxidation; and stage 3, subsequent continuation and
 discontinuation of rapid oxidation.
- 2. For the 5182 alloy, increased temperature brings about a shortening of the incubation/induction period. This had been linked to the effects that higher temperatures have on the formation of the initial oxide and the build-up of pressure and stresses leading to the rapid oxidation stage.
- 3. For the 5182 alloy, the presence of strontium prolonged the incubation/induction period of the breakaway oxidation behavior for over 25 hours at each of the temperatures used. It is proposed that the presence of strontium would offer an initial protectiveness due in part to the formation of different oxide species.

- 4. A356 and A357 exhibited similar oxidation behaviors with respect to the effects of strontium. The A357 samples exhibited slightly more oxidation with respect to their higher magnesium content compared to A356 samples.
- 5. The presence of strontium led to significantly lower weight gains in both the A356 and A357 alloy samples; but it also affected the overall kinetic behavior, which changed to a more logarithmic fit, suggesting protective behavior.
- 6. For both the A356 and A357 alloy samples, the total weight gains at the end of 30 hours were decreased by approximately four to six times with the presence of strontium.
- 7. A356/A357 samples without strontium yielded a cauliflower-like and cluster morphology of the oxide; samples with strontium mostly exhibited a much different surface oxide layer, which was dense and coherent.

7. SUGGESTED FUTURE WORK

Although the effects of strontium can be easily observed, the underlying mechanisms on exactly how strontium interacts with the 5182, A356 and A357 alloys are still uncertain. Additional work focusing on determining and identifying the oxide species that are formed with the presence of strontium would be extremely helpful in shedding a clearer light into the basis of the observed effects. The possible interactions between the metal and oxide layer, and the refractory material should also be verified to provide a further understanding of the industrial problems of oxide accretions.

The effects of different levels of strontium should also be investigated. At higher strontium levels, the depletion of available strontium should take longer to achieve or would be more difficult, possibly leading to more noticeable and significant effects, such as even lower weight gains in the A356/A357 alloys, and in the 5182 alloy, a prolongment of the observed incubation period during oxidation.

Larger scale experiments that can more closely resemble industrial practices should also be performed to verify the effects observed. The differences that exist between the TGA laboratory experiments and the industrial environment are quite significant and it would be extremely interesting to see if they can be easily correlated.

REFERENCES

- 1) Dennis, Keith, Effects of Magnesium, Silicon, and Strontium on the Oxidation of Molten Aluminum, M. Eng. Thesis, McGill University, Dept. of Mining and Metallurgy, (1999).
- 2) Emadi, D. Porosity Formation in Sr-Modified Al-Si Alloys, Ph. D. Thesis, McGill University, Dept. of Mining and Metallurgy, (1995).
- 3) Calister, William D. Jr., **Materials Science and Engineering: An Introduction**, John Wiley & Sons, Inc. 3rd ed., Canada. (1994), 577.
- 4) Guermazi, Mohamed, SiC-Reinforced Al₂O₃/Metal Composites by Directed Metal Oxidation, Ph. D. Thesis, McGill University, Dept. of Mining and Metallurgy, (1996).
- 5) M.S. Newkirk, H.R.Zwicker and A.W. Urquhart, "Composite Ceramic Articles and Methods of Making the Same," European Patent Application No. 8600739.9, Publ. No.0193292, Filed 04.02.86.
- 6) Pilling, N.B. Bedworth, R.E., *The Oxidation of Metals at High Temperatures*, **JIM**, Vol. 9, (1923), 529.
- 7) Dennis, Keith, Effects of Magnesium, Silicon, and Strontium on the Oxidation of Molten Aluminumn, M. Eng. Thesis, McGill University, Dept. of Mining and Metallurgy, (1999), 6.
- 8) Kubaschewski, O. Cibula, A. and Moore, D.C., *Gases and Metals*, American Elsevier Publishing Company, Inc. New York, (1970).
- 9) Dennis, Keith, Effects of Magnesium, Silicon, and Strontium on the Oxidation of Molten Aluminumn, M. Eng. Thesis, McGill University, Dept. of Mining and Metallurgy, (1999), 7.
- 10) Kubaschewski, O. Hopkins, B. E., *Oxidation of Metals and Alloys*, Butterworth and Co. Ltd. London, (1962).
- 11) Impey, S. A.; Stephenson, D. J.; and Nicholls, J. R., *Mechanism of Scale Growth on Liquid Aluminum*, **Materials Science and Tech.**, Vol. 4, (1988), 1126.

- 12) Bachrach, R. Z.; Flodstrom, S. A.; Bauer, R.S.; Hagstrom, S.B.M.; and Chadi, D.J., J. of Vacuum Science and Technology, Vol, 15, (1978), 488.
- 13) Cabrera, N. and Mott, N. F., Rep. Progr. Phys. 12, (1948-49), 163.
- 14) Cochran, C. N. and Sleppy, W. C., Oxidation of High-Purity Aluminum and 5052 Aluminum-Magnesium Alloy at Elevated Temperatures, J. Electrochem. Soc., Vol. 108, No. 4, (1961), 322.
- 15) S. J. Gregg and W. B. Jepson, ibid., 1958-59, 87, 187.
- 16) Dennis, Keith, Effects of Magnesium, Silicon, and Strontium on the Oxidation of Molten Aluminumn, M. Eng. Thesis, McGill University, Dept. of Mining and Metallurgy, (1999), 22.
- 17) L. de Brouchère, ibid., 1945, 71, 131.
- 18) Hine, R. A. and Guminski, R. D., *High Temperature Oxidation of Al-Mg Alloys in Various Gaseous Atmospheres*, **JIM. Vol. 89**, (1960), 417.
- 19) Smeltzer, W. W., Oxidation of An Aluminum-3 Per Cent Magnesium Alloy in the Temperature Range 200-550 °C, J. Electrochem. Soc., Vol. 105, No. 2, (1958), 67.
- 20) Impey, S. A.; Stephenson, D. J.; and Nicholls, J.R., A Study on the Effect of Mg Additions on the Oxide Growth Morphologies on Liquid Al Alloys, Microscopy of Oxidation, Vol. 27, (1989), 238.
- 21) Silva, M. P. and Talbot, D. E. J., Oxidation of Liquid Al-Mg Alloys, Light Metals, (1989), 1035.
- 22) Dennis, Keith, Effects of Magnesium, Silicon, and Strontium on the Oxidation of Molten Aluminumn, M. Eng. Thesis, McGill University, Dept. of Mining and Metallurgy, (1999), 47.
- 23) Dennis, Keith, Effects of Magnesium, Silicon, and Strontium on the Oxidation of Molten Aluminumn, M. Eng. Thesis, McGill University, Dept. of Mining and Metallurgy, (1999), 66.
- 24) Gruzleski, John E. and Closset, Bernard M., The Treatment of Liquid Aluminum-Silicon Alloys, American Foundrymen's Society, Inc., Illinois, USA. (1990), 31.
- 25) Dennis, Keith, Effects of Magnesium, Silicon, and Strontium on the Oxidation of Molten Aluminumn, M. Eng. Thesis, McGill University, Dept. of Mining and Metallurgy, (1999), 49.

- 26) Emadi, D. Porosity Formation in Sr-Modified Al-Si Alloys, Ph. D. Thesis, McGill University, Dept. of Mining and Metallurgy, (1995).
- 27) Dennis, Keith, Effects of Magnesium, Silicon, and Strontium on the Oxidation of Molten Aluminumn, M. Eng. Thesis, McGill University, Dept. of Mining and Metallurgy, (1999), 76-80.
- 28) Dennis, Keith, Effects of Magnesium, Silicon, and Strontium on the Oxidation of Molten Aluminumn, M. Eng. Thesis, McGill University, Dept. of Mining and Metallurgy, (1999), 46.
- 29) Dennis, Keith, Effects of Magnesium, Silicon, and Strontium on the Oxidation of Molten Aluminumn, M. Eng. Thesis, McGill University, Dept. of Mining and Metallurgy, (1999), 49.
- 30) Dennis, Keith, Effects of Magnesium, Silicon, and Strontium on the Oxidation of Molten Aluminum, M. Eng. Thesis, McGill University, Dept. of Mining and Metallurgy, (1999), 32, 34-35.
- 31) Dennis, Keith; Drew, R.A.L.; and Gruzleski, J.E., *Effects of Strontium on the Oxidation behavior of an A356 Aluminum Alloy*, Aluminum Transactions: An International Journal. (2000) 12.